JESCEE
Journal of Emerging Supply Chain, Clean Energy, and Process Engineering

p-ISSN 2963-8577
e-ISSN 2964-3511

Vol 4. No 2. 2025

JESCEE | Vol. 4 | No. 2 | pp. 39-116 | JAKARTA 2025 | ISSN 2963-8577

Faculty of
Industrial Technology
Universitas Pertamina

Universitas Pertamina

Journal of
Emerging Supply Chain, Clean Energy, and Process Engineering
Vol 4, No 2, 2025

Journal of
Emerging Supply Chain, Clean Energy, and Process Engineering
Vol 4, No 2, 2025

Journal of

Emerging Supply Chain, Clean Energy, and Process Engineering

Vol 4, No 2, 2025

Reviewers

Imprint

JESCEE is published by Faculty of Industrial Technology, Universitas Pertamina, Jakarta Selatan, Indonesia.

Postal Address

JESCEE Secretariat:

Universitas Pertamina

Jl. Teuku Nyak Arief, Simprug, Kebayoran Lama, Jakarta Selatan, 12220

Indonesias

Business hour: Monday to Friday

07:00 to 17:00 GMT+7

e-mail: jescee@universitaspertamina.ac.id

Journal of
Emerging Supply Chain, Clean Energy, and Process Engineering
Vol 4, No 2, 2025

PREFACE

The Journal of Emerging Supply Chain, Clean Energy, and Process Engineering (JESCEE) is published by the Faculty of Industrial Technology at Universitas Pertamina. It fosters communication among researchers, disseminates research findings, cultivates an academic culture, and encourages the development of new ideas in the fields of mechanical, electrical, chemical, and logistics engineering. The journal's Volume 4, Issue No. 2, has attracted significant attention from numerous researchers eager to publish their work.

On behalf of the Editor-in-Chief, I would like to extend my gratitude to everyone who supports this journal, especially the Dean of the Faculty of Industrial Technology for their direct and indirect assistance. I also appreciate the dedicated editors, the reviewers who provide valuable suggestions and constructive feedback on each submitted paper, and the authors who trust JESCEE with publishing their research.

We hope that this publication will continue to grow and present the latest information in the fields of mechanical, electrical, chemical, and logistics engineering. We also welcome collaborations from individuals and organizations that value this journal and wish to contribute to its ongoing development.

Jakarta, December 2025
Editor-in-Chief

Assoc. Prof. Dr. Eng. Ir. Muhammad Abdillah,
S.T., M.T., IPM

Journal of

Emerging Supply Chain, Clean Energy, and Process Engineering

Vol 4, No 2, 2025

List of Contents

Vol. 4, No. 2, December 2025, pp. 39-49
p-ISSN: 2963-8577
e-ISSN: 2964-3511
DOI: 10.57102/jescee.v4i2.101

JESCEE
Journal of Emerging Supply Chain, Clean Energy, and Process Engineering

SHORT-TERM ELECTRICAL LOAD FORECASTING USING LINEAR REGRESSION AND TIME SERIES MODELS: A CASE STUDY AT PT. PLN (PERSERO) TARAKAN

Kartika Putri Wardani[1*], Ismit Mado[1], Achmad Budiman[1], Sugeng Riyanto[1], Ghusaebi[2], Rustam Effendy[2]
[1]Department of Electrical Engineering, Universitas Borneo Tarakan, Jl. Amal Lama No.1, Tarakan, 77115, Indonesia
[2]PT.PLN (Persero) Kota Tarakan, Jl. P. Diponegoro No.18 Kelurahan Sebengkok, Kota Tarakan, 77114, Indonesia

Abstract
Electrical energy is a fundamental necessity and constitutes one of the most critical needs for society. Since electricity demand over a specific period cannot be determined with absolute certainty, PT. PLN (Persero) Tarakan, as the energy provider, must accurately predict daily load requirements. This study applies Time Series and Linear Regression methods. The optimal result using the ARIMA(1,1,0) model yielded a MAPE value of 14.68%. By incorporating seasonal components, the best model obtained was SARIMA(1,1,0)(1,0,0) with a MAPE of 6.13%. Meanwhile, load forecasting using the Linear Regression method resulted in the equation Y = 44,217.8 - 6.9X with a MAPE of 7.87%.

Keywords:
Linear Regression, Electrical Load, Time Series

Article History:

Corresponding Author:
Kartika Putri Wardani
Department of Electrical Engineering, Universitas Pertamina, Indonesia
Email:: kartikap.w@icloud.com

1. Introduction

Electrical energy is indispensable to modern society. Human activities aimed at fulfilling daily needs constitute a primary factor driving the increasing demand for electrical energy. Consequently, the electricity supply sector must anticipate this trend in terms of both future quantity and capacity. The magnitude of electricity demand over a specific period cannot be calculated with absolute certainty, leading to the challenge of operating power generation systems continuously to meet real-time demand. Conversely, if the power supplied significantly exceeds load demand, it results in the wastage of generation costs. On the other hand, if the generated power is insufficient to meet consumer needs, it leads to power outages. Therefore, efforts to predict electrical load demand are essential as a foundation for both operational planning and the future development of electric power systems.

The application of short-term electrical load forecasting based on Linear Regression and Time Series models at *PT. PLN (Persero)* in Tarakan is expected to assist the company in achieving more effective energy planning and management. With more accurate predictions, *PT. PLN* can optimize power plant operations, mitigate the risk of outages, and enhance energy usage efficiency. This not only positively impacts the continuity of electricity service in Tarakan but also contributes to the overall operational performance of *PLN*.

This study performs short-term electrical load forecasting modeling based on power generation data at *PT. PLN (Persero) Tarakan*. The data utilized in this research consists of hourly electrical load data from November 1 to November 15, 2023.

2. Experimental Section

A. Short-Term Electrical Load Forecasting

Forecasting is the process of estimating future events based on relevant historical data and projecting them forward using mathematical models. To achieve forecasting objectives, it is essential to employ methods compatible with the specific data and information being analyzed. This is particularly critical in electric power

system operations, which hold significant importance for both corporate management and operational efficiency. Short-term forecasting is defined as the prediction of conditions over a time horizon ranging from daily to hourly intervals. The objective of short-term forecasting in this context is to serve as a comparative study between forecasted and actual electrical loads.

1. ARIMA Modeling

The ARIMA method is also known as the Box-Jenkins method, a model extensively developed by George Box and Gwilym Jenkins in 1970. However, the Box-Jenkins method continues to dominate many research fields to this day. ARIMA utilizes two algorithms, namely autoregressive (AR) and moving average (MA), and combines an integrated element to address non-stationarity through a differencing method. A key prerequisite for stationarity is that the data pattern must not exhibit a significant trend. To identify AR properties, the Autocorrelation Function (ACF) is used, which represents the relationship between a series of observations in a time series. Conversely, the Partial Autocorrelation Function (PACF) is employed to identify MA properties. Generally, significant ACF and PACF values are observed at lag 1 or 2; it is rarely found that AR and MA properties possess values greater than 2.

ARIMA can be applied to data regardless of whether it exhibits seasonal patterns. In general, if an ARIMA model has an AR order of p, a degree of differencing d, and an MA order of q, the model is denoted as ARIMA(p,d,q), expressed by the following equation:

$$Z_t = (1+\phi_1)Z_{t-1} + (\phi_2-\phi_1)Z_{t-2} + \cdots + (\phi_p - \phi_{p-1})Z_{t-p} + \phi_p Z_{t-p-1} + a_t + \theta_1 a_{t-1} + \cdots + \theta_q a_{t-q} \quad (1)$$

or

$$\phi_p(B)(1-B)^d Z_t = \theta_0 + \theta_q(B)a_t \quad (2)$$

where

$\phi_p(B) = 1 - \phi_1 B - \phi_2 B^2 - \cdots - \phi_p B^p$

$\theta_q(B) = 1 - \theta_1 B - \theta_2 B^2 - \cdots - \theta_q B^q$.

A stationary time series possesses an Autocorrelation Function (ACF) that declines linearly and slowly. The same applies to the estimated ACF derived from the data. If there is a tendency for the ACF and the estimated ACF (f_k) not to decay rapidly, the function is classified as non-stationary.

The seasonal time series is described as follows:

Seasonal Autoregressive Moving Average (SARIMA) Model

The general form of SARIMA is

$$\phi_p(B)\Phi_{P_1}(B^{s_1})(1-B)^d(1-B^{s_1})^{D_1}Z_t = \theta_0 + \theta_q(B)\Theta_{Q_1}(B^{s_1})a_t \quad (3)$$

where

$\phi_p(B) = 1 - \phi_1 B - \phi_2 B^2 - \cdots - \phi_p B^p$

$\Phi_P(B^s) = 1 - \Phi_{1_1} B^{s_1} - \Phi_{2_1} B^{2s_1} - \cdots - \Phi_{P_1} B^{P_1 s_1}$

$\theta_q(B) = 1 - \theta_1 B - \theta_2 B^2 - \cdots - \theta_q B^q$

$\Psi_{Q_1}(B^{s_1}) = 1 - \Theta_{1_1} B^{s_1} - \Theta_{2_1} B^{2s_1} - \cdots - \Theta_{Q_1} B^{Q_1 s_1}$

1) Box-Jenkins ARIMA Model Procedure

Data analysis was performed using the ARIMA method assisted by statistical software, specifically MINITAB 14. The sequential steps for applying the ARIMA method are as follows:

a. Data preparation, including stationarity checks.
b. Model identification. Through ACF and PACF plots, the appropriate model for ARIMA prediction can be determined.
c. Determination of ARIMA parameters *p*, *d*, and *q*.
d. Formulation of the ARIMA model equation. The coefficients utilized are derived from model analysis parameters yielding the lowest Mean Squared Error (MSE) value.
e. Validation of predictive parameters.
f. Forecasting.

The subsequent step involves utilizing the optimal model for prediction. Once the best model has been determined, it is ready to be employed for daily electrical load forecasting at *PT. PLN (Persero) Tarakan*.

2. Linear Regression Modeling

The linear regression model is a statistical framework used to understand and predict the relationship between a dependent variable (target) and one or more independent variables (predictors).

The relationship between the dependent and independent variables can be expressed as a function. The simple linear regression equation is defined as follows:

$$Y = \alpha + bX \tag{4}$$

Where:

Y = Dependent Variable

X = Independent Variable

α = Constant (Intercept)

b = Magnitude of the response induced by the predictor (Slope)

To obtain Equation (4), the initial step is to determine the constant and the regression coefficient. The formulas used to calculate these variables are as follows:

$$\alpha = \frac{\sum y - b \sum x}{n} \tag{5}$$

$$b = \frac{n \sum (xy) - \sum x \sum y}{n \sum x^2 - (\sum x)^2} \tag{6}$$

3. Forecasting Model Evaluation

Forecasting accuracy is essential in data analysis to evaluate the suitability of the utilized forecasting models. In this study, the criterion employed to evaluate forecasting accuracy is the Mean Absolute Percentage Error (MAPE). The equation for calculating MAPE is as follows:

$$MAPE = \sum_{t=1}^{n} \left(\frac{Yreal - Yforcast}{Yforcast} \right) \times 100\% \tag{7}$$

3. Result and Discussion

The data utilized in this study is secondary data, specifically electrical load data obtained from *PT. PLN (Persero) Tarakan* spanning from November 1 to November 15, 2023. This dataset consists of hourly measurements. The training set comprises 336 data points covering the period from August 1 to August 14, 2023, while the testing set consists of 24 data points recorded on November 15, 2023.

A. Electrical Load Forecasting Study Based on Time Series Models

1. Data Stationarity

The initial step is to assess the stationarity of the electrical load data using a time series plot. Based on visual observation, the data exhibits trend components, as it tends to fluctuate (increase and decrease) over time. Consequently, the data is considered non-stationary. Figure 1 shows the plot after data differencing.

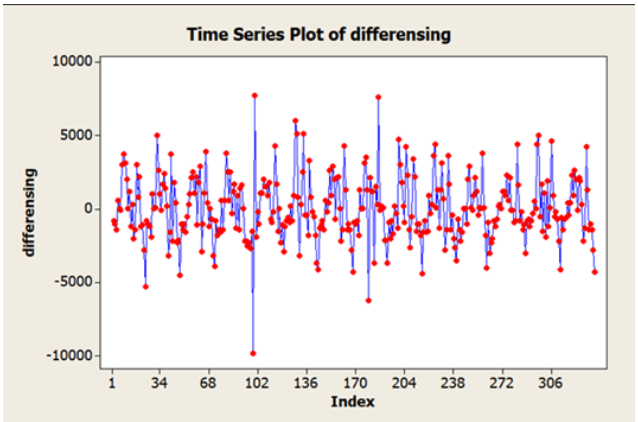

Figure 1. Time series plot after differencing.

Meanwhile, the ACF plot after differencing is presented in Figure 2.

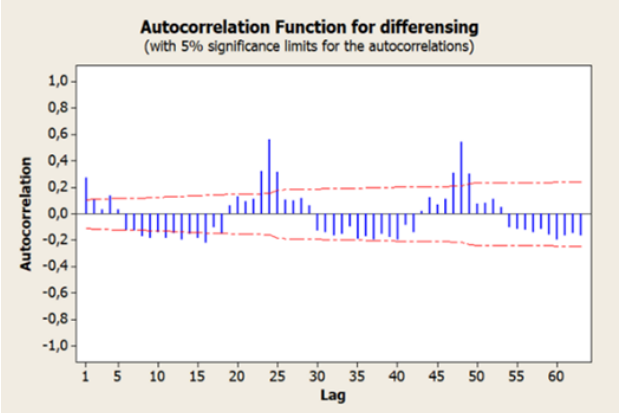

Figure 2. Autocorrelation Function (ACF) plot after differencing.

In addition to the time series plot, data stationarity can also be assessed using the ACF plot. The initial ACF plot indicates that the data is non-stationary, as it decays slowly and exhibits high correlation at early lags. Based on this identification, differencing is required. Figure 2 demonstrates that the data has become stationary, as the correlations at various lags rapidly approach zero, indicating the absence of any remaining trend patterns. The PACF plot is also necessary for model analysis, as presented in Figure 3.

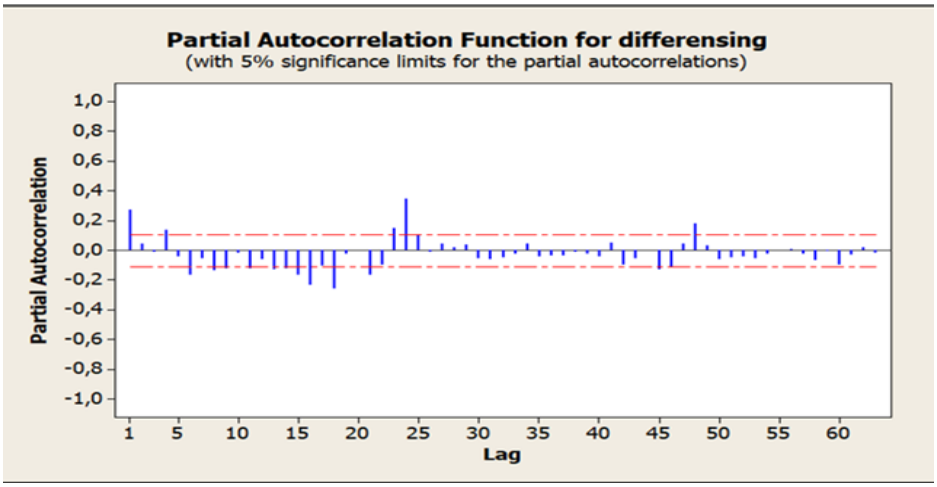

Figure 3. Partial Autocorrelation Function (PACF) plot after differencing.

The criteria used for model determination are as follows:

a. If the ACF exhibits a "dying down" (tailing off) pattern and the PACF shows a "cut off," the ARIMA model is identified as a pure Autoregressive (AR) process.

b. If the ACF shows a "cut off" and the PACF exhibits a "dying down" pattern, the ARIMA model is identified as a pure Moving Average (MA) process.

c. If both the ACF and PACF exhibit "dying down" patterns, the ARIMA model is considered a mixed AR and MA process.

The ACF plot in Figure 2 demonstrates a dying down pattern, characterized by lags that gradually decrease towards zero. Additionally, the T-value at the first lag is 5.08, which slowly declines and approaches zero. With significant spikes observed initially at lags 1 and 3, the parameter p can be determined to be between 1 and 2. Consequently, it can be concluded that $p = 1$ (denoted as AR 1) or $p = 2$ (denoted as AR 2).

Meanwhile, the PACF plot in Figure 3 exhibits a "dying down" pattern, declining towards zero with insignificant T-values after the first lag; thus, the parameter q is determined to be 1. Regarding the parameter d (differencing), the value is 1, as the data achieved stationarity after the first differencing. Consequently, the model to be utilized is the ARIMA(p,d,q) model.

To validate the determination of the ARIMA model, it is necessary to evaluate several candidate models by selecting the one with the lowest Mean Squared Error (MSE) value derived from the identification results.

Table 1. ARIMA Model determination using MSE.

No	ARIMA Model	MSE
1	(1,1,1)	4403641
2	(1,1,2)	4415008
3	(1,1,0)	4400358
4	(0,1,1)	4454668
5	(0,1,2)	4399166
6	(2,1,0)	4404417

7	(2,1,1)	4414802
8	(2,1,2)	4428689

Based on the eight models evaluated above, the ARIMA(1,1,0) model yielded the lowest MSE value of 4,400,358; therefore, this model is selected for forecasting. Based on the forecasting results of the selected model, the resulting MAPE is 14.68%.

Although the plot of the differenced data is stationary, it exhibits indications of a Seasonal ARIMA (SARIMA) process. This is evidenced by the presence of multiple significant lags or repetitive significant spikes at specific intervals, occurring at lags 24, 48, and so forth. Consequently, a re-analysis incorporating the seasonal pattern is required. To understand the model's behavior, the ACF and PACF plots are interpreted with reference to Table 2 as follows.

Table 2. Seasonal ACF and PACF Patterns.

Model	ACF	PACF
AR (P)	*Dying down* (exponential decay) at seasonal lags	*Cut off* (abrupt drop)
MA (Q)	*Cut off* (abrupt drop)	*Dying down* (exponential decay) at seasonal lags
ARIMA (P,d,Q)	*Dying down* (exponential decay) at seasonal lags	*Dying down* (exponential decay) at seasonal lags

The SARIMA model is denoted as $(p,d,q)(P,D,Q)_{24}$, where the non-seasonal parameters (p,d,q) are derived from the previously determined optimal ARIMA model, specifically (1,1,0). Consequently, eight estimated SARIMA models are compared. To facilitate analysis, the MSE values for each model are presented below.

Table 3. SARIMA Model determination using MSE.

SARIMA Model	MSE
(1,1,0)(1,0,0)24	2932520
$(1,1,0)(1,0,1)_{24}$	-
(1,1,0)(0,0,1)24	3674686
(1,1,0)(2,0,0)24	-
(1,1,0)(2,0,1)24	-
(1,1,0)(2,0,2)24	-
$(1,1,0)(0,0,2)_{24}$	3194503

(1,1,0)(1,0,2)24	3545555

Berdasarkan Among the eight SARIMA models evaluated above, the model with the lowest MSE is the SARIMA$(1,1,0)(1,0,0)_{24}$ model, with an MSE value of 2,932,520. Consequently, this model is selected for forecasting. Based on the forecasting results of the selected model, the Mean Absolute Percentage Error (MAPE) is 6.136030879%, or approximately 6.13%. When comparing the MAPE values of the seasonal and non-seasonal models, the seasonal model demonstrates superior performance, as indicated by its lower MAPE value compared to the non-seasonal counterpart.

B. Short-Term Electrical Load Forecasting Study Based on Linear Regression Models

1. Determination of Normal Equation Coefficients

To obtain the coefficients for the linear regression equation, the normal equations must be constructed. Prior to forming these equations, the value of each element is calculated by organizing the variables as shown in the following table.

Table 4. Determination of normal equation elements.

N	X	Y	Xy	x^2
1	1	40.600	40.600	1
2	2	39.800	79.600	4
.	.	.	.	.
.	.	.	.	.
335	335	45.700	15.309.500	112.225
336	336	41.400	13.910.400	112.896
n = 336	Σx= 56.616	Σy = 14.463.700	Σxy = 2.415.155.500	Σx^2 = 12.700.856

Subsequently, the values of coefficients α and b are determined using Equations 5 and 6, yielding:

$$b = \frac{336(2.415.155.500) - 56.616 \,.14.463.700}{336(12.700.856) - (56.616)^2}$$

$$b = -6,95$$

Subsequently, to determine the value of coefficient α using the equation above, yielding:

$$\alpha = \frac{14.463.700 - (-6,95).56.616}{336}$$

$$\alpha = 44.217,8$$

2. *Forecasting*

Calculating the short-term electrical load forecast using the linear regression model via Equation 4 yields:

$$Y = \alpha + b \, . \, X$$
$$= 44.217{,}8 + (-6{,}95) \, . \, 337$$
$$= 41.875{,}65$$

Subsequently, the comparison between the actual data (specifically from November 15, 2023) and the results obtained from the linear regression model is presented in a tabulated format in Table 5 below.

Table 5. Overall results of $|Y_{real} - Y_{forecast}|$ values.

No	Date	Time	X	Y_{real}	$Y_{forecast}$	$\lvert Y_{real} - Y_{forecast} \rvert$
1	15-Nov-23	01.00	337	40.000	41.875,65	-1.875,65
2	15-Nov-23	02.00	338	38.300	41.868,7	-3.562,70
3	15-Nov-23	03.00	339	36.900	41.861,75	-4.961,75
4	15-Nov-23	04.00	340	35.400	41.854,8	-6.454,80
5	15-Nov-23	05.00	341	36.300	41.847,85	-5.547,85
6	15-Nov-23	06.00	342	37.000	41.840,9	-4.840,90
7	15-Nov-23	07.00	343	37.700	41.833,95	-4.133,95
8	15-Nov-23	08.00	344	41.900	41.827	73
9	15-Nov-23	09.00	345	45.600	41.820,05	3.779,95
10	15-Nov-23	10.00	346	46.700	41.813,1	4.886,90
11	15-Nov-23	11.00	347	47.600	41.806,15	5.793,85
12	15-Nov-23	12.00	348	48.500	41.799,2	6.720,80
13	15-Nov-23	13.00	349	50.600	41.792,25	8.807,75
14	15-Nov-23	14.00	350	51.200	41.785,3	9.414,70
15	15-Nov-23	15.00	351	51.700	41.778,35	9.921,65
16	15-Nov-23	16.00	352	48.300	41.771,4	6.528,60
17	15-Nov-23	17.00	353	47.500	41.764,45	5.735,55
18	15-Nov-23	18.00	354	51.900	41.757,5	10.142,50

19	15-Nov-23	19.00	355	52.900	41.750,55	11.149,45
20	15-Nov-23	20.00	356	51.700	41.743,6	9.956,40
21	15-Nov-23	21.00	357	50.600	41.736,65	8.863,35
22	15-Nov-23	22.00	358	48.800	41.729,7	7.070,30
23	15-Nov-23	23.00	359	46.900	41.722,75	5,177,25
24	15-Nov-23	00.00	360	43.200	41.715,8	1.484,20
	Total		8364	1.087.200	1.003.097,4	78.951,35

3. MAPE Accuracy Test

After obtaining the absolute values, the MAPE accuracy test for the short-term electrical load on November 15, 2023, is performed as follows:

$$MAPE = \sum_{t=1}^{n} \left(\frac{78.951,35}{1.003.097,4}\right) \times 100\%$$

$$= 7,87075612$$

$$= 7,87\%$$

Based on the accuracy testing conducted using MAPE, an error value of 7.87% was obtained.

4. Conclusion

Following the forecasting analysis conducted on electrical load data from PT PLN (Persero) Tarakan utilizing both time series and linear regression methods, the following conclusions are drawn:

a. The MAPE for the ARIMA model is 14.67% and for the SARIMA model is 6.13%. These results generally fall within the 10–20% range, indicating "Good" forecasting accuracy.

b. The MAPE for the Linear Regression model is 7.87%, which is also interpreted as "Good".

c. Forecasting using the SARIMA model proved to be the best approach, demonstrating the smallest error margin among the three methods utilized.

Acknowledgment

The authors express their gratitude for the collaboration between the Department of Electrical Engineering at Universitas Borneo Tarakan and PT PLN Kota Tarakan, which serves as a manifestation of the synergy between academia and practitioners.

References

[1]. Putra, A A. & Budiono, H. (2017). Peramalan Beban Listrik dengan Metode Time Series. Jurnal Teknik Elektro, Vol 9 No 2, 58-65.

[2]. Dewi, I. A. M. C., Nrartha, M. A., & Suksmadana, M. B. (2016). Peramalan Beban Listrik Jangka Pendek pada Sistem Kelistrikan Jawa Timur dan Bali Menggunakan Fuzzy Time Series. Jurnal Ampere Vol 3 No 1, 1–6.

[3]. Aswathappa. (2005). Time Series Forecasting for Financial Applications. Jurnal of Applied Business Research. Vol 21 No 4, 115-130 .

[4]. Khair, Aulia. (2011). Peramalan Beban Listrik Jangka Pendek Menggunakan Kombinasi Metode Autoregresif Integrated Moving Avarage (ARIMA) Dengan Regresi Linier Antara Suhu Dan Daya Listrik". Universitas Indonesia.

[5]. Helmi Wibowo, Yadi Mulyadi, Ade Gafar Abdullah. (2012). Peramalan Beban Listrik Jangka Pendek Terklasifikasi Berbasis Metode Autoregressive Integrated Moving Average. Jurnal, Electrans, Vol 11 NO.2, 44-50.

[6]. Juliasari, Yossi. (2020). Peramalan Beban Listrik Jangka Pendek Menggunakan Metode Regresi Linier-Algoritma Genetika. Universitas Hasanuddin.

[7]. Hartono, D. (2021). Penerapan Model Regresi Linier untuk Peramalan Beban Listrik. Jurnal Elektronika Indonesia.

[8]. Haryanto, R. (2019). Analisis Peramalan Beban Listrik Menggunakan Model ARIMA pada PT. PLN (Persero). Prosiding Seminar Nasional Teknik Elektro, 243-250. Surabaya: Universitas X.

[9]. I Mado, A Soeprijanto, S Suhartono. (2018). Applying of Double Seasonal ARIMA Model for Electrical Power Demand Forecasting at PT. PLN Gresik Indonesia. International Journal of Electrical and Computer Engineering 8 (6), 4892.

[10]. I Mado, A Rajagukguk, A Triwiyatno, A Fadllullah. (2014). Short-Term Electricity Load Forecasting Model Based DSARIMA. International Journal of Electrical, Energy and Power System Engineering 5(1), 6-11.

[11]. I Mado, A Budiman, A Triwiyatno. (2023). Short-Term Forecasting Daily Electricity Loads Using Seasonal Arima Patterns of Generation Units at PT. PLN (PERSERO) Tarakan City. Jurnal Ilmiah Kursor 12 (2), 93-100.

[12]. I Mado. (2020). Electric Load Forecasting an Application of Cluster Models Based on Double Seasonal Pattern Time Series Analysis. Forecasting in Mathematics-Recent Advances, New Perspectives and Applications

Biographies of Authors

Kartika Putri Wardani is an Electrical Engineering Student at the University of Borneo Tarakan in 2019. The author was born in Tarakan on April 07 1999. Before becoming a student, the author had completed his education at SMA Negeri 1 Pulau Bunyu.

Ismit Mado graduated from the ITS Surabaya Doctoral Program in 2019. Currently he serves as Head of the Power System Stability Laboratory at the Department of Electrical Engineering, University of Borneo, Tarakan. He is interested in stability and control studies of power generation systems, forecasting studies based on time series models, and fuzzy modeling.

Achmad Budiman is an Electrical Engineering Lecturer since 2002. He obtained his Bachelor's degree in Electrical Engineering from Gadjah Mada University, Yogyakarta. He obtained his Master's degree in Electrical Engineering from ITS Surabaya. Currently, he serves as the Head of Electrical Engineering Study Program, Borneo Tarakan University. He is interested in the field of stability in power distribution and transmission systems.

Sugeng Riyanto is an Electrical Engineering Lecturer since 2002. Currently, he serves as a lecturer in the Electrical Engineering Study Program, University of Borneo Tarakan. He is interested in the fields of drawing electrical engineering, basic electrical installations and transformers.

Ghusaebi graduated with a Bachelor's degree in Electrical Engineering from the University of Indonesia in 2015. He has been working at PT PLN (Persero) since 2016, specializing in power distribution. Currently, he serves as the Manager of PT PLN (Persero) ULP Tarakan.

Rustam Effendy Graduated from Hang Tuah Tarakan High School in 1998. He has been working at PT PLN (Persero) since 2010. Currently, he serves as a Junior Load Regulator Technician at PT PLN (Persero) ULP Tarakan.

Vol. 4, No. 2, December 2025, pp. 51-59
p-ISSN: 2963-8577
e-ISSN: 2964-3511
DOI: 10.57102/jescee.v4i2.118

JESCEE
Journal of Emerging Supply Chain, Clean Energy, and Process Engineering

FERMENTATION OF CHICKEN SLAUGHTERHOUSE WASTEWATER (CSWW) WITH WHITE SUGAR AS A CARBON SOURCE FOR MANUFACTURING OF LIQUID FERTILIZER

Eduardus Budi Nursanto[1, 2, 3*], Akbar Angga Handjaya[1], Nur Layli Amanah[1, 4], Muhammad Fairuzt Fathin Faundra[1], Andika Yudistira[1], Alifiana Permata Sari[1,2], Catia Angli Curie[1,2]
[1]Department of Chemical Engineering, Faculty of Industrial Engineering, Universitas Pertamina
[2]Center of Downstream Chemical Industry, Universitas Pertamina, Jalan Teuku Nyak Arif, Jakarta Selatan, 12220, Indonesia
[3]Graduate Program of Science in Sustainability, Universitas Pertamina, Jalan Teuku Nyak Arif, Jakarta Selatan, 12220, Indonesia
[4]The Petroleum and Petrochemical College, Chulalongkorn University, Bangkok 10330, Thailand

Abstract
Along with the increase in the production of broilers, the amount of liquid waste produced will increase. Liquid waste resulting from chicken slaughterhouse activities will cause odor pollution and aquatic pollution. Chicken slaughterhouse wastewater (CSWW) is suitable for use as a raw material for Liquid Organic Fertilizer (LOF) production, based on nutrient analysis results of waste samples collected from a facility in South Jakarta. According to the results of the analysis, the Biochemical Oxygen Demand (BOD) was measured at 214.52 mg/L, and the Chemical Oxygen Demand (COD) was significantly higher at 2310 mg/L. Furthermore, the samples contained 37.39 mg/L of oil and fat, and an ammonia (NH_3) concentration of 37.39 mg/L. The presence of high concentrations of organic substances, such as protein, oil, and fat, confirms the potential of CSWW as a valuable raw material to produce LOF. To facilitate this study, bioconversion, the fermentation method was employed. In this study, four formulations of (LOF) were prepared using varied concentrations of a carbon source (sucrose) and Effective Microorganisms 4 (EM4) solution bacterial inoculum. The efficacy of these formulations was subsequently evaluated via a bioassay on land kangkong (Ipomoea reptans Poir). The results revealed that the greatest positive effect on plant growth was achieved by the LOF variation, which incorporated 150 g of sucrose and 0.05 L of EM_4 solution. Samples of plants that were given the addition of LOF showed the highest number of leaves, as many as 24 strands and the highest plant height value of 18 cm.

Keywords:
Liquid waste, chicken slaughterhouse, fermentation, organic fertilizer

Article History:
Received: November 19th, 2025
Revised: December 10th, 2025
Accepted: December 21st, 2025
Published: December 31st, 2025

Corresponding Author:
Eduardus Budi Nursanto
Department of Chemical Engineering, Universitas Pertamina, Indonesia
Email::
eduardus.bn@universitaspertamina.ac.id

1. Introduction

Waste, as an unavoidable by-product of human and natural activities, requires proper management and processing, ideally through conversion into economically valuable raw materials. Waste streams are generally categorized into solid, liquid, and gaseous forms. Among these forms, wastewater generated by one chicken slaughterhouse poses a significant environmental challenge, especially for facilities located in residential areas. The discharge of this organic-rich waste highly contributes to water and air pollution, leading to a decline in overall environmental sanitation and water quality [1]. Therefore, developing effective strategies to enhance the value of this specific organic wastewater stream is crucial for mitigating its environmental impact.

In 2022, the demand for broiler chicken meat in Indonesia was recorded at 3.11 billion [2]. Due to this high consumption of broiler chickens, chicken slaughtering production activities and the resulting CSWW will

inevitably increase. Generally, waste has the potential to cause negative impacts on the environment and human health in surrounding settlements. However, CSWW can be enhanced in value by processing it into organic fertilizer [1]. The large-scale development of organic fertilizer has already been carried out. Various types of organic sources can be used as raw materials, such as livestock solid waste, agricultural waste, and organic industrial waste [3]. Fertilizer derived from organic materials is one that can play a role in enhancing the soil's biological, chemical, and physical activities, which are crucial for soil and plant fertility [4].

While organic fertilizer can be derived from liquid and solid livestock waste, the focus of this research is on the liquid waste generated by chicken slaughterhouses. The liquid waste (effluent) from slaughterhouse production contains 0.5–9% macro and micro nutrients, 11–15.2% organic carbon (C-organic), and 0.15–13.6% amino acids [5]. Liquid waste, which constitutes 80% of the total waste content, exists as a poorly digested substrate. This presents a significant potential for its use as a raw material for organic fertilizer [5].

With the aim of increasing the value of this CSWW, this research focuses on the production process of Liquid Organic Fertilizer (LOF). This process utilizes supporting materials such as water (as a solvent), EM4 bacteria solution, and sucrose. EM4 solution contains several bacteria (such as *Lactobacillus* sp, photosynthetic bacteria, *Streptomyces* sp). The sucrose acts as the carbon source for the EM4 bacteria solution during the fermentation process that converts the waste into LOF [6]. This fermentation proceeds through four distinct stages: hydrolysis, acidogenesis, acetogenesis, and methanogenesis. Furthermore, the resulting LOF product is tested directly using land kangkong plant samples with varying fertilizer concentrations.

2. Experimental Section

A. Materials

The Chicken Slaughterhouse Wastewater (CSWW) was obtained from a chicken slaughterhouse located in Cipulir, Kebayoran Lama, Jakarta Selatan, DKI Jakarta. The Effective Microorganisms 4 (EM4) bacterial solution, which contains *Lactobacillus* sp, photosynthetic bacteria, and *Streptomyces* sp, was purchased commercially, while the sucrose source was derived from local crystalline sugar. The detailed ratio of EM4 to sucrose can be seen in Table 1. The liquid organic fertilizer (LOF) testing was practiced on land kangkong sourced from the East West Seed Company, using various LOF concentrations as clearly presented in Table 3.

B. Pre-treatment of CSWW

The CSWW sample was subjected to sampling and testing at the Chemical Engineering Laboratory, Faculty of Industrial Technology Universitas Pertamina and the Environmental Laboratory DKI Jakarta. The sampling was carried out to analyze the content of the acquired sample before it was processed into LOF.

C. Fabrication of LOF

The sampled CSWW was subsequently poured into a fermented vessel. It was then mixed with clean water, the EM4 bacterial solution, and sucrose, according to the ratio variations presented in Table 1. Stirring was carried out for 2 minutes, and the fermenter vessel was sealed. The fermentation process lasted for 14 days. The resulting LOF was then subjected to sample testing at the Chemical Engineering Laboratory of Universitas Pertamina.

Table 1. Variations of LOF samples.

Sampel No.	Waste (L)	Em4 (L)	Water (L)	Carbon Source (Kg)
1	2	45	0.2	0.15
2	2	45	0.2	0.2
3	2	45	0.2	0.25
4	2	45	0.2	0.25

D. Parameter

Observations were conducted during the 14-day fermentation process and immediately after the LOF sample was produced. The observation variables included color, odor, pH, the presence of gas in the sample, and the total

sample volume percentage (yield) at the beginning of fermentation and after 14 days of fermentation. The yield volume can be calculated using Equation 1, where Vi and Vf denote the initial and final volumes, respectively.

$$Yield = \frac{V_i V_f}{V_i} \times 100\% \quad (1)$$

E. Plant Testing

The plant experiment was conducted using land kangkong seeds as the research object. The seeds were planted in polybags(15×15) cm using burnt rice husks, obtained from a local ornamental plant store, as the planting medium. Five treatments were performed: four plant samples were given the LOF with an equal addition of 30 ml for each sample, and one sample was used as a comparator (control) without the addition of the LOF.

Three land kangkong seeds were used for each experimental plant. The development of the land kangkong lasted for 21 to 30 days, with watering done once a day [7]. The application of the LOF sample to the treated plants was done once every 3 days during the planting process. Specifically, the LOF was applied on days 7, 14, and 21. The parameters observed during the planting process were plant height and number of leaves.

3. Result and Discussion

A. Characteristic of CSWW

Prior to the production of the LOF, the CSWW sample was first tested for its nutrient content. This was aimed at determining the potential and composition of the CSWW sample originating from the chicken slaughterhouse. 30 $Liter$ sample of the CSWW was collected and analyzed at an environmental. The detailed results of the CSWW sample content analysis can be seen in Table 2.

The results of the CSWW sample testing showed that several parameters exceeded the quality standards issued by the Environmental Ministry of the Special Capital Region of Jakarta Province [8]. Nearly all parameters were found to be above the standard quality, except for the oil and fat test. Thus, it can be concluded that the CSWW discharged by the chicken slaughterhouse poses a potentially dangerous risk to living organisms in the environment surrounding the slaughterhouse [1].

Specifically, the value of Biochemical Oxygen Demand (BOD) is a measure of the amount of oxygen consumed by the microbial population present in a water sample in response to the introduction of biodegradable organic matter. The high BOD value of 215.52 mg/L indicates the high potential of organic matter in processing the organic substances contained within the sample [9]. Chemical Oxygen Demand (COD) represents the total organic material, both difficult and easy to decompose. The COD value of 2310 mg/L obtained from the CSWW sample analysis in this study is significantly higher than the standard BOD value. This difference arises because the COD value includes a larger number of organic substances in the sample that can be chemically oxidized but are not susceptible to biological oxidation (non-biodegradable) [10].

Similarly, the high amount of ammonia can serve as an energy source for the bacterial nitrification process during fermentation, and this ammonia can also enhance the fertility of a planting medium within an ecosystem [10]. Therefore, with this CSWW testing, it can be stated that through processing, the value of CSWW can be enhanced by converting it into LOF, which is more beneficial for other living organisms.

Table 2. Analysis of fluid waste sample content of chicken slaughterhouse.

No.	Parameter	Unit	Test Results	Waste Quality Standard
1	BOD	mg/L	214.52	100
2	COD	mg/L	2310	200
3	TSS	mg/L	530	100
4	Oil And Fat	mg/L	0.82	15
5	Ammonia	mg/L	37.39	25
6	pH	mg/L	7.9	6 – 9

B. Fermentation effect on LOF

The production of LOF was carried out using several materials that have been mentioned. Additional ingredients such as the EM4 bacterial solution and sucrose are substances that can accelerate the LOF production process and improve the quality. This is justifiable because the EM4 solution contains 90% Lactobacillus sp. (lactic acid-producing bacteria), photosynthetic bacteria, and Streptomyces sp. Which function to optimize the utilization of organic substances contained in the CSWW [5]. Therefore, the components in EM4 can directly digest sucrose, cellulose, starch, sugars, protein, and fats in the CSWW [11]. This anaerobic fermentation process comprises four stages, which include [5]:

1. Hydrolysis

   Hydrolysis is the initial stage of the digester process, where organic matter is converted into simpler forms, making it easier for microorganisms to decompose. This digester process is often referred to as depolymerization, breaking down the macromolecules contained within the CSWW sample. More specifically, the hydrolysis reaction of the glucose macromolecule can be seen in Equation 2. This equation involves water (H_2O) and EM4 bacteria, which are capable of breaking down sucrose into glucose and hydrogen (H_2).

$$CSWW + H_2O \xrightarrow[Bacteria]{Facultative} C_6H_{12}O_6 + 2H_2 \quad (2)$$

2. Acidogenesis

   Acidogenesis is the stage where glucose, fatty acids, and amino acids resulting from the hydrolysis process are converted into organic acids such as acetic acid (CH_3COOH), propanoic acid (CH_3CH_2COOH), butyric acid ($CH_3CH_2CH_2COOH$), and alcohol. The process of converting glucose into alcohol, propanoic acid, and acetic acid, which is carried out by Lactobacillus bacteria or bacteria with acidogenic content, corresponds to Equations 3 to 5.

$$C_6H_{12}O_6 \leftrightarrow 2CH_3CH_2OH + CO_2 \quad (3)$$

$$C_6H_{12}O_6 + 2H_2 \leftrightarrow 2CH_3CH_2COOH + CH_3(CH_2)_2COOH + 2H_2O \quad (4)$$

$$C_6H_{12}O_6 \rightarrow 3CH_3COOH \quad (5)$$

3. Acetogenesis

   Acetogenesis is the process that converts organic acids and alcohol into acetic acid (CH_3COOH). In the acetogenesis stage, the residual products from acidogenesis, such as propanoic acid, butyric acid, and alcohol, are converted by acetogenic bacteria (Lactobacillus) into hydrogen, carbon dioxide, and acetic acid. The corresponding fermentation reactions can be seen in Equations 6 and 7.

$$CH_3CH_2COOH + 2H_2O \rightarrow CH_3COOH + CO_2 + 3H_2 \quad (6)$$

$$CH_3(CH_2)_2COOH2 \rightarrow CH_3COOH + 2H_2 \quad (7)$$

4. Methanogenesis

   During the methanogenesis process, methanogenic microorganisms convert the hydrogen and acetic acid formed in the preceding process into methane gas (CH_4) and carbon dioxide (CO_2) via fermentation reactions. The detailed reactions can be seen in Equations 8–9.

$$CO_2 + 4H_2 \rightarrow CH_4 + 2H_2O \quad (8)$$

$$CH_3COOH \rightarrow CH_4 + CO_2 \quad (9)$$

Based on the graph obtained, as shown in Figure 1, the pH value started to decrease on the first day. This indicates that the CSWW underwent a fermentation process which had entered the first stage, is the Hydrolysis stage [12]. Hydrolysis is a decomposition process carried out by facultative bacteria, converting organic matter into fatty acids and amino acids. This is followed by the Acidogenesis stage, where the glucose, amino acids, and fats present in the LOF sample are converted by hydrolase bacteria into organic acids [5]. This entire process takes place under anaerobic conditions (without oxygen), which initially causes the pH value to rise, before the sample LOF's pH subsequently begins to decrease as it becomes more acidic due to the formed acids [13].

The second stage is Acetogenesis. In this phase, the sugar components produced from the preceding fermentation stage undergo acidification and become a food source for the microbial bacteria present in the LOF sample. Subsequently, the organic acid compounds and ethanol formed earlier are broken down by Acetogenic Bacteria into acetic acid, as well as CO_2 and H_2 [13]. This breakdown process is what further caused the average pH value of the sample to decrease until the third day. Overall, the fermentation process leads to an increase in microbial activity, a decrease in the pH value, and an increase in the acid content of the fermented product.

From the third to the fourteenth day, it can be observed that the pH value began to stabilize, maintaining a consistent range of 3 to 4 (Figure 1). This indicates that the LOF sample is entering the final stage of the fermentation process in LOF production, which is Methanogenesis. Methanogenesis is the fermentation process that produces methane gas [13]. The presence of methane gas is attributed either to the process of converting acetic acid into carbon dioxide or to the reduction of carbon dioxide by hydrogen [13].

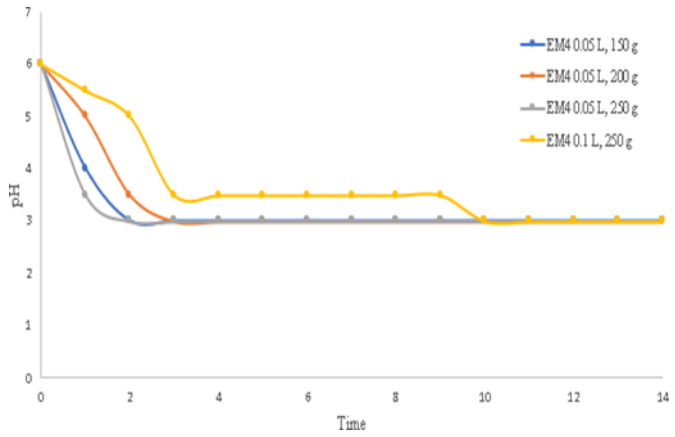

Figure 1. pH observation data for liquid organic fertilizer samples.

C. Plant Response

Table 3. Effect of LOF from CSWW on land kangkong plant growth.

Treatment	Crop Height (cm)			Leaf Number		
	7 days	14 days	21 days	7 days	14 days	21 days
Added Fertilizer	8.5	13.1	18	12	19	24
Without Fertilizer	5.8	9.7	11	8	13	16

Table 3 shows the effect of the LOF application on land kangkong plants. It can be concluded that the addition of the LOF had a positive influence on the growth of the land kangkong samples. This positive effect is due to the additional nutrients contained within the LOF sample. This also confirms that the LOF sample contains essential nutrients such as N, P, and K. The N, P, and K elements are highly required by plants for physiological and metabolic processes, thus increasing the height of the sample plants [14], [15]. Consequently, the number of leaves formed is correlated with the plant height; the taller the plant, the greater the number of leaves formed [19].

Table 4. Data volume of LOF

Sampel Number	Initial volume (L)	Final volume (L)
1	2.25	2.065
2	2.25	2.045
3	2.25	2.040
4	2.30	2.190

Table 5. Yield value of LOF

Sampel Number	Yield (%)
1	8.222
2	9.111
3	9.333
4	4.782

Using the data obtained from Table 4 and the yield equation, the resulting yields are shown in Table 5. It is observed that the quantity of the LOF sample produced in this study decreased. The Optimal Condition showed the highest yield of 9.333% in Sample 3, which indicates that the fermentation conditions, specifically the CSWW to EM4 ratio, were optimal. In contrast, Sample 4 indicated a suboptimal yield value of 4.782%, which could be caused by several factors, including an incomplete fermentation process and an unfavorable ratio that did not mutually support each other [14].

4. Conclusion

There are four stages of fermentation that occur in the process of producing liquid organic fertilizer (LOF) from chicken slaughterhouse waste CSWW: Hydrolysis, Acidogenesis, Acetogenesis, and Methanogenesis. The plant samples treated with an addition $30\ ml$ of the LOF showed a positive effect on the growth of the land kangkong samples. Based on the growth observation data obtained in this study, the plant samples treated with the LOF sample performed better than the blank (control) sample. Specifically, the optimal plant height reached $24\ cm$ with a leaf count of 24 leaves by the twenty-first day of planting. Therefore, it can be assumed that the LOF sample produced in this study already contains the expected nutrient content.

Acknowledgment

The author is thankful to Universitas Pertamina for their support.

References

[1]. M. A. Yaakob, R. M. S. Radin Mohamed, A. Algheethi, and A. H. mohd kassim, “Characteristics of Chicken Slaughterhouse Wastewater,” Chem. Eng. Trans., vol. 63, Jul. 2018, doi: 10.3303/CET1863107.

[2]. Sumiati, R. Fadilah, A. Darmawan, and R. Nadia, “— Invited Review — Challenges and constraints to the sustainability of poultry farming in Indonesia,” Anim Biosci, vol. 38, no. 4, pp. 802–817, Apr. 2025, doi: 10.5713/ab.24.0678.

[3]. S. R. Shanmugam, R. Schorer, W. Arthur, E. Drabold, M. Rudar, and B. Higgins, “Upcycling nutrients from poultry slaughterhouse wastewater through cultivation of the nutritional yeast, Yarrowia lipolytica,” J. Environ. Chem. Eng., vol. 13, no. 1, p. 115245, 2025, doi: https://doi.org/10.1016/j.jece.2024.115245.

[4]. M. Boru, “Review of Organic Fertilizer and Its Role in Organic Farming,” Int. J. Energy Environ. Sci., vol. 10, pp. 31–37, Apr. 2025, doi: 10.11648/j.ijees.20251002.11.

[5]. Y. Sastro, B. Bakrie, and N. Sudolar, “The effect of fermentation method, microbes inoculation and carbon source proportion on the quality of organic fertilizer made from liquid wastes of chicken slaughterhouse,” J. Indones. Trop. Anim. Agric., vol. 38, Dec. 2013, doi: 10.14710/jitaa.38.4.257-263.

[6]. N. E. A. Nasution and C. R. Rizka, "Production of Liquid Compost with EM4 Bio Activator Volume Variation from Vegetable and Fruit Waste," META J. Sci. Technol. Educ., vol. 1, no. 1 SE-Articles, pp. 87–99, Jun. 2022, [Online]. Available: https://meta.amiin.or.id/index.php/meta/article/view/7

[7]. C. Anselmo, "Phytoremediation Potential of Kangkong (Ipomoea Reptans Poir) in Lead-Induced Hydroponic System," Int. J. Res. Sci. Innov., vol. Volume 11, pp. 909–921, Jul. 2024, doi: 10.51244/IJRSI.2024.1107072.

[8]. M. Aprilia, H. Effendi, and S. Hariyadi, "Water quality status based on Pollution Index and Water Quality Index of Ciliwung River, DKI Jakarta Province," IOP Conf. Ser. Earth Environ. Sci., vol. 1109, p. 12051, Nov. 2022, doi: 10.1088/1755-1315/1109/1/012051.

[9]. Sugito, K. Diah, Binawati, and M. Al Kholif, "The effect of BOD concentrate influet to remove pollutant load in waste water of a chicken slaughterhouse," ARPN J. Eng. Appl. Sci., vol. 11, pp. 3519–3524, Mar. 2016.

[10]. T. Karchiyappan, P. Ettiyagounder, P. S. Selvaraj, D. Veeraswamy, J. Ponnusamy, and K. Ramanujam, "A review on sustainable poultry slaughterhouse wastewater management based on electrochemical technology," Desalin. Water Treat., vol. 322, p. 101212, 2025, doi: https://doi.org/10.1016/j.dwt.2025.101212.

[11]. T. M. Patria and W. Suwito, "Sustainability Engineering on Chicken Slaughterhouse Waste as a Source of Liquid Biofertilizers Supporting Eco-Farming," IOP Conf. Ser. Earth Environ. Sci., vol. 1246, p. 12003, Sep. 2023, doi: 10.1088/1755-1315/1246/1/012003.

[12]. S. Chainetr, R. Khiewwijit, N. Maneetien, and S. Chaiwongsar, "Chicken Slaughterhouse Wastewater Characteristics, Current Treatment and Future Challenges: A review," RMUTL Eng. J., vol. 5, no. 1 SE-Review Article, pp. 41–55, Jun. 2020, doi: 10.14456/rmutlengj.2020.6.

[13]. H. ali, J. Faraj, and F. Hussien, "Effect of pH on biogas production during anaerobic digestion," J. Univ. Shanghai Sci. Technol., vol. 23, pp. 224–231, Aug. 2021, doi: 10.51201/JUSST/21/08369.

[14]. A. Ranasinghe, R. Jayasekera, S. Kannangara, and R. M. C. S. Ratnayake, "Effect of Nutrient Enriched Organic Liquid Fertilizers on Growth of Albemonchus esculentus," pp. 96–106, Sep. 2019.

[15]. S. Kataki, S. Hazarika, and D. Baruah, "Assessment of by-products of bioenergy systems (anaerobic digestion and gasification) as potential crop nutrient (SCI IF 2020: 7.15, NAAS IF:13.15)," Waste Manag., vol. 59, Oct. 2016, doi: 10.1016/j.wasman.2016.10.018.

[16]. H. Setiadi *et al.*, "An Extreme Learning Machine Based Adaptive VISMA for Stability Enhancement of Renewable Rich Power Systems," Electronics, vol. 11, no. 2, 2022, doi: 10.3390/electronics11020247.

[17]. J. C. Maxwell, A Treatise on Electricity and Magnetism, 3rd ed., no. 2. Oxford: Clarendon Press, 1892.

[18]. R. Tschuncky, K. Szielasko, and I. Altpeter, "Hybrid methods for materials characterization," in *Materials Characterization Using Nondestructive Evaluation (NDE) Methods*, G. Hübschen, I. Altpeter, R. Tschuncky, and H.-G. Herrmann, Eds. Woodhead Publishing, 2016, pp. 263–291. doi: 10.1016/B978-0-08-100040-3.00009-2.

[19]. S. Hastuty, H. A. Prasetyo, N. N. Kirana, A. Nugroho, H. S. Oktaviano, and M. Awwaluddin, "The Effectivity of Oil Palm Inhibitor Processed by Aminolysis to Control Corrosion on Steel in Sodium Chloride Environment," in *Journal of Physics: Conference Series*, 2021, vol. 2080, no. 1, p. 12027.

[20]. A. Dahliyanti, C. A. Curie, and W. I. Dyah, "Production and Characterization of Silica as a Multifunctional Material from Corn Waste [Produksi dan Karakterisasi Silika sebagai Material Multifungsi dari Limbah Jagung]," J. Teknol., vol. 2, no. 1, p. 1, 2019, [Online]. Available: https://aperti.e-journal.id/teknologia/article/view/22

Biographies of Authors

Eduardus Budi Nursanto graduated his doctoral degree majoring in clean energy and chemical engineering from Korea University of Science and Technology, South Korea. Currently, he is active faculty member at Chemical Engineering Department, Universitas Pertamina, Indonesia.

Akbar Angga Handjaya graduated his bachelor's degree from Chemical Engineering Department, Universitas Pertamina, Indonesia.

Nur Layli Amanah graduated her bachelor's degree from Chemical Engineering Department, Universitas Pertamina, Indonesia. Currently, she is a Ph.D student at The Petroleun and Petrochemical Technology, Chulalongkorn University, Thailand

Muhammad Fairuzt Fathin Faundra graduated his bachelor's degree from Chemical Engineering Department, Universitas Pertamina, Indonesia.

Andika Yudistira graduated his bachelor's degree from Chemical Engineering Department, Universitas Pertamina, Indonesia.

Alifiana Permata Sari graduated her master degree majoring in Advanced Chemical Engineering, University of Birmingham, Birmingham, Inggris. Currently, she is active faculty member at Chemical Engineering Department, Universitas Pertamina, Indonesia.

Catia Angli Curie graduated her doctoral degree majoring in chemical engineering from Universitas Indonesia, Indonesia. Currently, she is active faculty member at Chemical Engineering Department, Universitas Pertamina, Indonesia.

Vol. 04, No. 2, December 2025, pp. 61-75
p-ISSN: 2963-8577
e-ISSN: 2964-3511
DOI: 10.57102/jescee.v4i2.119

JESCEE
Journal of Emerging Supply Chain, Clean Energy, and Process Engineering

AN EMPIRICAL STUDY OF REVERSE LOGISTICS IN NATURAL COSMETIC PRODUCTS ON CONSUMER SATISFACTION

Resista Vikaliana[1*], Fatih Wahid Satrio[2]
[1,2]Logistics Engineering Department, Universitas Pertamina, Indonesia

Abstract
This study aims to analyze the influence of reverse logistics on consumer satisfaction with cosmetic products at PT Nectars Natura Karya. Reverse logistics, which involves the management of product returns for recycling, repairs, or waste handling, is a crucial element in enhancing sustainability while meeting the expectations of modern consumers. The study employs a simple linear regression analysis method to understand the relationship between reverse logistics as the independent variable and consumer satisfaction as the dependent variable. Data were collected through questionnaires distributed to consumers of PT Nectars Natura Karya's best-selling product, Tamanu Daycream. Based on the simple linear regression test results, the simple linear regression equation obtained is Y = 0.666 + 0.464X, indicating that if the reverse logistics variable is zero or constant, consumer satisfaction increases by 0.666 units. The coefficient value for the reverse logistics variable is 0.464, meaning that a one-unit increase in reverse logistics will increase consumer satisfaction by 0.464 units or 46.4%. Furthermore, the R value (correlation coefficient) is 0.876, signifying a very strong relationship between reverse logistics and consumer satisfaction. The R2 value (coefficient of determination) is 0.767, indicating that 76.7% of the variation in consumer satisfaction can be explained by reverse logistics in the model, while the remaining 23.3% is explained by other factors outside the model. With an R2 of 0.767, the model is categorized as substantial, implying a very strong relationship between reverse logistics and consumer satisfaction. In the hypothesis testing, the t_calculated value of 17.778 far exceeds the t_table value of 1.664. Thus, H0 is rejected, and Ha is accepted, confirming that the relationship between reverse logistics and consumer satisfaction is highly significant.

Keywords:
reverse logistics; consumer's; satisfaction; natural cosmetics; linear regression

Article History:
Received: September 25th, 2025
Revised: October 28th, 2025
Accepted: October 30th, 2025
Published: October 31st, 2025

Corresponding Author:
Resista Vikaliana
Logistics Engineering Department
Universitas Pertamian
Email:
resista.vikaliana@universitaspertamina.ac.id

1. Introduction

Companies that sell skincare products have the potential to damage the environment because mass production is labor-intensive, uses raw materials that cannot be recycled, and generates hazardous waste. To reduce their impact on the environment, businesses should incorporate green marketing into their sustainable strategies [1]. The production, delivery to consumers, and disposal of goods and services through green marketing can reduce environmental damage such as the effects of global warming, non-degradable waste, and harmful pollutants [2].

There is a change in consumer shopping behavior driven by concern for environmental issues. 74% of consumers have or are willing to adjust their shopping preferences based on their impact on the environment. This change is most prevalent among Gen Z and Millennial shoppers, where more than half of consumers aged 45 and

below have adjusted their shopping habits. In contrast, only 45% of consumers aged 45 and above have done the same [3].

Reverse logistics, which involves returning products or packaging from consumers for recycling or reuse, is an integral part of green supply chains. Such programs not only reduce waste, but also create closer relationships between companies and consumers. The importance of understanding the impact of reverse logistics on consumer satisfaction has been supported by research such as that published in the Journal of Cleaner Production (2023), the study showed that 55% of consumers felt more satisfied when companies offered recycling or packaging return programs, and 48% of them felt more satisfied when they were given the option. Currently PT Nectars Natura Karya anticipates a packaging return program for recycling.

Based on the product sales, Tamanu Daycream is the highest selling product with 269 products sold. Followed by Facial Foam Citrus with 211 products sold and Seabuckthorn Daycream with 196 products sold which also show significant sales figures. Tamanu Daycream's sales figures are the highest, indicating the high consumer demand for this product. Therefore, Tamanu Daycream is the right choice as the object of research to find out how the influence of reverse logistics aspects on consumer satisfaction at PT Nectars Natura Karya.

Tamanu Daycream products are designed to soften the surface structure of the skin, treat sunburn symptoms, treat acne and eczema, and prevent premature wrinkles. This product is packaged in a 10ml travel size and is sold at Rp 88,200 in the marketplace. This product also managed to make its consumers satisfied, this is stated based on the ratings and reviews on the Tamanu Daycream sales product page, the rating obtained is 4.9 out of 5, reviews or reviews given by Tamanu Daycream consumers also show that they are satisfied with the quality of Tamanu Daycream products.

Making Tamanu Daycream as the focus of observation in this study is expected to provide a more comprehensive understanding of how reverse logistics aspects can affect consumer satisfaction on the products that consumers are most interested in. The selection of products with the highest sales also allows the company to identify and optimize the potential for improving reverse logistics aspects on products that make the largest contribution to the company's revenue.

People today are increasingly selective in choosing brands when buying goods or services. Indonesia, as a fast-growing country, shows an increasing demand for natural and eco-friendly skincare [2]. Environmentally friendly aspects influence consumer choice in choosing skincare. Consumers' environmental awareness and behavior are contributing to purchasing patterns that support sustainability. Consumers are increasingly concerned about the adverse effects of environmentally unfriendly skincare products [4]. around 73% of global consumers stated that they are willing to change their consumption patterns to reduce their negative impact on the environment. This awareness is a major factor driving changes in business strategies across industries, including cosmetics [5].

Companies in various sectors, including the cosmetics industry, are starting to show their commitment to sustainability by creating environmentally friendly products. This commitment is important because a McKinsey report shows that products with sustainability labels tend to have higher growth rates than conventional products. PT Nectars Natura Karya is committed to producing natural and sustainable skincare products [6], this phenomenon is in line with the growing trend of green consumerism, where more and more consumers are concerned about environmental issues and tend to choose products that are more friendly to nature [7]. The company's focus on natural ingredients and sustainability reflects consumer preferences for attributes such as safety, product performance, and natural ingredients in eco-friendly skincare products [2]. Similar to PT Yagi Natural Indonesia, PT Nectars Natura Karya implements environmentally friendly marketing strategies, including the use of organic ingredients, and promotional activities that emphasize an eco-friendly approach [8].

Reverse logistics is one of the key practices in sustainability efforts. Reverse logistics includes all activities related to managing the reverse flow of products, including recycling and waste management. This implementation not only supports the environment but also strengthens the company's relationship with consumers through social responsibility [9]. The following is the reverse logistics process at PT Nectars Natura Karya.

Fig.1. Reverse Logistics Process

Based on Figure 1, the reverse logistics process carried out at PT Nectars Natura Karya starts from consumers returning their empty packaging, the empty packaging is returned directly to the PT Nectars Natura Karya factory. After the empty packaging is received by PT Nectars Natura Karya, the company team directs the empty packaging that has been returned by consumers to a recycle disposal site or such as a collector who recycles.

According to data provided by the Plastic Pollution Coalition, the self-care and beauty industry worldwide produces more than 120 billion pieces of packaging every year. It is unfortunate that most of these bottles are not recyclable, leading to more waste in landfills. The composition of waste at the national level by type of waste in 2023, plastic is the second largest contributor after food waste at 18.77% based on the Directorate of Waste Management.

The Body Shop runs reverse logistics activities as a form of their commitment to environmental sustainability. One of the programs implemented is the return of empty packaging, otherwise known as Bring Back Our Bottle (BBOB). This program aims to encourage consumers to be more environmentally responsible by contributing to reducing the amount of waste that ends up in landfills. Based on journals and sources, packaging that can be returned is all products with plastic or glass containers, consumers who return empty packaging will get awards such as points as feedback from The Body Shop [10]. This is similar to what PT Nectars Natura Karya does, PT Nectars Natura Karya has an empty packaging return program and also provides a reward in the form of a shopping voucher worth IDR 120 thousand for every 40 empty packaging returned.

The most appropriate analysis method to be used in this research is Simple Linear Regression, this is because the research only involves one independent variable (reverse logistics) which is assumed to have a direct effect on one dependent variable (consumer satisfaction). Simple linear regression is used to model the linear relationship between two variables, so as to provide relevant results and clear interpretation of the effect of the independent variable on the dependent variable [11].

The Simple Linear Regression analysis method is considered appropriate for this research because it is simple and focuses on the direct effect of one variable on another without involving the relationship of mediating or moderating variables, as is usually analyzed using more complex methods such as SEM or Path Analysis. By using simple linear regression, this research can identify and explain the effect of reverse logistics on consumer satisfaction efficiently and purposefully.

Based on the background description, there are objectives to be achieved in this study, namely analyzing the effect of reverse logistics on consumer satisfaction of PT Nectars Natura Karya

2. Literature Review

A. Green Skincare Product

Green products are sustainable products that are designed and marketed by considering their impact on the environment. These products utilize environmentally friendly raw materials, minimize energy use during the production process, and can be recycled after use [12]. Green skincare products are skincare products that are made using natural ingredients without the addition of chemicals, artificial colors, or other synthetic ingredients. This type of cosmetics is often referred to as organic cosmetics. All ingredients used in these products are obtained from natural resources, such as plants or other natural materials [13].

B. Consumer Satisfaction

According to Tjiptono dan Chandra, consumer satisfaction refers to the extent to which the product or service provided is able to meet consumer expectations. [14]. In addition, Daryanto and Setyobudi reveal the emotional response that arises after consumers use the product, when their needs and expectations have been achieved [15].

The main goal of a business is to provide satisfaction for consumers. Consumer satisfaction brings a number of benefits, such as strengthening the relationship between the company and consumers, strengthening the basis for repeat purchases, and building consumer loyalty. In addition, consumer satisfaction can also generate word of mouth which provides great benefits for the company [16].

C. Reverse Logistics

Reverse logistics is a process that includes efficient and effective planning, implementation, and control in managing the flow of goods and information from the point of consumption back to the point of origin [9]. Reverse logistics primarily aims to recover the value of returned goods or manage them in a more environmentally friendly way. Effective and efficient management in reverse logistics has the ability to generate economic value as well as improve the company's image in the eyes of consumers and in product distribution. With the right efficiency, reverse logistics can create economic value through various activities, such as the reuse of salvageable goods, material recycling, repair, or remanufacturing for resale [17].

D. Data Analysis Method

Data analysis is a step taken after all data has been collected from respondents or other sources. This step involves grouping data based on variables and categories of respondents, tabulating data based on variables from all respondents, and presenting accurate and relevant data. Sugiyono stated that each variable in the study needs to be analyzed to answer the formulation of the problem that has been prepared, while the calculation process is carried out to test the hypothesis proposed [18].

Simple regression analysis is a statistical method that aims to describe the linear relationship between one independent variable (x) and one dependent variable (y). This method is applied to analyze the extent to which the independent variable affects the dependent variable, as well as predict the value of y based on the value of x [19]. According to Sugiyono, the simple regression equation can be formulated as follows [20]:

$$Y = a + bX$$

Description:
Y : consumer satisfaction
a : simple regression constant
b : regression coefficient
A. X : reverse logistics

3. Research Methodology

The method applied in this research is Simple Linear Regression, where quantitative data obtained from questionnaires will be used to test hypotheses between research variables, the data will be processed using IBM SPSS 26 software. The following are the steps taken by researchers to facilitate the research process and problem solving.

A. Problem Identification

The initial stages of the research began with identifying problems by looking at real conditions based on phenomena that occurred at PT Nectars Natura Karya. The problem is related to reverse logistics implemented by PT Nectars Natura Karya. Generally, research to assess or measure consumer satisfaction is measured in terms of product quality, product durability, and so on, but in this research consumer satisfaction is measured based on reverse logistics, this is because based on information from the Director of Operations of PT Nectars Natura Karya that the company needs reverse logistics to strengthen their branding as a company that is friendly and cares about the environment. Although there has been no research measuring consumer satisfaction with the quality of their products, the researcher considers consumers to be satisfied with the quality of products from PT Nectars Natura Karya, this is reinforced by the ratings and reviews of PT Nectars Natura Karya products in the marketplace, besides that based on interviews, the lack of complaints from consumers about their products makes PT Nectars Natura Karya consider measuring consumer satisfaction with the quality of their products not an urgency. Thus, the researcher aims to examine the effect of reverse logistics on consumer satisfaction.

B. Literature Study

Literature study is conducted to collect references that can support this research. The literature obtained includes theoretical foundations and methods relevant to the research, where this information comes from journals, books, websites, and other reliable sources. Some of the references used in this research are reverse logistics and consumer satisfaction.

C. Variable Identification

Variable identification is carried out to determine the variables that act as influencing factors and influenced variables. Variable identification is determined based on the results of the literature study. The following are the variables in this study.

TABLE 1
VARIABLE IDENTIFICATION

No	Variable	Definition	Reference
1	Reverese Logistics	Reverse Logistics refers to the process of flowing products or components back after use, for the purpose of repair, recycling, or reprocessing. In green supply chain management,	[21]

No	Variable	Definition	Reference
		reverse logistics is used by companies as a tool to manage waste recycling, thus preventing environmental pollution. Reverse logistics provides significant benefits, especially in increasing the company's production output.	
2	Consumer Satisfaction	Consumer satisfaction refers to the feelings that arise after a person compares the performance of the product or service received with the expectations he has. High satisfaction can reduce the negative impact of unavoidable errors due to variations in the service delivery process. In another sense, consumer satisfaction is defined as a response to the fulfillment of consumer needs, where consumers assess whether the product or service has succeeded in meeting their needs and expectations. If the product or service matches consumer expectations, it can be considered that consumers are satisfied.	[22]

There are several dimensions and indicators on the reverse logistics variable and the consumer satisfaction variable adopted from several references for use in this study, in adopting several dimensions and indicators for each variable, adjustments are made from each dimension and indicator to the activities carried out at PT Nectars Natura Karya. The following are the dimensions and indicators used in this study.

TABLE 2
DIMENSIONS AND INDICATORS OF VARIABLES IDENTIFICATION

No	Variable	Dimension	Indicator	Reference
1	Reverse Logistics	Return Initiation	Product return request	[23]
		Select Disposition	Recycling action	
		Credit Consumer	Rewards for consumers	
2	Consumer Satisfaction	Expectations	Consumer expectations	[24]
		Satisfaction Toward Quality	Service feedback	[25]

D. Model Making

The following is a structural model based on previous research as a reference which is adjusted to the variables used in this study.

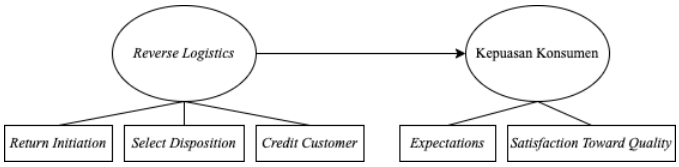

Fig. **2** Structural Model

Based on Figure 2, this research involves two types of variables, namely independent variables and dependent variables. Independent variables are variables that exert influence on other variables, while dependent variables are variables that receive influence from other variables. In this study, the independent variable is reverse logistics with the dimensions of Return Initiation, Select Disposition, and Credit Consumer, while the dependent variable is consumer satisfaction with the dimensions of Expectations and Satisfaction Toward Quality.

E. Hypothesis Generating

Effective and efficient reverse logistics management can create economic value, strengthen the company's positive image, and improve performance in the distribution chain [17]. Responsiveness in reverse logistics describes a company's ability to manage the returns process quickly and according to consumer needs, which includes efficient returns management, such as providing easy and fast authorization options. This responsiveness not only contributes to improving consumer satisfaction, but also supports the company's competitiveness. In order for the returns process to be effective, good collaboration between the marketing and logistics functions is required to ensure smooth credit management and settlement for consumers [26]. Based on this, the following hypothesis is proposed.

H0: Reverse Logistics has no effect on consumer satisfaction

Ha: Reverse Logistics affects consumer satisfaction

F. Determination of Sample Size

The population in this study is 120 people, of which 120 people are considered end-customers because there is no reseller/reselling system at PT Nectars Natura Karya. From a population of 120 people, the Slovin formula was used to determine the number of samples to be used in the study. The Slovin formula is used because the population in this study has been identified [27].

$$n = N / 1 + N(e)^2$$

Description:

n : number of samples

N : total population

e : error tolerance limit (0.05)

Based on the Slovin formula, researchers obtained the minimum number of samples needed in this study, namely:

$$n = N / 1 + N(e)^2$$
$$n = 120 / 1 + 120(0.05)^2$$
$$n = 120 / 1 + 0.3$$
$$n = 120 / 1.3$$
$$n = 92.307692$$

Based on the results of the application of the Slovin formula, with a total population of consumers who buy Tamanu Daycream products of 120 people and the error tolerance limit used is 0.05, the minimum number of samples needed in this study is 92 people. The sampling technique used in this study is simple random sampling which is one of the sampling techniques from probability sampling, simple random sampling is used because there is no population segmentation in this study [28].

G. Questionnaire Design and Distribution

Data collection is done through distributing questionnaires to consumers who have purchased Tamanu Daycream products. The questionnaire is structured in the form of a statement with a Likert scale, where number 1 means “strongly disagree” and number 5 means “strongly agree” [29]. The selection of respondents was carried out using the simple random sampling method, because there were no differences in strata and other provisions used in the respondents of this study. The statements are made based on dimensions and indicators to be used in the questionnaire as a tool that describes how reverse logistics affects consumer satisfaction.

TABLE 3
STATEMENT FOR EACH DIMENSION

Dimensions	Statement
Return Initiation	I find it easy to find information about the procedure for submitting empty packaging returns
	I find the process of requesting empty packaging returns easy to do
	The team from PT Nectars Natura Karya responded quickly to my empty packaging return request
Select Disposition	I am satisfied with the recycling program for returned empty packaging
	I am confident that the empty packaging I return is directed to a disposal facility that can recycle it
	I support the recycling actions taken by PT Nectars Natura Karya
Credit Consumer	I feel that the shopping vouchers given are very profitable for me
	I am more motivated to return empty packaging because of the shopping voucher provided by PT Nectars Natura Karya
Expectations	PT Nectars Natura Karya's empty packaging return program has met my expectations of environmental stewardship
	I feel that PT Nectars Natura Karya's empty packaging return program is in line with its branding as a company that supports environmental sustainability
Satisfaction Toward Quality	I am satisfied with the responsiveness of PT Nectars Natura Karya's team in returning empty packaging
	I am satisfied with the responsiveness of the PT Nectars Natura Karya team in the process of claiming shopping vouchers after returning empty packaging

H. Questionnaire Test

1. Validity Test

The validity test serves to assess the accuracy of the measuring instrument and can describe the concept or phenomenon being measured. The validity test is applied to assess whether a questionnaire is valid or not. A questionnaire is considered valid if the questions or statements contained in it can reveal what you want to measure. If the significance value is <5% (level of significance), it means that the statements are valid [20].

2. Reliability Test

The reliability test serves as a tool to assess the questionnaire which functions as an indicator of the variable. The questionnaire is considered reliable if a person's response to a statement remains consistent or stable over time. In this study, reliability testing was carried out using the Cronbach's Alpha formula [20].

I. Classical Assumption Test

1. Normality Test

The normality test aims to check whether the data obtained is normally distributed in each variable. Data that is considered good is data that has a normal distribution in its residual values, so that data analysis can be carried out appropriately and validly. This residual test is very important to do before proceeding to simple linear regression analysis [30]. Some normality test methods that can be applied include the histogram test, normal P-Plot test, Chi Square test, Skewness and Kurtosis or Kolmogorov Smirnov test. [30].

2. Linearity Test

The purpose of the linearity test is to determine whether the model specification applied is correct. Good data should show a linear relationship between the independent variable and the dependent variable. [31].

The linearity test is applied to evaluate whether there is a significant linear relationship between two variables. The regression model is considered good if the linear relationship between variables x (reverse logistics) and y (consumer satisfaction) is significant.

J. Simple Linear Regression Test

Simple linear regression is used to obtain a mathematical relationship expressed in the form of an equation between one independent variable (reverse logistics) and the dependent variable (consumer satisfaction), which involves only one independent variable.

K. Correlation Coefficient (R) dan Determination Coefficient (R^2) Test

Correlation coefficient test (R) is a test to determine how strong the relationship between variables is, while the determination coefficient test (R^2) is a test to determine how much the percentage of the independent variable (reverse logistics) affects the dependent variable (consumer satisfaction).

L. Hypothesis Test

In simple linear regression, the hypothesis test applied is the T test. The T test is a test for partial regression coefficients individually which aims to determine whether the independent variable (x) has an influence on the dependent variable (y) individually [32].

The T test is used to test whether an independent variable actually affects the dependent variable. In this study, researchers want to know whether if separately / partially, the independent variable (reverse logistics) still has a significant effect on the dependent variable (consumer satisfaction).

M. Analysis of Results

Based on the results of the tests that have been carried out, namely the questionnaire test which consists of validity and reliability tests, the classical assumption test which consists of normality test and linearity test, simple linear regression test, correlation coefficient test and determination coefficient, and hypothesis testing, namely the T test, the next step is to analyze how reverse logistics affects consumer satisfaction.

N. Conclusions and Suggestions

The last stage of this research is drawing conclusions and providing suggestions. Drawing conclusions aims to answer research objectives based on data processing and analysis of results. Recommendations in the form of suggestions will also be given to PT Nectars Natura Karya as a reference in an effort to improve the implementation of reverse logistics.

4. Result and Discussion

A. Validity and Reliability Test

1. Pearson Correlation Validity Test

The Pearson Correlation method is used to test the validity of a questionnaire by correlating the score of each question with the total score obtained from respondents. According to Ghozali, this method compares the r_calculated value with the r_table value to determine whether the questionnaire is valid. The r_table value used is 0.1968 (df = 96; α = 5%), as the sample consists of 98 respondents. A questionnaire is considered valid if the r_calculated value for each variable indicator is greater than the r_table value [33]. The following are the results of the validity test using Pearson Correlation.

TABLE 4
PEARSON CORRELATION VALIDITY TEST RESULTS

Variable	Indicator	r_calculated value	r_table value	Description
Reverse Logistics (x)	RI1	0.720	0.1986	Valid
	RI2	0.864		Valid
	RI3	0.869		Valid
	SD1	0.838		Valid
	SD2	0.819		Valid
	SD3	0.681		Valid
	CC1	0.823		Valid
	CC2	0.862		Valid
Consumer Satisfaction (y)	E1	0.888		Valid
	E2	0.768		Valid
	STQ1	0.908		Valid
	STQ2	0.894		Valid

All indicators in the Reverse Logistics (x) and Consumer Satisfaction (y) variables are declared valid because they meet the criteria for the value r_calculated > r_table. Therefore, the questionnaire is worth using for further analysis.

2. Cronbach's Alpha Reliability Test

After the validity test, the next step is to carry out a reliability test to assess the consistency and accuracy of the questionnaire [34]. Reliability testing is important because it will provide an idea of the extent to which the questionnaire that has been built has good reliability, where a Cronbach's Alpha value greater than 0.6 indicates the questionnaire is reliable, while a value below 0.6 indicates the questionnaire is unreliable [35]. Testing was carried out using 98 respondents with 2 variables and 12 statement indicators, 8 statement indicators for the reverse logistics variable and 4 statement indicators for the consumer satisfaction variable. Following are the results of the reliability test.

TABLE 5
CRONBACH'S ALPHA VARIABLE X RELIABILITY TEST

Cronbach's Alpha	N of Items
0.924	8

TABLE 6
CRONBACH'S ALPHA VARIABLE Y RELIABILITY TEST

Cronbach's Alpha	N of Items
0.888	4

Based on Tables 5 and 6, both variables (reverse logistics and consumer satisfaction) have Cronbach's Alpha values which show very good reliability, namely 0.924 > 0.6 for the reverse logistics variable and 0.888 > 0.6 for the consumer satisfaction variable. Therefore, the questionnaire is worth using for further analysis.

B. Classical Assumption Test

1. Normality Test

The normality test is carried out to determine whether the residual or confounding variables in the regression model are normally distributed. One way to detect normal distribution in a model is through a P-Plot graph. The ideal regression model will show a normal data distribution, characterized by the distribution of data following the diagonal line on the normal distribution graph. Residuals are considered normally distributed if the points on the P-Plot graph are parallel to the diagonal line. Here is a P-Plot graph that illustrates it [36].

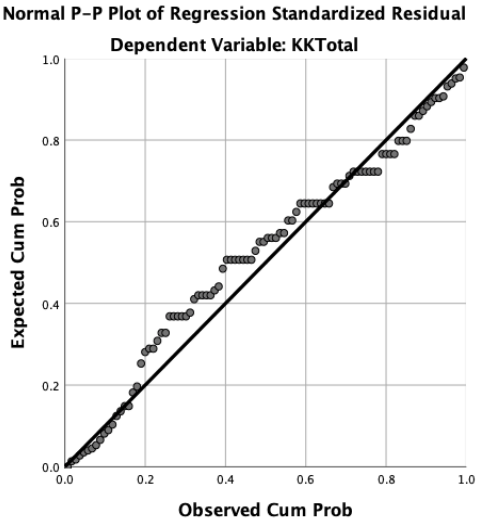

Fig. 1 P-Plot Graph

The P-P Plot graph in Fig. 10, most of the residual points appear to be around the diagonal line, both at the beginning, middle and end of the graph. With this, the residual distribution shows a pattern that is close to a diagonal line, therefore the residuals from the regression model meet the normality assumption. Because the normality test shows good results, the regression model used can be considered valid in terms of the residual normality assumption.

2. Linearity Test

The linearity test is carried out to determine whether there is a significant and linear relationship between the variables. This linearity test is carried out through the linearity test contained in the ANOVA table. The criteria for decision making in the linearity test is if linearity $\geqslant 0.05$, then there is no linear relationship. If linearity < 0.05, then there is a linear relationship.

TABLE 7
ANOVA TABLE LINEARITY TEST RESULTS

	Sum of Squares	**df**	***Mean Square***	**F**	**Sig**
Linearity	543.971	1	543.971	300.832	0.000
Deviation from Linearity	24.181	18	1.343	0.743	0.757

Based on Table 7, it can be seen that the significance value for Linearity is 0.000 < 0.05, with this the relationship between the two variables is significantly linear. The significance value for Deviation from Linearity is 0.757 > 0.05, this indicates that there is no significant deviation from the linear relationship. Based on the results of the linearity test, the relationship between the reverse logistics variable and consumer satisfaction is significantly linear, apart from that there are no significant deviations, this shows that the relationship between the two is indeed consistent in a linear pattern.

C. Simple Linear Regression Test

The simple linear regression test aims to analyze the effect of reverse logistics on cosmetic products on consumer satisfaction at PT Nectars Natura Karya. Simple linear regression analysis was carried out with the help of IBM SPSS 26 software, meanwhile the confidence level used in simple linear regression calculations was 95% or with a significance level of 0.05 ($\alpha = 0.05$).

TABLE 8
SIMPLE LINEAR REGRESSION CALCULATION RESULTS

Variabel X	**B**
Constant	0.666
RL Total	0.464

Based on Table 8, the simple linear regression equation can be seen as follows:

$$Y = a + bX$$
$$Y = 0.666 + 0.464X$$

Based on the simple linear regression equation, it can be stated that the regression coefficient is constant at 0.666, indicating that if the reverse logistics variable is zero or fixed, it will increase consumer satisfaction by 0.666 units. The coefficient value of the reverse logistics variable is 0.464, indicating that if the reverse logistics variable increases by one unit, it will increase consumer satisfaction by 0.464 units or 46.4%.

D. Correlation Coefficient (R) dan Determination Coefficient (R^2) Test

Correlation coefficient test (R) used to find out how strong the relationship between variables is, while the determination coefficient test (R^2) is a structural model analysis used to measure how well independent variables influence the dependent variable in a model [37]. R^2 is an indicator that shows how accurate predictions are for the structure that has been built. The R^2 value ranges from 0 to 1, where values close to 1 indicate a high level of prediction accuracy. R and R^2 values can be categorized into three strength levels: $\geqslant$ 0.25 (weak), $\geqslant$ 0.50 (moderate), and $\geqslant$ 0.75 (substantial) [35]. The following are the results for the correlation coefficient and determination coefficient test.

TABLE 9
RESULTS OF CORRELATION COEFFICIENT (R) AND DETERMINATION COEFFICIENT (R^2)

	R	**R-Square**
RL Total * KK Total	0.876	0.767

Based on Table 9, the R value/correlation coefficient is 0.876, meaning that the relationship between the reverse logistics variable and the consumer satisfaction variable is very strong. Furthermore, it is known that the R^2 value is 0.767, which means that 76.7% of the variation in the consumer satisfaction variable can be explained by the reverse logistics variable in the model, the remaining 23.3% is explained by other factors outside the model. With R^2 of 0.767, it can be concluded that this model is in the substantial category, which means the relationship between the reverse logistics variable and consumer satisfaction is very strong.

E. Hypothesis Test

The t-test is used to measure the significance of the relationship between two variables. Before determining whether such a relationship exists, the first step is to identify the t_table value based on the degrees of freedom (df) = 98. This is done by considering the degrees of freedom and the predetermined two-tailed significance level, which corresponds to a 95% confidence level and a 5% statistical error rate ($\alpha = 0.05$). The t_table value for df = 98 is 1.664. If the t_calculated is greater than the t_table value (t_calculated > t_table), it indicates a significant relationship between the two variables. Below are the t_calculated values.

TABLE 10
T_CALCULATED VALUE RESULTS

	t
RL Total	17.778

Based on Table 10, the t_calculated is 17,778 which is much greater than the t_table, namely 1,664. Therefore, **H0** is rejected and **Ha** is accepted, so that the relationship between the reverse logistics variable and the consumer satisfaction variable in this research is very significant.

F. Discussion of Research Results

After completing the validity and reliability tests, the classical assumption test, the simple linear regression test, the correlation coefficient and determination coefficient tests, as well as the hypothesis test (t-test), a proper analysis of the existing problem needs to be conducted. The findings or calculations are explained according to real-world conditions and supported by relevant previous studies to provide a clear and well-rounded explanation.

The study on the impact of reverse logistics on consumer satisfaction at PT Nectars Natura Karya consists of a total of five dimensions across two variables—three dimensions for the reverse logistics variable (X) and two dimensions for the consumer satisfaction variable (Y). The dimensions for variable X include Return Initiation (with an indicator of submitting empty packaging returns), Select Disposition (with an indicator of recycling actions), and Credit Consumer (with an indicator of rewards for consumers). Meanwhile, the dimensions for variable Y include Expectations (with a service feedback indicator) and Satisfaction Toward Quality (with a consumer expectations indicator).

Referring to the results of the tests conducted using IBM SPSS 26, all indicators for both reverse logistics and consumer satisfaction variables are deemed valid, as confirmed by the r_calculated values being significantly greater than the r_table values. Additionally, the reliability of each variable also shows excellent results, indicating that the questionnaire is consistent and accurate. This is further supported by the Cronbach's Alpha value being greater than 0.6, demonstrating that the questionnaire is reliable.

The residuals of the regression model follow a normal distribution, meaning they fulfill the assumption of normality. Since the normality test produced favorable results, the regression model used can be considered valid regarding the assumption of residual normality. This is reinforced by the fact that most residual points on the P-Plot graph appear close to the diagonal line, whether at the beginning, middle, or end of the graph, indicating a residual distribution pattern that closely follows the diagonal line.

The relationship between reverse logistics and consumer satisfaction is also significantly linear, with no significant deviations. This is supported by the significance value for Linearity, which indicates that the relationship between the two variables is statistically significant and linear. Additionally, the significance value for Deviation from Linearity suggests that there are no significant deviations from a linear relationship. These results confirm that the relationship between the two variables is indeed consistently linear.

The relationship between reverse logistics and consumer satisfaction in this study is highly significant. This is confirmed by the rejection of the null hypothesis (H0: Reverse logistics has no impact on consumer satisfaction) and the acceptance of the alternative hypothesis (Ha: Reverse logistics affects consumer satisfaction). This conclusion is based on the t_calculated value being significantly higher than the t_table value. Furthermore, this model falls into the substantial category, indicating a strong relationship between reverse logistics and consumer satisfaction. This statement is supported by the fact that 76.7% of the variation in consumer satisfaction can be explained by reverse logistics in the model, while the remaining 23.3% is influenced by other factors outside the model.

Based on the tests conducted, the findings align with previous research on The Impact of Reverse Logistics on Customer Satisfaction. That study stated that reverse logistics has a significant impact on customer satisfaction because it helps ensure a positive experience for customers when returning products. One of the most important effects of reverse logistics on customer satisfaction is the improvement of customer service. By offering return policies, companies can provide a better overall experience for consumers [38].

G. Managerial Implications

The analysis results indicate that reverse logistics has a significant impact on consumer satisfaction. Therefore, the company needs to integrate reverse logistics as part of its core business strategy to ensure a positive consumer experience. The first step to achieving this is simplifying the empty packaging return process, making it easily accessible to consumer. Implementing technology-based return services, such as a digital application that allows for real-time tracking of return statuses, can enhance consumer convenience. Additionally, the company must ensure that return locations are strategically distributed to be easily reachable, particularly in areas with high consumer volume.

Next, the company must ensure that the processing of shopping vouchers and responses to return requests or confirmations is swift and efficient. Excessive processing time can lead to a decline in consumer satisfaction. The company should regularly monitor its performance on the empty packaging return program using specific key performance indicators (KPIs), such as the average return processing time.

Beyond speed, the quality of consumer interaction during the reverse logistics process should also be a primary focus. The company should provide intensive training for consumer service staff responsible for handling returns to ensure they offer friendly, solution-oriented, and professional assistance. For instance, staff should be able to clearly explain the empty packaging return policy and provide satisfactory solutions in case of any issues. Effective communication will help reduce potential consumer frustration and strengthen brand loyalty.

Furthermore, the management of returned empty packaging should be optimized to create added value for the company. Eligible returned packaging can be inspected, refurbished, and reused for packaging purposes or repurposed into creative projects and other initiatives. This not only helps reduce product waste but also provides financial benefits for the company. On the other hand, damaged or unusable packaging should be responsibly managed, either through recycling or environmentally friendly disposal methods, reinforcing the company's image as a sustainability-conscious entity.

Beyond operational aspects, the company should actively communicate the advantages of its reverse logistics process to consumers. Marketing campaigns that highlight flexible and consumer-friendly packaging return policies can enhance brand appeal among both new and existing consumer. For example, the company could emphasize how its return process contributes to a risk-free shopping experience, thereby boosting consumer trust in the brand.

With this integrated approach, reverse logistics will not only serve as a support function in the supply chain but also as a strategic tool to enhance consumer satisfaction and strengthen long-term consumer relationships. A well-managed reverse logistics system will yield a significant competitive advantage for the company in an increasingly competitive market.

5. Conclusion

The core objective of this research was to analyze the effect of reverse logistics on consumer satisfaction at PT Nectars Natura Karya. The findings from the simple linear regression analysis strongly support a positive and significant relationship between the two variables. The regression model revealed that the reverse logistics variable explains a substantial portion of consumer satisfaction, demonstrating a very strong correlation ($R = 0.876$). Specifically, the coefficient of determination (R^2) indicated that 76.7% of the variation in consumer satisfaction can be attributed to the implementation of reverse logistics practices.The calculated t-value of 17.778 far exceeded the required critical value ($t_{table}=1.664$), confirming that the alternative hypothesis (Ha) is accepted: reverse logistics has a positive and significant influence. Quantitatively, the equation $Y = 0.666 + 0.464X$ suggests that a one-unit increase in effective reverse logistics translates to a 0.464 unit increase in consumer satisfaction. These results underscore a crucial trend: modern consumers are increasingly factoring sustainability and corporate responsibility into their purchasing decisions. Successful management of reverse logistics dimensions—such as efficient product return requests, proactive recycling actions, and consumer rewards—is paramount. By implementing these effective practices, the company can build a positive brand image and foster enhanced consumer loyalty.

Based on these findings, it is recommended that PT Nectars Natura Karya maintains and continuously develops its reverse logistics programs to drive both environmental sustainability and further increases in consumer satisfaction. Future researchers are encouraged to expand the scope and incorporate additional variables, such as brand image and consumer loyalty, to gain a broader understanding of consumer satisfaction drivers

.

References

[1] K. K. Papadas, G. J. Avlonitis, and M. Carrigan, “Green marketing orientation: Conceptualization, scale development and validation,” *J Bus Res*, vol. 80, pp. 236–246, Nov. 2017, doi: 10.1016/j.jbusres.2017.05.024.

[2] N. U. Ramadhani, B. M. Wibawa, and J. Gunawan, “Analisis Sikap Konsumen Perempuan terhadap Produk Green Skincare: Pendekatan Multiatribut Fishbein,” *JURNAL SAINS DAN SENI ITS*, vol. 8, no. 1, pp. 2337–3520, 2019.

[3] I. Gusmiarti, “Pengaruh Produk Ramah Lingkungan Terhadap Preferensi Belanja Konsumen.” Accessed: Dec. 08, 2024. [Online]. Available: https://data.goodstats.id/statistic/pengaruh-produk-ramah-lingkungan-terhadap-preferensi-belanja-konsumen-Q2Gn2#:~:text=Lebih%20lanjut%2C%20Sustainability%20in%20Ecommerce,pembelian%20mereka%20berdasarkan%20dampak%20lingkungan.

[4] B. B. Schlegelmilch, G. M. Bohlen, and A. Diamantopoulos, “The link between green purchasing decisions and measures of environmental consciousness,” *Eur J Mark*, vol. 30, no. 5, pp. 35–55, 1996.

[5] Nielsen, “Basis Data: Apa Arti Keberlanjutan Saat Ini.” Accessed: Dec. 08, 2024. [Online]. Available: https://www.nielsen.com/id/insights/2018/what-sustainability-means-today/

[6] Y. H. Lubis, D. Indrawan, and R. Hasbullah, “The Development Strategy of Natural Skincare (Case Study PT Nectars Natura Karya),” *International Journal of Research and Review*, vol. 10, no. 11, pp. 83–92, Nov. 2023, doi: 10.52403/ijrr.20231110.

[7] A. M. Kalifa, A. M. Wahyudi, Istijanto, and N. Amelia, “Pengaruh Nilai Konsumen dan Pengalaman Masa Lalu terhadap Niat Pembelian Konsumen untuk Membeli Produk Perawatan Tubuh Organik,” *Kajian Branding Indonesia*, vol. 2, no. 2, pp. 337–378, 2020.

[8] L. Moza, A. Suryana, and P. Trulline, “Implementasi Green Marketing pada PT Yagi Natural Indonesia dalam Memasarkan Produk Perawatan Tubuh Ramah Lingkungan,” *Telangke: Jurnal Telangke Ilmu Komunikasi*, vol. 6, no. 1, pp. 72–87, Feb. 2024, doi: 10.55542/jiksohum.v6i1.949.

[9] Dr. D. S. Rogers and Dr. R. S. Tibben-Lembke, *Going Backwards: Reverse Logistics Trends and Practices*. Reverse Logistics Executive Council, 1998.

[10] S. M. Rahman and E. Nurtjahjadi, “Pengaruh Kampanye Hijau ‘Bring Back Our Bottles’ terhadap Citra Merek (Studi Kasus Pada Konsumen The Body Shop di Kota Bandung),” *J-MAS (Jurnal Manajemen dan Sains)*, vol. 9, no. 2, p. 1157, Oct. 2024, doi: 10.33087/jmas.v9i2.1855.

[11] M. A. Yusuf, Herman, H. Trisnawati, A. Abraham, and H. Rukmana, “Analisis Regresi Linier Sederhana dan Berganda Beserta Penerapannya,” *Journal on Education*, vol. 06, no. 02, 2024.

[12] L. Mubarokhah, D. Purnomo, and A. W. Utomo, “Sustainable Beauty : Pengaruh Green Product, Green Marketing, Dan Brand Terhadap Keputusan Pembelian Produk Kecantikan,” *INNOVATIVE: Journal Of Social Science Research*, vol. 4, no. 3, 2024.

[13] C. D. Sekartaji, C. T. S., and B. Andriyani, "Pengaruh Sosial, Bauran Promosi, Kondisi Ekonomi Dan Keuangan, Serta Green Skincare Lifestyle Terhadap Keputusan Pembelian Green Skincare Product," *JEKU (Jurnal Ekonomi dan Kewirausahaan)*, vol. 22, no. 4, Dec. 2022.
[14] Munarsih and B. P. Adi, "PENGARUH KUALITAS PELAYANAN DAN PROMOSI TERHADAP KEPUASAN PELANGGAN PADA PT. INDOMARCO PRISMATAMA CABANG KEMIRI RAYA KOTA TANGERANG SELATAN," *Indonesian Journal of Economy, Business, Entrepreneurship and Finance*, vol. 2, no. 1, 2022, doi: 10.53067/ijebef.
[15] N. W. W. Premayani and G. A. D. M. Yoga, "PENGARUH KEWAJARAN HARGA DAN KUALITAS PRODUK TERHADAP KEPUASAN KONSUMEN WINA RUMAH KEBAYA," *Widya Manajemen*, vol. 1, no. 2, pp. 113–157, 2019.
[16] H. A. Susanto and I. O. Narto, "PENGARUH KUALITAS PELAYANAN TERHADAP KEPUASAN KONSUMEN PADA PT ASTRA INTERNASIONAL TBK HONDA CABANG MAROS," *Jurnal Brand*, vol. 2, no. 1, 2020, [Online]. Available: https://ejournals.umma.ac.id/index.php/brand
[17] I. Zai, F. Winnerko, H. Suandri, D. Yosuky, and V. Linardo, "Jurnal Mirai Management Peran Reverse Logistic Dalam Meningkatkan Efisiensi Dan Efektivitas Perusahaan Dalam Rantai Pasokan Studi Kasus: Pt. Graha Auto Perkasa," *Jurnal Mirai Management*, vol. 8, no. 3, 2023.
[18] A. Rachman, E. Yochanan, A. I. Samanlangi, and H. Purnomo, *Metode penelitian kuantitatif, kualitatif, dan R&D*. Saba Jaya Publisher, 2024.
[19] Mulyono, "Analisis Regresi Sederhana," BBS - MANAGEMENT PROGRAM. Accessed: Dec. 10, 2024. [Online]. Available: https://bbs.binus.ac.id/management/2019/12/analisis-regresi-sederhana/
[20] M. I. A. Imran, "PENGARUH KEPUASAN PELANGGAN TERHADAP MINAT BELI ULANG MAKANAN DI RUMAH MAKAN AYAM BAKAR WONG SOLO ALAUDDIN KOTA MAKASSAR," *Jurnal Profitability Fakultas Ekonomi Dan Bisnis*, vol. 2, no. 1, 2018, [Online]. Available: https://journal.unismuh.ac.id/index.php/profitability
[21] V. Jayaraman, L. Yadong, and E. M. Findlay, "Creating competitive advantages through new value creation: A reverse logistics perspective," *Academy of Management Perspectives*, vol. 21, no. 2, pp. 56–73, 2007, doi: 10.5465/AMP.2007.25356512.
[22] R. L. Oliver, *Satisfaction: A behavioral perspective on the consumer: A behavioral perspective on the consumer*. Routledge, 2014.
[23] D. S. Rogers, D. M. Lambert, K. L. Croxton, and S. J. Garcia-Dastugue, "The Returns Management Process," vol. 13, 2002.
[24] A. Christian and D. Dharmayanti, "PENGARUH EXPERIENTIAL MARKETING TERHADAP CUSTOMER SATISFACTION DAN CUSTOMER LOYALTY THE LIGHT CUP DI SURABAYA TOWN SQUARE," *JURNAL MANAJEMEN PEMASARAN PETRA*, no. 2, 2013.
[25] M. Hassanah, E. Sentosa, and Marnis, "Pengaruh Kepuasan Pelanggan, Kualitas Produk Dan Citra Merek Terhadap Loyalitas Pelanggan Kosmetik Wardah Di Lingkungan Mahasiswi Universitas Persada Indonesia Y.A.I.," *JURNAL IKRAITH-EKONOMIKA*, vol. 6, no. 2, 2023.
[26] T. Adabayo, "An evaluation of reverse logistics responsiveness and customer satisfaction in retailing," *International Journal of Research in Business and Social Science (2147- 4478)*, vol. 11, no. 1, pp. 93–98, Feb. 2022, doi: 10.20525/ijrbs.v11i1.1570.
[27] S. Maimunah, A. Yusuf, and H. Sunarya, "ANALISIS SIKAP, MINAT DAN MOTIVASI MAHASISWA TERHADAP KEPUTUSN MENEMPUH PENDIDIKAN PROFESI AKUNTANSI," *Jurnal Akuntansi*, vol. 7, no. 1, Jan. 2020.
[28] N. Suryani, Risnita, and M. S. Jailani, "Konsep Populasi dan Sampling Serta Pemilihan Partisipan Ditinjau Dari Penelitian Ilmiah Pendidikan," *IHSAN: Jurnal Pendidikan Islam*, vol. 1, 2023, [Online]. Available: http://ejournal.yayasanpendidikandzurriyatulquran.id/index.php/ihsan
[29] Z. Zainuddin, Y. Hamja, and S. H. Rustiana, "Analisis faktor dalam pengambilan keputusan nasabah memilih produk pembiayaan perbankan syariah (Studi kasus pada PT Bank Syariah Mandiri Cabang Ciputat)," *Jurnal Keuangan dan Perbankan*, vol. 13, no. 1, 2016.
[30] A. D. A. S. Budi, L. Septiana, and B. E. P. Mahendra, "Memahami Asumsi Klasik dalam Analisis Statistik: Sebuah Kajian Mendalam tentang Multikolinearitas, Heterokedastisitas, dan Autokorelasi dalam Penelitian," *Jurnal Multidisiplin West Science*, vol. 03, no. 01, pp. 1–11, 2024.
[31] T. Lauvira, Y. Syafitri, and R. Parlindungan, "Pengaruh Persepsi Wajib Pajak Mengenai ProgramPerpajakan Tax Amnesty danWacana Transparasi Data Nasabah Bank (Bank Secrecy) Tahun 2018 Terhadap Kepatuhan WajibPajak (Studi Empiris pada KPP Pratama Ilir Barat Palembang)," 2018.
[32] S. Wardani and R. I. Permatasari, "PENGARUH PENGEMBANGAN KARIER DAN DISIPLIN KERJA TERHADAP PRESTASI KERJA PEGAWAI NEGERI SIPIL (PNS) STAF UMUM BAGIAN

PERGUDANGAN PENERBANGAN ANGKATAN DARAT (PENERBAD) DI TANGERANG," *JURNAL ILMIAH M-PROGRESS*, vol. 12, no. 1, 2022.
[33] R. Slamet and S. Wahyuningsih, "VALIDITAS DAN RELIABILITAS TERHADAP INSTRUMEN KEPUASAN KERJA," *Aliansi: Jurnal Manajemen dan Bisnis*, vol. 17, no. 2, 2022.
[34] O. Pasianus and A. A. Kana, "PENGARUH KUALITAS LAYANAN TERHADAP LOYALITAS PELANGGAN MELALUI KEPUASAN SEBAGAI VARIABEL INTERVENING PADA SWALAYAN PAMELLA ENAM YOGYAKARTA," *CAKRAWANGSA BISNIS*, vol. 2, no. 2, pp. 197–216, 2021.
[35] J. F. Hair, G. Tomas, M. Hult, C. M. Ringle, and M. Sarstedt, "Partial Least Squares Structural Equation Modeling (PLS-SEM) Using R: A workbook," 2021, doi: 10.1007/978-3-030.
[36] N. P. Sari and N. Rina, "PENGARUH KONTEN MEDIA SOSIAL INSTAGRAM @LAAKFKB TERHADAP PEMENUHAN KEBUTUHAN INFORMASI MAHASISWA AKHIR FKB," *Jurnal Education and Development*, vol. 10, no. 3, 2022.
[37] J. F. Hair, J. J. Risher, M. Sarstedt, and C. M. Ringle, "When to use and how to report the results of PLS-SEM," *European Business Review*, vol. 31, no. 1, pp. 2–24, Jan. 2019, doi: 10.1108/EBR-11-2018-0203.
[38] I. Melanakis, "THE IMPACT OF REVERSE LOGISTICS ON CUSTOMER SATISFACTION," 2023.

Vol. 4, No. 2, December 2025, pp. 77-91
p-ISSN: 2963-8577
e-ISSN: 2964-3511
DOI: 10.57102/jescee.v4i2.120

JESCEE
Journal of Emerging Supply Chain, Clean Energy, and Process Engineering

PRODUCTION SIMULATION HYDROGEN GAS FROM HEAVY FUEL OIL GASIFICATION AND LIFE CYCLE ASSESSMENT (LCA)USING UNISIM DESIGN R460.1 AND GABI TS SOFTWARE

Rinaldi Medali Rachman[1,2*], Dionisius Fransisco Rupang Pangkung[1]
[1]Department of Chemical Engineering, Faculty of Industrial Engineering, Universitas Pertamina
[2]Center for Downstream Chemical Industry, Universitas Pertamina

Abstract
Heavy fuel oil utilization via combustion leads to negative impacts towards the environment. A cleaner way of heavy fuel oil utilization should be implemented, gasification is one. Gasification process can convert heavy fuel oil feed into valuable gas like hydrogen. Based on the simulation result, hydrogen purity (on dry basis) was obtained at 98,02% (volume). Study on temperature and addition of gasifying agent was also done. At high gasification temperature, more hydrogen tends to be produced. Steam addition also gives positive effect on hydrogen yield. Environmental impacts evaluation using life cycle assessment method has been performed. Based on the simulation, this process significantly contributes to climate change with the score of 2.630 kgCO2eq. Carbon dioxide utilization via enhanced oil recovery can overcome this problem. From economical point of view, annual net income after tax is at Rp 45.956.031.943,16 with the annual return on investment rate of 59,46%, which is economically justified.

Keywords:
Heavy fuel oil gasification, hydrogen, life cycle assessment

Article History:
Received: December 10th, 2025
Revised: December 20th, 2025
Accepted: December 27th, 2025
Published: December 31st, 2025

Corresponding Author:
Rinaldi Medali Rachman
Department of Chemical Engineering, Universitas Pertamina, Indonesia

Email:
rinaldi.rachman@universitaspertamina.ac.id

1. Introduction

Global energy sources are currently still dominated by fossil-based hydrocarbon fuels, one of which is heavy fuel oil. Heavy fuel oil (HFO) is a residue from the distillation and cracking of petroleum, consisting of saturated, aromatic and olefinic hydrocarbons with a carbon number range of C9 to C50. This fraction has a boiling point of approximately 160–600°C and contains organometallic compounds, including heavy metals such as vanadium and nickel in low concentrations. [1]. In general, heavy fuel oil contains 85–90% carbon and 8–13% hydrogen, with small amounts of sulphur, nitrogen and oxygen. [2]. The sulphur and heavy metal content means that direct combustion of heavy fuel oil produces significant pollutant emissions and has the potential to increase the environmental burden. With increasing energy demands and the need to reduce emissions, cleaner HFO utilisation technologies are required.

Gasification is a thermochemical conversion technology capable of converting heavy fuel oil into synthesis gas (syngas) containing hydrogen (H_2), carbon monoxide (CO), carbon dioxide (CO_2), and methane (CH_4). [3]. The main reactions in gasification include partial oxidation, steam reforming, water–gas shift, and cracking[4] heavy hydrocarbon compounds affected by temperature, gasification agent ratio, and feed characteristics. Heavy oil gasification has been studied under various operating conditions—for example, increasing the temperature has been shown to increase hydrocarbon conversion and hydrogen yield, while adding water vapour increases the H_2/CO ratio through the water–gas shift reaction [5]. Hydrogen produced by gasification is very important in the petroleum industry, especially for hydrotreating and hydrocracking processes.

Modelling using process simulation software, such as UniSim Design R460.1, provides the ability to comprehensively study gasification phenomena without the need for large-scale experiments. Simulation

enables process sensitivity evaluation, mass–energy balance calculations, hydrogen purity analysis, and optimisation of operating parameters based on relevant thermodynamic and kinetic conditions, as has been done by [6], [7], [8]. In addition to technical analysis, a quantitative assessment of the environmental impacts arising throughout the process life cycle is required. The Life Cycle Assessment (LCA) method is used to assess the contribution of impact categories such as climate change, acidification, eutrophication, and resource use in accordance with the ISO 14040 standard. [9]. The GaBi software is used to calculate the environmental impact of each stage of the system, from feed preparation, gasification, hydrogen purification, to process emissions. On the other hand, economic feasibility must also be reviewed, given that the sustainability of the process is largely determined by profitability and return on investment.

Therefore, this study was conducted to provide a comprehensive understanding of the utilisation of heavy fuel oil through gasification technology. This study includes the development of a simulation model for the gasification-based hydrogen production process using UniSim Design R460.1, evaluation of environmental impacts through a Life Cycle Assessment (LCA) approach with the help of GaBi software, and economic feasibility analysis based on investment estimates, operating costs, and profitability parameters. The results of this study are expected to provide a scientific basis for the development of cleaner and more sustainable HFO utilisation technology.

2. Method

This research method consists of three main stages, namely simulation of the heavy fuel oil gasification process for hydrogen production using UniSim Design R460.1, environmental impact analysis through Life Cycle Assessment (LCA) with GaBi software, and economic feasibility analysis based on investment parameters and profitability. The general flow diagram of the research includes feed characterisation, process modelling, environmental evaluation, and economic analysis.

A. Process Simulation Using UniSim Design

1) Feed Characterization

This research method consists of three main stages, namely simulation of the heavy fuel oil gasification process for hydrogen production using UniSim Design R460.1, environmental impact analysis through Life Cycle Assessment (LCA) with GaBi software, and economic feasibility analysis based on investment and profit parameters. The general flow chart of the research includes raw material characterisation, process modelling, environmental evaluation, and economic analysis.

2) Fluid Package

Heavy fuel oil (HFO) is modelled as an assay using atmospheric distillation data and available physical properties. Pseudo-components are generated according to the boiling point range of heavy fuel oil fractions. The selection of thermodynamic models can be accessed in the Simulation Basis Manager menu. In this simulation, two types of thermodynamic models are used, namely Peng-Robinson (PR) and Amine Package.

3) Process Simulation

This simulation process consists of five main stages, namely:

- **Feed preheating**, namely heating heavy fuel oil and oxygen using steam through a heat exchanger until it reaches the gasifier operating temperature.
- **Gasification,** represented using a Gasifier block, where partial oxidation, pyrolysis, and subsequent reactions take place. At this stage, the HFO feed is reacted with air and steam under specific operating conditions. The operating variables set include:
    - Gasification temperature with a temperature range of 1000-2000°C
    - Steam-to-feed ratio (S/F) with the ratio of steam mass flow rate to feed (Steam/Feed) varying from 0.2-2.0.

  This model produces an initial syngas composition of H_2, CO, CO_2, CH_4, H_2O, and other minor gases. The hot gas produced is then fed into a waste-heat boiler to generate utility steam.

- **Quenching**, performed using an absorption column that brings hot gas into contact with water, thereby lowering the temperature and separating suspended carbon particles.
- **CO conversion,** modelled using an equilibrium reactor to represent the water-gas shift reaction isothermally at low temperatures.
- **Gas purification/gas sweetening,** using an MEA absorption-desorption system to remove CO_2 and H_2S, with the amount of MEA used based on the process. [10] , sehingga dihasilkan gas hidrogen dengan kemurnian minimal 98% volume sesuai standar ISO 14687.

B. Life Cycle Assessment (LCA)

This LCA study was conducted entirely with the assistance of GaBi ts software.

1) Goal and Scope Definition

The LCA study conducted in this research was evaluated using a gate-to-gate approach, where observations began from the point of entry of raw materials into the product system to the point where hydrogen gas was produced by the system. The impact assessment method used was the ReCiPe 2016 v1.1 Midpoint method. The category selected was midpoint, where the impact focused only on several environmental impacts caused by the product system. The boundaries of the product system can be illustrated as follows

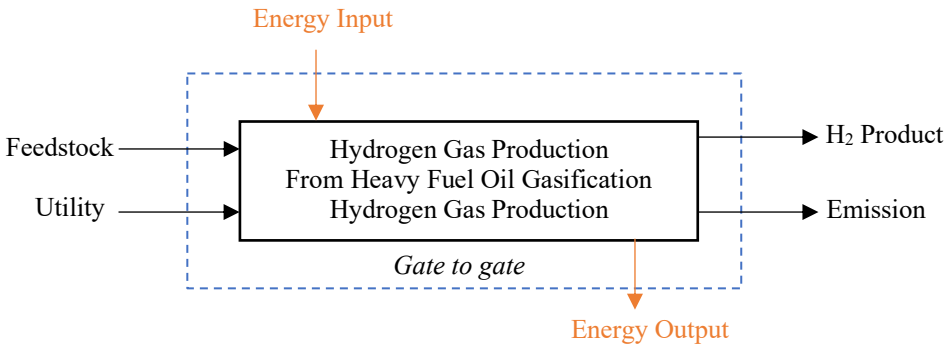

Figure 1. Product System Boundary

2) Life Cycle Inventory (LCI)

This process is carried out by inventorying all inflows and outflows from the system based on UniSim simulation data. The data recorded includes flows of raw materials, utilities, energy, main products, by-products, and emissions released into the environment. The inventory is carried out based on an operating basis of 1000 kg/hour of heavy fuel oil as feed, in accordance with the capacity design specified in the simulation. The data is then entered into the inventory table in GaBi for use in the impact assessment stage.

3) Impact Assessment

The third stage is the phase in which inventory data is translated into environmental impact values through a process of classification, characterisation, normalisation and weighting. This procedure follows the Life Cycle Impact Assessment (LCIA) flow as stipulated in the British Standards, which served as a reference in the previous simulation process. During the characterisation stage, each emission stream is converted into an equivalent impact value, such as CO_2 equivalents for the global warming category. The ReCiPe 2016 method is used for mapping and assessing impact categories.*Economic Feasibility Analysis*

An economic analysis method was used to assess the financial feasibility of hydrogen production from heavy fuel oil gasification. Calculations were made taking into account the initial investment costs, annual operating costs, and revenue from hydrogen sales. Cost components included the main equipment requirements, utilities, raw materials, and maintenance. Economic assessment was carried out using the net present value (NPV), payback period, and return on investment (ROI) parameters to determine the overall profitability and feasibility of the project.

3. Result and Discussion

A. Process Simulation

The results of simulations of hydrogen production through heavy fuel oil gasification show that the process configuration built in UniSim Design R460.1 is capable of producing a hydrogen flow with a purity of 98.02% vol, in accordance with the ISO 14687 standard for Grade A hydrogen, with the following details:

Table 1. Key Product Specifications Based on Simulation Results (Dry Basis)

Component	Value	Unit
H_2	98,02%	%vol.
CO	0,00%	%vol.
CO_2	0,00%	%vol.
H_2S	0,8891	ppm
CH_4	0,04%	%vol.
N_2	1,87%	%vol.

With the overall mass balance showing a total inflow and outflow of 8,634.70 kg/hour, this indicates that the model has achieved good stability and convergence, as follows:

Table 2. Mass Balance of Simulation Results

Input		Output	
Stream	Mass Flowrate (kg/jam)	Stream	Mass Flowrate (kg/hour)
Feed	1000,00	*Steam*	2424,00
Oxygen	1160,00	*Quench Water*	2814,95
Steam	750,00	*WGSR Bottom*	251,48
CW Gasifier	300,70	*Produk Utama (Sweet Gas)*	299,80
BFW	2424,00	*Sour Gas*	2697,40
Quench Water	3000,00	*Slag*	147,07
Total	**8634,70**	**Total**	**8634,70**

- Syngas Production

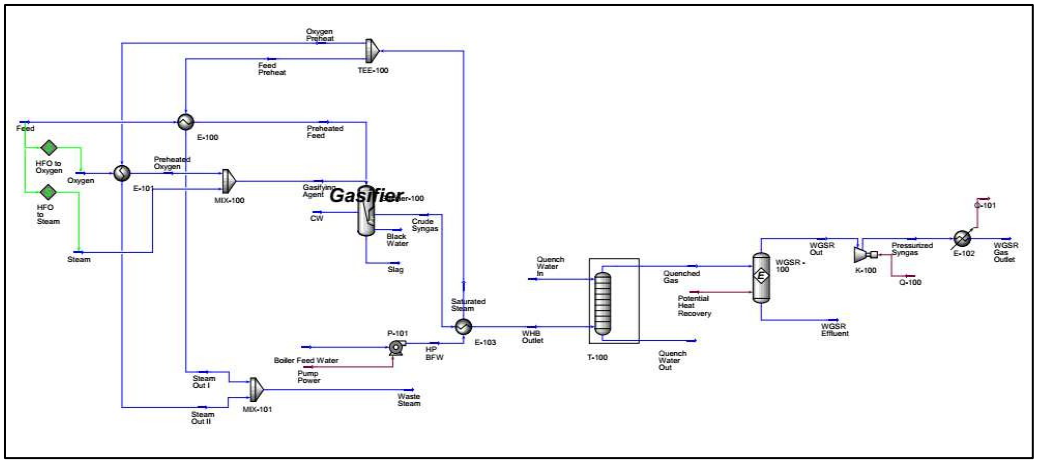

Figure 2. Process Flow Diagram of the Syngas Production Simulation Stage

The image shows the complete configuration of the syngas production simulation process built using UniSim Design R460.1. In the syngas production process using the heavy fuel oil gasification method, various process equipment is used in accordance with the operating conditions applied in this simulation, including the following:

Table 3. List of Equipment for Heavy Fuel Oil Gasification Process Simulation

No	Equiptment	Operation Condition		Description
		Temp. (ºC)	Pressure (kPa)	
1.	Heat Exchanger, E-100 (*Feed steam preheater*)	200	308,2	Heating Heavy Fuel Oil Feed ΔP: 20 kPa
2.	Heat Exchanger, E-101 (*Oxygen steam preheater*)	210	4238	Oxygen Warming ΔP: 20 kPa
3.	Mixer, MIX-100	-	-	Mixing of Gasification Agents
4.	Gasifier, Gasifier-100	1680	307,2	-
5.	Heat Exchanger, E-103 (Waste-heat boiler)	250	101,3	ΔP: 20 kPa
6.	Quench Tower, T-100	50,56	30 (*Top Stage Pressure*)	-
7.	Reactor, WGSR-100	25	30	Isotermik
8.	Compressor, K-100	164,7	100	Eficiency (adiabatic), 75%
9.	Cooler, E-102	25	100	-

As can be seen in the composition of the gasification product stream, a molar ratio of H2 to CO of 0.98 and a volume ratio of 0.80 were obtained. When compared to the results of experiments on a research scale conducted by Ashizawa, Hara, Kidoguchi, & Inumaru [5] The H2/CO volume ratio obtained was 1.01, so using this value as a reference, the absolute error percentage was 21%. This shows that the gasification model in UniSim is capable of representing the reaction phenomena that occur, particularly pyrolysis, partial oxidation, and gasification reactions that take place at a temperature of 1680 °C.

Within the gasifier, the process takes place in three zones—pyrolysis, gasification and quench—each of which contributes to the formation of char, devolatilisation and syngas production. In the pyrolysis zone, drying and thermal cracking (devolatilisation) occur, significantly reducing the volatile components in the heavy fuel oil feed from 41,530 kgmol/hour to 3,0017 kgmol/hour.

Name	Pyrolysis Feed	Pyrolysis Prod
Temperature [C]	990.7434	800.0000
Pressure [kPa]	308.1682	307.1682
Total Molar Flow [kgmole/h	173.6735	157.1969

Figure 3. Operating Conditions Between Feed and Pyrolysis Zone Products

Name	Pyrolysis Feed	Pyrolysis Prod
Coal [kgmole/h]	95.6062	55.9674
Fixed C [kgmole/h]	51.3771	51.3771
Volatile [kgmole/h]	41.530	3.0017
Ash [kgmole/h]	1.5886	1.5886
Moisture [kgmole/h	1.1102	0.00000

Figure 4. Proximate Content of Feed and Pyrolysis Zone Products

At a temperature of 800°C [11], All feedstock is converted into char and volatile substances, where char serves as fuel to provide heat energy when reacting with oxygen and steam. Simulation results show that the pyrolysis zone output stream contains CO_2 from char combustion and H_2S formed as a result of the reaction of sulphur in the feedstock with hydrogen released during pyrolysis.

Component	Inlet Mole Flow [kgmole/h]	Outlet Mole Flow [kgmole/h]
Hydrogen	0.00000	0.00000
CO	0.00000	0.00000
CO2	0.00000	8.2611
H2O	41.632	84.874
H2S	0.00000	0.98595
Methane	0.00000	0.00000
Nitrogen	1.4892	1.4892
Oxygen	34.946	5.6192
Heavy Fuel Oil*	95.606	55.967

Figure 5. Proximate Content of Feed and Pyrolysis Zone Products

In the gasification zone, syngas begins to form when the temperature reaches 800°C. Based on simulation results, this zone extends 6.592 m inside the gasifier vessel. Gasification occurs as indicated by a decrease in the fixed carbon fraction in the product compared to the feed, as a result of the water–gas and Boudouard reactions. In the water-gas reaction, carbon reacts with steam to form an equimolar mixture of H_2 and CO, while the Boudouard reaction produces CO through the interaction of carbon with CO_2.

Length [m]	Coal [kgmole/h]	Fixed Carbon [kgmole/h]	Volatile [kgmole/h]	Ash [kgmole/h]	Moisture [kgmole/h]
0.0000	55.967	51.377	3.0017	1.5886	0.00000
6.592	4.7488	0.15857	3.0017	1.5886	0.00000

Figure 6. Proximate Composition of Feedstock and Gasification Zone Products

Further steam consumption confirms the ongoing gasification process, primarily through water–gas and water–gas shift reactions, in which CO reacts again with steam to produce H_2 and CO_2. This is evident from the increase in the number of moles of CO_2 at the end of the gasification zone. Hydrogenation reactions with carbon also occur, as indicated by the formation of methane (CH_4) at the outlet of this zone.

Length [m]	Hydrogen [kgmole/h]	CO [kgmole/h]	CO2 [kgmole/h]	H2O [kgmole/h]	H2S [kgmole/h]	Methane [kgmole/h]	Nitrogen [kgmole/h]	Oxygen [kgmole/h]	Heavy Fuel Oil* [kgmole/h]
0.0000	0.00000	0.00000	8.2611	84.874	0.98595	0.00000	1.4892	5.6192	55.967
6.592	45.153	45.991	13.486	39.680	0.98595	2.6332e-002	1.4892	0.00000	4.7488

Figure 7. Flow Rate of Feedstock and Product Components in the Gasification Zone

In the quench zone, based on simulation results, hot gas is brought into contact with cooling water so that the outlet temperature drops to around 1300°C. This quench process produces 4.7488 kgmol/hour of slag, while the cooling water evaporates and is carried away with the gas flow, as evidenced by the absence of water content in the slag that comes out. Slag is a solid residue left over from the gasification process. The simulation results also show that hydrogen gas exits the gasifier at a rate of 45.153 kmol/hour, formed through a series of reactions inside the gasifier. To determine the contribution of each reaction to hydrogen production, a more in-depth study of reaction kinetics is required.

Name	Temperature [C]	Pressure [kPa]	Molar Flow [kgmole/h]
Cooling Feed	25.0000	101.3250	27.7545
Internal Feed	1680.3365	307.1682	151.5598
Vap Prod	1299.8809	101.3250	174.5655
Liq Prod	1299.8809	101.3250	0.0000
Slag Prod	1299.8809	101.3250	4.7488

Figure 8. Operating Conditions of the Quench Zone

And for the water–gas shift reactor, which functions to increase hydrogen yield through the conversion of carbon monoxide (CO). Based on the simulation results, CO conversion reached 99.99%, indicating that almost all CO in the inlet stream reacted with steam to produce hydrogen and CO_2. The isothermal reaction conditions provide a high equilibrium constant so that the reaction shift is strongly directed towards product formation. Since CO is used as the base component, the amount of H_2 and CO_2 formed follows the amount of CO entering the reactor. This conversion value is in line with Callaghan's findings[12], which shows that equilibrium conversion can reach around 99%.

 p-ISSN: 2963-8577
e-ISSN: 2964-3511

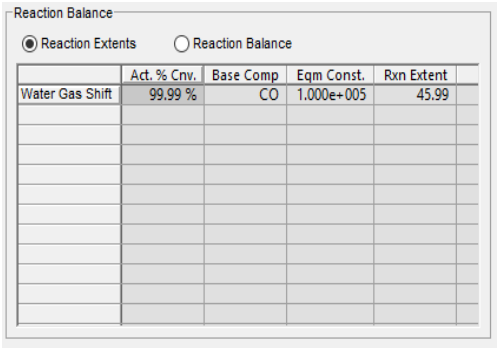
Reaction Balance

Reaction Extents Reaction Balance

	Act. % Cnv.	Base Comp	Eqm Const.	Rxn Extent
Water Gas Shift	99.99 %	CO	1.000e+005	45.99

Figure 10. Water Gas Shift Reaction Performance

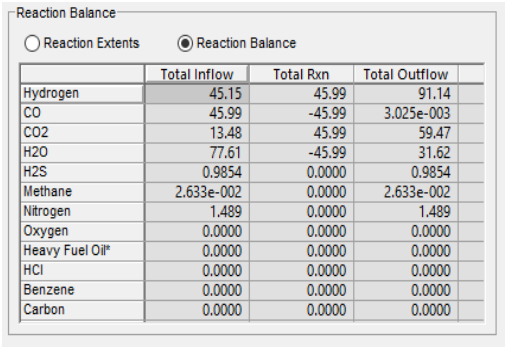
Reaction Balance

Reaction Extents Reaction Balance

	Total Inflow	Total Rxn	Total Outflow
Hydrogen	45.15	45.99	91.14
CO	45.99	-45.99	3.025e-003
CO2	13.48	45.99	59.47
H2O	77.61	-45.99	31.62
H2S	0.9854	0.0000	0.9854
Methane	2.633e-002	0.0000	2.633e-002
Nitrogen	1.489	0.0000	1.489
Oxygen	0.0000	0.0000	0.0000
Heavy Fuel Oil*	0.0000	0.0000	0.0000
HCl	0.0000	0.0000	0.0000
Benzene	0.0000	0.0000	0.0000
Carbon	0.0000	0.0000	0.0000

Figure 9. Flow of Mol Entering and Leaving the Reactor

- Purification

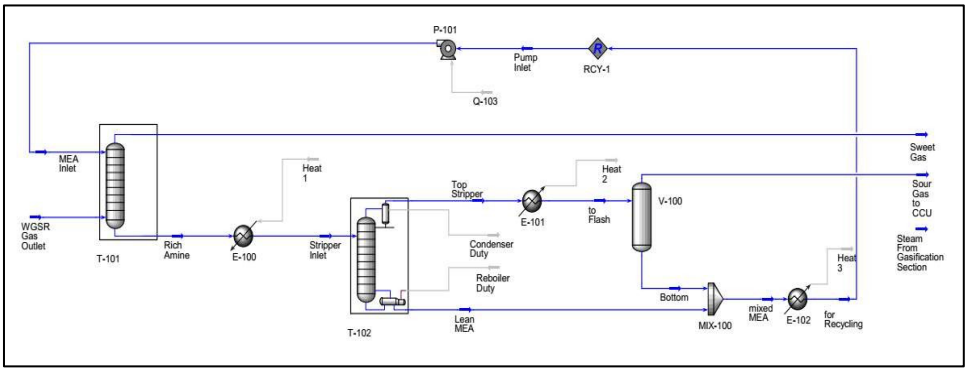

Figure 11. Process Flow Diagram of Purification

The image shows the complete configuration of the purification resistance simulation process built using UniSim Design R460.1. In this process, various process equipment is used in accordance with the operating conditions applied in this simulation, including the following:

Table 4. List of Equipment for Gasification Product Purification Process Simulation

No	Equipment	Operation Condition		Description
		Temp. (ºC)	Pressure (kPa)	
1.	Absoprtion Column, T-101	25	100	-
2.	Heater, E-100	50	90	No difference in pressure
3.	Desorption Column (Stripper), T-101	50	90	-
4.	Cooler, E-101	25	80	No difference in pressure
5.	Separator, V-100	25	80	-
6.	Mixer, M-100	-	-	Mixing of liquid product from the separator with the bottom product of the desorption column
7.	Pump, P-101	25	100	-
8.	Cooler, E-102	25	-	No difference in pressure

- Study of Variable Effect

  The study of variable effects in this research was conducted with the help of the case studies feature in the UniSim Design R460.1 software. Case studies can be accessed in the Databook menu option, Tools tab of the UniSim Design R460.1 software.

  a. The Effect of Gasification Temperature on the Volumetric Composition of H_2 and CO Gases

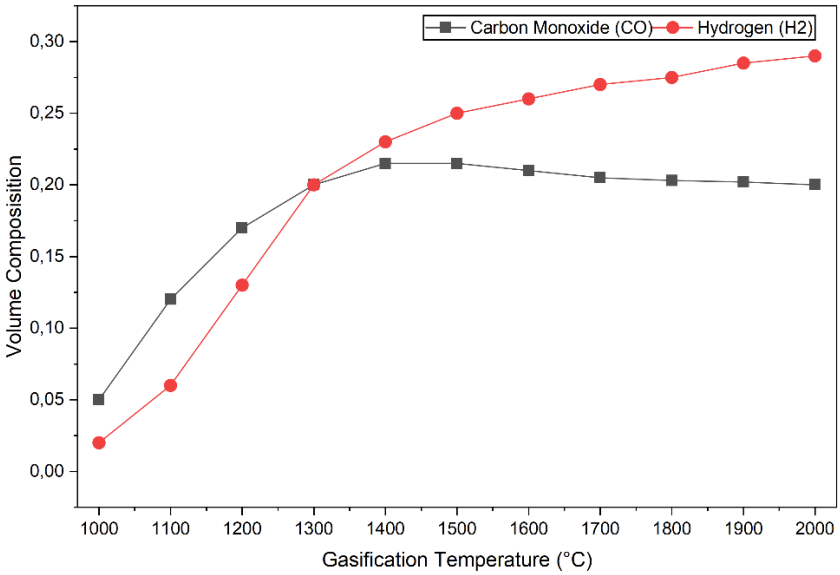

Figure 12. Graph of the Effect of Gasification Temperature on H_2 and CO Composition

Gasification temperature variations were conducted to observe the volume composition profiles of the two main gasification products, namely hydrogen and carbon monoxide. Using a gasification temperature range of 1000-2000°C, hydrogen formation tended to increase continuously. Meanwhile, carbon monoxide formation appears to be constant above a gasification temperature of 1500°C. This is due to the limited availability of oxygen used in the gasifier, which also limits the rate of CO formation. More hydrogen is obtained when gasification is carried out at high temperatures. This is because high temperatures can aid in the cracking process of heavy fractions found in fuel oil.Efek Temperatur Gasifikasi Terhadap Komposisi Volum Gas H_2 dan CO

p-ISSN: 2963-8577
e-ISSN: 2964-3511

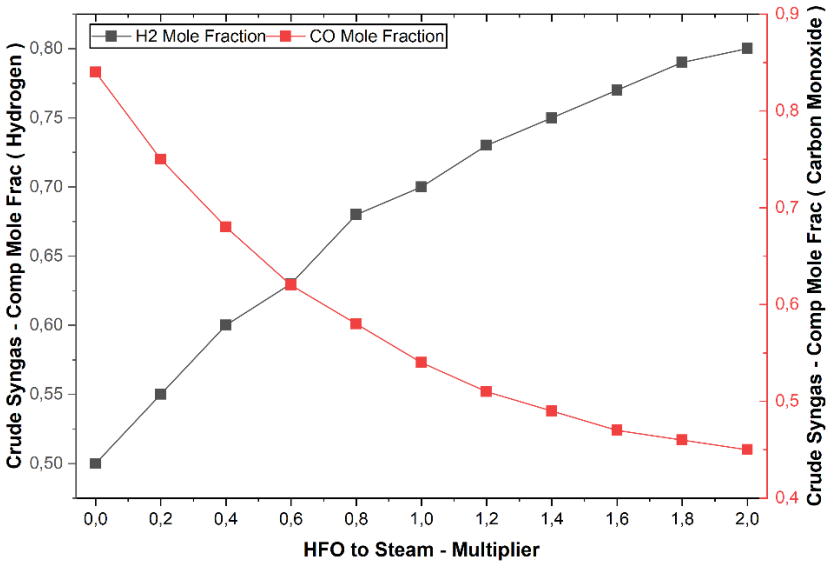

Figure 13. Graph showing the effect of steam volume on the composition of H_2 and CO

In this study, the oxygen mass flow rate to feed ratio (O_2 /Feed) was kept constant to observe the effect of steam on the gasification product. The steam mass flow rate to feed ratio (Steam/Feed) was varied from 0.2 to 2.0. Based on the results graph below, the addition of steam will increase the hydrogen gas composition and suppress the carbon monoxide composition. Thus, the presence of steam can increase the effectiveness of the gasification process by increasing the H_2 /CO ratio.

B. Life Cycle Assessment (LCA)

After entering all flow data from the process simulation results into the GaBi ts software, several environmental impacts resulting from hydrogen production through heavy fuel oil gasification were obtained. There are six categories of impacts, namely:

- Climate Change

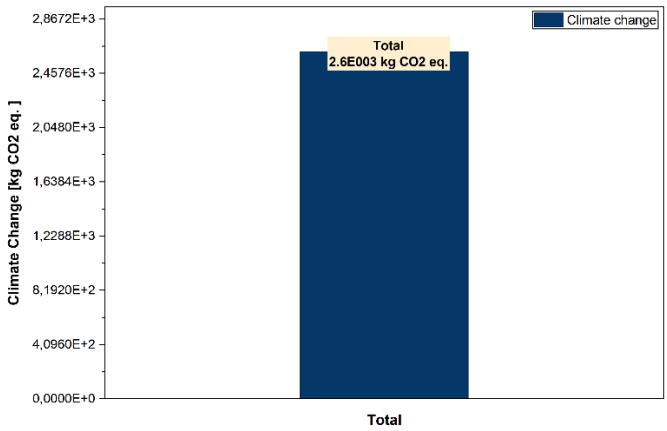

Figure 14. Climate Change

This category describes the impact on climate change expressed in kg CO2 equivalent. The graph below shows that this hydrogen production process contributes 2,620 kgCO2 equivalent (per hour) for a process base of 1,000 kg/hour of feed input.

- Freshwater Ecotoxicity

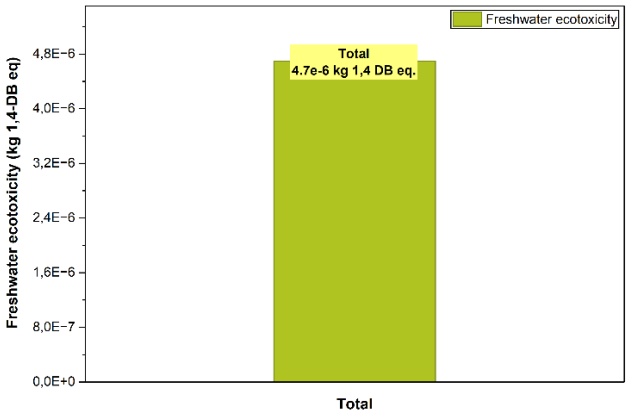

Figure 15. • Freshwater Ecotoxicity

This category describes the impact on water pollution expressed in kg of 1,4-dichlorobenzene equivalent. The graph below shows that this hydrogen production process contributes 4.7x10-6 kg of 1,4-dichlorobenzene equivalent (per hour) for a process basis of 1000 kg/hour of feed input.

- Marine Etoxicity

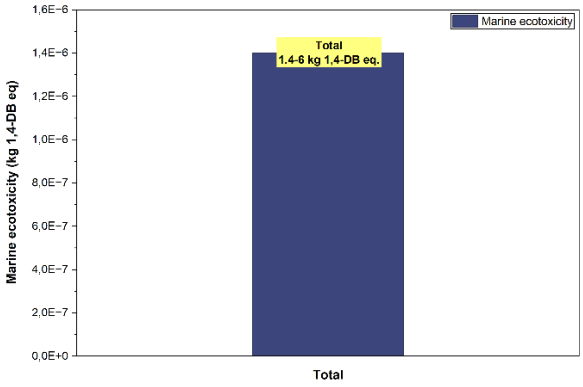

Figure 16. Pencemaran Laut

This category describes the impact on marine pollution expressed in kg of 1,4-dichlorobenzene equivalent. The graph below shows that this hydrogen production process contributes 1.4x10-6 kg of 1,4-dichlorobenzene equivalent (per hour) for a process basis of 1000 kg/hour of feed input.

- Marine Eutrophication

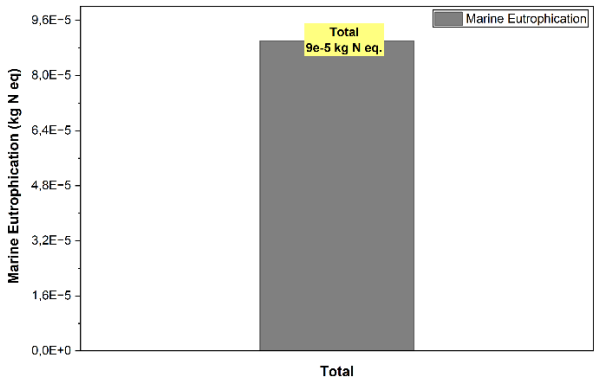

Figure 17. Marine Eutrophication

This category describes the impact on eutrophication of marine ecosystems expressed in kg N equivalent. The graph below shows that this hydrogen production process contributes 9x10-5 kg N (per hour) equivalent for a process base of 1000 kg/hour of feed input.

- Terrestrial Ecotoxicity

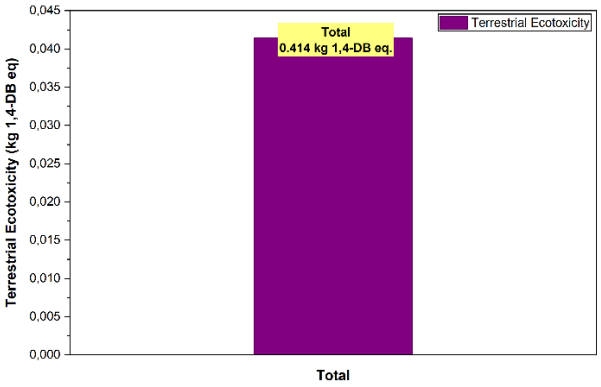

Figure 18. Terrestrial Ecotoxicity

This category describes the impact on soil contamination expressed in kg of 1,4-dichlorobenzene equivalent. The graph below shows that this hydrogen production process contributes 0.0414 kg of 1,4-dichlorobenzene equivalent (per hour) for a process basis of 1000 kg/hour of feed input.

To minimise the environmental impact, there are solutions that can be implemented. The following table recommends several alternatives for utilising CO2 gas produced by the product system, so that it is not released as emissions into the surrounding environment, based on Hepburn. [13] :

Table 5. Alternatif Utilisasi CO2

No	Alternative	Potential for CO_2 Removal (Mt CO_2/year)
1	Manufacture of Building Materials Based on CO_2	100-1400
2	Enhanced Oil Recovery	100-1800
3	Bioenergy with Carbon Capture and Storage	500-5000

Perbandingan dampak lingkungan terhadap penggunaan minyak bakar berat secara konvensional juga dilakukan. Penggunaan minyak bakar berat dengan cara pembakaran 1000 kg/jam umpan menghasilkan emisi sebagai berikut:

Table 6. Heavy Fuel Oil Combustion Emissions

Component	Flowrate	Unit
CO_2	850	kg/hour
H_2O	110	
SO_2	40	

These emission results are based on the assumption that combustion occurs completely, so that all ultimate components in the feed are oxidised into non-combustible gases in the form of carbon dioxide, water and sulphur dioxide.

The following is a comparison of the environmental impact of the two heavy fuel oil utilisation methods:

Table 7. Comparison of Environmental Impacts of Heavy Fuel Oil Utilisation Methods

Environmental Impacts	Methode	
	Gasification + 80% CO_2 *Sequestration*	Burning
Climate Change Potention (kg CO2 eq.)	520	850
Acidification Potention (kgSO2 eq.)	0	40

Based on the comparison results, it was found that the environmental impact is minimal when using the gasification method accompanied by CO2 sequestration. It is assumed that the injected carbon dioxide is 80% of the total emissions and the rest is considered to be released back into the atmosphere.

C. Economic Feasibility Analysis

In evaluating a project, information about the project's economic viability is required. According to [14], There are several factors that control the success of a business. These factors are based on the project's ability to generate profits. An economic evaluation is carried out to determine the following aspects:

- Capital Investment
  After evaluation, this hydrogen gas production project requires a total investment capital of IDR 121,243,430,694.96 per year, consisting of fixed investment capital of IDR 103,046,693,204.49 per year.
- Production costs
  The production costs required for this project amount to Rp47,193,691,710.60 per year.
- Revenue
  On the sales side, if all products are successfully sold, the income that will be obtained per year during the project is IDR 108,776,314,080.00 per year. The net profit that can be reaped after tax deductions is IDR 45,956,031,943.16.
- Return Of Investment (ROI)
  By knowing the costs required for production and the profit value, the rate of return on capital can also be determined using the return on investment parameter. From the calculations, the pre-tax and post-tax rates of return on investment were obtained as follows: 59.46% and 44.60%. By referring to the following minimum rate of return reference table, this project is declared feasible because it exceeds the minimum threshold. This project is categorised as a high-risk project because it is classified as a new process.

4. Conclusion

Based on the simulation results, the hydrogen gas production process through heavy fuel oil gasification has been successfully carried out with a final hydrogen gas purity of 98.02% (volume) and a production flow rate of 299.8 kg/hour. The production process involves several main stages, namely: gasification, quenching, conversion, and finally gas purification. An environmental impact analysis was also conducted using the life cycle assessment method. In terms of the environmental impact of the process, hydrogen gas production through gasification contributes to several categories of environmental impact. This hydrogen production process contributes to climate change, soil pollution, eutrophication of marine ecosystems, and water pollution. In addition, the economic aspects of the process were also reviewed. With the Return on Investment parameter, the pre-tax rate of return on this project is 59.46%, which exceeds the minimum threshold of 44%.

Acknowledgment

References

[1] D. King *et al.*, 'Environmental classification of petroleum substances - summary data and rationale', *CONCAWE*, no. 01, p. 51, 2001.
[2] H. A. Romp, *Oil Burning*. Dordrecht: Springer Netherlands, 1937. doi: 10.1007/978-94-017-6069-0.
[3] M. Vaezi, M. Passandideh-Fard, M. Moghiman, and M. Charmchi, 'Gasification of heavy fuel oils: A thermochemical equilibrium approach', *Fuel*, vol. 90, no. 2, pp. 878–885, Feb. 2011, doi: 10.1016/j.fuel.2010.10.011.
[4] Robert C. Brown and Tristan R. Brown, *Biorenewable Resources Engineering New Products from Agriculture*. in Second Edition. Lowa State University: WILEY Blackwell, 2014. [Online]. Available:

chrome-extension://efaidnbmnnnibpcajpcglclefindmkaj/https://download.e-bookshelf.de/download/0005/0284/22/L-G-0005028422-0002720397.pdf
[5] M. Ashizawa, S. Hara, K. Kidoguchi, and J. Inumaru, 'Gasification characteristics of extra-heavy oil in a research-scale gasifier', *Energy*, vol. 30, no. 11–12, pp. 2194–2205, Aug. 2005, doi: 10.1016/j.energy.2004.08.023.
[6] X. Yang, A. Hamidzadeh, M. Ilkhani, A. Foroughi, M. J. Esfahani, and M. Motahari-Nezhad, 'Aspen plus simulation of heavy oil gasification in a fluidized bed gasifier', *Petroleum Science and Technology*, vol. 34, no. 17–18, pp. 1530–1533, Sep. 2016, doi: 10.1080/10916466.2016.1208227.
[7] H. F. Fasih, H. Ghassemi, and H. K. M. Shahi, 'Gasification of a Heavy Fuel Oil: A Parametric Study on Energy and Exergy Analysis for Different Gasifying Agents', *Pet. Chem.*, vol. 61, no. 2, pp. 162–171, Feb. 2021, doi: 10.1134/S0965544121020055.
[8] M. Hosseinpour, A. H. Hajialirezaei, M. Soltani, and J. Nathwani, 'Thermodynamic analysis of in-situ hydrogen from hot compressed water for heavy oil upgrading', *International Journal of Hydrogen Energy*, vol. 44, no. 51, pp. 27671–27684, Oct. 2019, doi: 10.1016/j.ijhydene.2019.08.223.
[9] J. Wang, R. Iwasaki, A. M. Bayen, and J. Harvey, 'Future road transportation technology', *International Journal of Transportation Science and Technology*, vol. 5, no. 1, pp. iii–iv, Aug. 2016, doi: 10.1016/j.ijtst.2016.09.001.
[10] M. I. Stewart, 'Overview of Gas-Handling, Conditioning, and Processing Facilities', in *Surface Production Operations*, Elsevier, 2014, pp. 1–8. doi: 10.1016/B978-0-12-382207-9.00001-9.
[11] Speight , James G, *Gasification of Unconventional Feedstocks*, First Edition. Gulf Professional Publishing, 2014. [Online]. Available: https://www.sciencedirect.com/book/9780127999111/gasification-of-unconventional-feedstocks
[12] C. A. Callaghan, 'Kinetics and Catalysis of the Water-Gas-Shift Reaction: A Microkinetic and Graph Theoretic Approach', *WORCESTER POLYTECHNIC INSTITUTE*, Mar. 2006, [Online]. Available: chrome-extension://efaidnbmnnnibpcajpcglclefindmkaj/https://my.che.utah.edu/~ring/Design%20II/Articles/Water%20Gas%20Shift%20Kinetics-c%20callaghan%20thesis.pdf
[13] C. Hepburn *et al.*, 'The technological and economic prospects for CO2 utilization and removal', *Nature*, vol. 575, no. 7781, pp. 87–97, Nov. 2019, doi: 10.1038/s41586-019-1681-6.
[14] R. S. Aries and R. D. Newton, *Chemical Engineering Cost Estimation*, Second. Universitas Michigan: McGraw-Hill, 1955, 1955. [Online]. Available: https://books.google.co.id/books?id=NjhPAAAAMAAJ&hl=id&source=gbs_book_other_versions_r&cad=3

Biographies of Authors

Author 1 short CV and photograph
Please write your short CV and insert the photograph inside the frame on the left side.

Author 2 short CV and photograph
To Add author please insert row above this line.

Vol. 4, No. 2, December 2025, pp. 93-101
p-ISSN: 2963-8577
e-ISSN: 2964-3511
DOI: 10.57102/jescee.v4i2.127

JESCEE
Journal of Emerging Supply Chain, Clean Energy, and Process Engineering

IMPLEMENTATION OF DIGESTER MACHINE AUTOMATION USING AN ARDUINO UNO AND MULTISENSING SENSORS TO IMPROVE CRUDE PALM OIL PRODUCTION EFFICIENCY

Putri Maharani[1], A Alfisyahrin[2], S Syukriyadin[3*]
[1]Diploma Program in Electrical Engineering, Faculty of Engineering, Universitas Syiah Kuala
[2,3]Department of Electrical and Computer Engineering, Faculty of Engineering, Universitas Syiah Kuala

Abstract

The production of crude palm oil was highly dependent on the operational efficiency of the digester unit, in which improper control of temperature, material level, and stirring speed often resulted in reduced productivity and unstable operating conditions. This study aimed to address these issues by developing an automated control system to improve digester performance through integrated sensing and motor control. An automation system based on a microcontroller was designed and simulated using multisensing technology, including temperature monitoring within an optimal range of 90–95 °C, material level detection with a minimum threshold of 75%, and direct current motor speed regulation through a motor driver module. System logic and operational behavior were evaluated using Proteus simulation software prior to hardware implementation. The simulation results showed that the proposed system was able to automatically stop the digester motor when the operating temperature exceeded 95 °C or when the material level dropped below the predefined threshold, thereby preventing unsafe operating conditions and potential equipment damage. The automated response ensured more stable digester operation and reduced the risk of process inefficiencies. The overall findings indicated that the proposed low-cost automation system effectively enhanced process control and operational reliability. Furthermore, the implementation of this system demonstrated a potential improvement in production efficiency of approximately 20–30%. These results confirmed that microcontroller-based automation with multisensing integration provided a practical and efficient solution for optimizing digester operations in crude palm oil processing plants.

Keywords:
Industrial automation; multisensing sensors; digester system; crude palm oil; process simulation

Article History:
Received: November 2nd, 2025
Revised: November 29th, 2025
Accepted: December 1st, 2025
Published: December 31rd, 2025

Corresponding Author:
S Syukriyadin
Department of Electrical and Computer Engineering, Universitas Syiah Kuala, Indonesia
Email: syukriyadin@usk.ac.id

1. Introduction

The palm oil industry is one of the most strategic industrial sectors in Indonesia, with annual fresh fruit bunch (FFB) production exceeding 40 million tons. During the early stages of crude palm oil (CPO) processing, the digester machine plays a critical role by agitating sterilized fruit to facilitate oil release from the cellular structure. Optimal oil extraction is achieved when the digester operates within a temperature range of 90–95 °C and maintains stable agitation, resulting in oil yields of approximately 22–24% of FFB weight. However, in many processing

plants, digester operation still relies on conventional manual control, which often fails to maintain consistent operating conditions [1].

Uncontrolled fluctuations in temperature and material level represent major operational challenges in digester systems. Excessive temperatures can trigger accelerated hydrolysis reactions, leading to a reduction in crude palm oil quality of up to 15–20% [2]. Similarly, material levels below the optimal threshold, particularly under 75%, increase energy consumption without improving oil extraction efficiency. These conditions not only reduce production efficiency but also impose additional mechanical stress on equipment, increasing the risk of premature wear and failure [3].

With the advancement of industrial automation technologies, microcontroller-based systems have emerged as promising solutions for improving process stability and operational efficiency. Arduino Uno, as an open-source microcontroller platform, has been widely applied in various agricultural industrial automation systems, including irrigation and drying processes, resulting in efficiency improvements of up to 25% compared to manual methods [4]. The integration of multisensing technology enables real-time monitoring of process parameters with adequate accuracy. The DHT11 sensor has been reported to measure temperature with a deviation of approximately ±2 °C, while the HC-SR04 ultrasonic sensor has proven effective for material level detection within a range of 2–400 cm, making it suitable for digester applications [5]. Furthermore, control of the agitator motor speed using an L293D motor driver with pulse width modulation techniques plays an important role in maintaining mechanical stability and preventing damage caused by uncontrolled agitation [6]. The real-time display of operational data has also been shown to reduce operator errors by up to 30% [7].

Despite extensive research on automation in the palm oil industry, studies focusing on an integrated system that simultaneously controls temperature, material level, and agitation speed in digester machines remain limited [8]. This gap highlights the need for a comprehensive automation approach that not only monitors key parameters but also responds automatically to unsafe or non-optimal operating conditions [9].

Based on these considerations, this study presents the design and simulation of an Arduino Uno–based digester automation system integrated with multisensing sensors. The proposed system maintains operating temperature within 90–95 °C, ensures a minimum material level of 75%, and regulates agitator motor speed in real time. System performance and reliability were validated through Proteus simulation prior to physical implementation. The system is expected to enhance operational stability, minimize human error, and contribute to improved efficiency in crude palm oil production [10].

2. Method

A. System Design

The proposed system was designed as a closed-loop control system for digester operation. Temperature and material level were continuously monitored using a DHT11 temperature sensor and an HC-SR04 ultrasonic sensor, respectively. The material level was calculated as a percentage of the digester volume, assuming a maximum digester height of 100 cm. All sensor data were processed by an Arduino Uno microcontroller, which executed control logic based on predefined operating thresholds. The digester motor was activated through an L293D motor driver only when operating conditions were within the optimal range, namely a temperature between 90–95 °C and a material level of at least 75%. If either parameter exceeded or fell below the specified limits, the system automatically stopped motor operation to prevent inefficient or unsafe conditions. A red LED was used as a visual indicator to display system status during operation. Prior to hardware implementation, the entire system was modeled and evaluated using Proteus simulation software to verify control logic and operational behavior.

B. Hardware Components

The hardware architecture of the proposed digester automation system consists of a microcontroller unit, sensing devices, actuators, display modules, and a power supply. A summary of the hardware components and their functions is presented in Table 1.

Table 1. Hardware Components of the Proposed Digester Automation System

No.	Component	Specification	Function in System
1	Arduino Uno	ATmega328P, 16 MHz, 14 digital I/O, six supporting PWM	Main controller for data processing and control logic
2	DHT11	Temp. range 0–50 °C, ±2 °C accuracy	Monitoring digester operating temperature
3	HC-SR04	Range 2–400 cm, ±3 mm accuracy	Detecting material level inside digester
4	L293D	H-bridge, 4.5–36 V, 600 mA/channel	Controlling DC motor speed via PWM
5	LCD 32 × 2	HD44780-based	Displaying temperature and material level
6	DC Motor	12 V, 100–200 rpm	Digester agitator
7	LED (Red)	With 220 Ω resistor	System operation indicator
8	Power Supply	5 V and 12 V DC, ≥2 A	Supplying system power

Arduino Uno was employed as the central control unit responsible for processing sensor data and executing control decisions [11]. The microcontroller compared real-time temperature and material level values with predefined thresholds and generated output signals for motor control and system indicators. The selection of Arduino Uno was based on its open-source architecture, ease of integration with industrial sensors, and proven effectiveness in palm oil automation applications [12].

Temperature monitoring was performed using a DHT11 sensor installed within the digester chamber. Although the sensor operates within a nominal range of 0–50 °C, it was utilized to simulate thermal control behavior around the optimal digester operating range of 90–95 °C. The sensor provides temperature readings with an accuracy of approximately ±2 °C and has been reported to perform reliably in humid industrial environments such as palm oil processing facilities When the measured temperature exceeded 95 °C, the system automatically disabled motor operation to prevent oil degradation.

Material level detection was achieved using an HC-SR04 ultrasonic sensor mounted at the top of the digester. The sensor measured the distance between its position and the surface of the material, which was then converted into a percentage of digester fill level based on the assumed maximum digester height. System operation was permitted only when the material level was equal to or greater than 75%, preventing inefficient agitation under low-load conditions. Previous studies have confirmed the reliability of HC-SR04 sensors in dusty industrial environments, including palm oil mills [13].

The digester agitator motor was controlled using an L293D motor driver, which enabled speed regulation through pulse width modulation (PWM). This approach allowed the system to maintain stable agitation while reducing excessive mechanical stress and energy consumption. PWM-based motor control using H-bridge drivers contributes to improved energy efficiency and mechanical stability in industrial mixing applications.

Operational data, including temperature and material level, were displayed in real time using a 32 × 2 character LCD module installed on the external control panel. Real-time visualization of system parameters has been shown to reduce operator error rates by up to 30% in industrial control systems. A red LED indicator was also incorporated to provide immediate visual feedback on system status, illuminating only when operating conditions were within acceptable limits.

The system was powered using a dual DC power supply configuration consisting of a 5 V supply for the microcontroller, sensors, and display, and a 12 V supply for the DC motor via the L293D driver. This configuration ensured stable system operation and minimized voltage fluctuations during motor startup.

C. Simulation and Testing Procedure

The control program was developed using Arduino IDE 2.0 with the DHT.h and LiquidCrystal.h libraries. The program continuously read temperature and material level data, compared the values with predefined thresholds, and controlled motor operation accordingly. The motor operated only when the temperature remained within 90–95°C and the material level was at least 75%. If the temperature exceeded 95°C or the material level fell below the threshold, the system automatically stopped motor operation and turned off the LED indicator.

All system logic and component interactions were tested through a Proteus simulation, as illustrated in Figure 1. This figure provides a schematic representation of the entire system, highlighting the connections between the Arduino Uno, sensors, motor driver, and other components. The simulation procedure was designed to ensure the reliability of the system in controlling operational parameters (temperature 90–95°C and material level ≥75%) and to assess its overall efficiency and responsiveness.

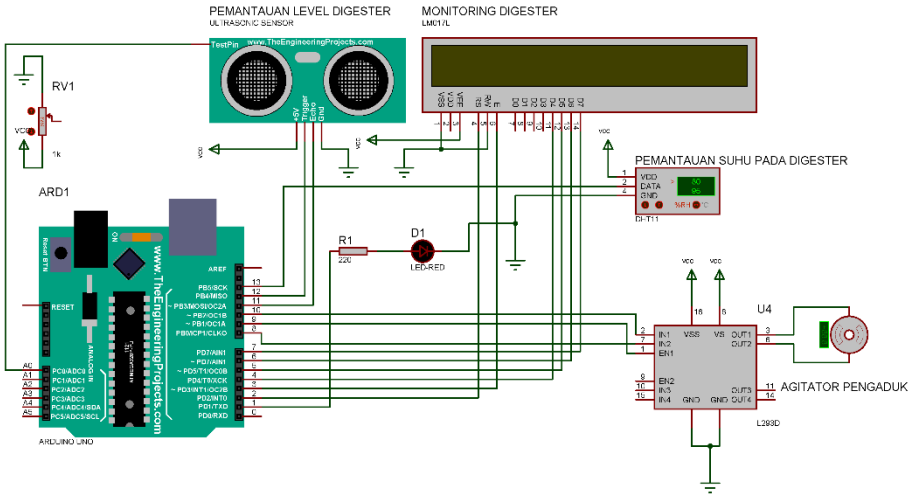

Figure 1. Simulation Circuit

Before starting the simulation, a virtual circuit was constructed in Proteus with all necessary components (Arduino Uno, DHT11, HC-SR04, L293D, LCD 32×2, DC motor, and red LED). The Arduino code was uploaded to the virtual microcontroller using the Virtual Terminal feature for debugging. The sensor inputs were simulated as follows:

- Temperature (DHT11): A variable signal generator in Proteus was used to simulate temperature readings (85–100°C) with fluctuations of ±1°C per second, representing the heating conditions inside the digester (Siregar et al., 2018).
- Material Level (HC-SR04**)**: The echo distance variable was adjusted to simulate material levels (50-100%, equivalent to a range of 50–200 cm for a 200 cm digester height), including random noise of ±2 cm to simulate agitation vibrations.

The power supply was stabilized at 5V/12V, and a virtual oscilloscope was attached to the motor's PWM pin to monitor the output signals. Data was recorded every second using the Graph feature in Proteus and external logs.

The testing was divided into four main scenarios to assess both normal and abnormal operational conditions. Each scenario was repeated three times for statistical reliability (average and standard deviation), with a duration of 5–10 minutes per scenario. The input transitions were gradual to avoid simulation artifacts.

1. Scenario 1: Optimal Condition (Normal Operation)
    - Input: The temperature started from 85°C and increased linearly to 92°C (within the 90–95°C range), with the material level stabilized between 80–90%.

- Procedure: Run the simulation for 5 minutes. Observe if the DC motor is active (PWM 150, ~150 rpm), the red LED is on, and the LCD displays real-time values (e.g., "Temperature: 92°C, Level: 85%").
- Criteria: The system should operate stably without shutdown.

2. Scenario 2: Overheating (Temperature >95°C)
   - Input: The temperature gradually increased from 92°C to 97-100°C, with the material level maintained ≥75%.
   - Procedure: Monitor for 3 minutes. Verify that the Arduino detects temperatures >95°C, stops the motor (PWM 0), turns off the LED, and updates the LCD (e.g., "Temperature: 97°C - STOP").
   - Criteria: The shutdown should occur in <1 second to prevent damage, with 100% motor power savings when off.
3. Scenario 3: Low Level (<75%)
   - Input: The material level decreased from 80% to 60–70%, while the temperature remained at 92°C.
   - Procedure: Run the simulation for 4 minutes, observing that the system stays off until the material level rises back to ≥75%. The LCD should display "Level: 70% - IDLE".
   - Criteria: Prevent energy-wasting operation, with a material level detection accuracy of ±2%.
4. Scenario 4: Combined and Stress Condition (Extreme Variations)
   - Input: Rapid fluctuations, such as temperature 85–100°C and material level 50–100% (including fast transitions like temperature jumping 5°C/second and level decreasing 10%/minute).
   - Procedure: Run the simulation for 10 minutes to test the system's robustness with external disturbances such as humidity (80% RH) or vibrations.
   - Criteria: The system should handle 95% of scenarios without failure, with an average response time of <1.5 seconds.

D. Success Criteria and Limitations

The system is considered successful if:

1. 100% detection of optimal conditions triggers operation.
2. 100% shutdown occurs under abnormal conditions.
3. Sensor accuracy >90%.
4. Energy efficiency >15% compared to the manual baseline.

Limitations of the testing include Proteus's inability to simulate physical factors such as extreme humidity, so further physical testing is required. This procedure ensures the system is ready for real-world applications in CPO industries, with a total testing time of around 2 hours.

3. Result and Discussion

A. Scenario 1

The temperature increased linearly from 85°C to 92°C, entering the optimal range at the 50th second, while the material level remained stable between 80% and 85%. When the temperature reached above 90°C and the material level exceeded 75%, the motor operated at PWM 150 (~150 rpm) and the LED turned on, indicating that the system was functioning correctly. The LCD displayed the status "RUNNING" and updated the temperature and material level readings in real-time. The response time from detection to motor and LED activation was recorded to be very fast, under two seconds. The detailed test results are summarized in Table 2.

The system operated effectively under optimal conditions, with the motor and LED activated when the temperature was within the 90°C to 95°C range and the material level was above 75%. The system's ability to control the motor only under these conditions indicates efficient energy use and protection against system damage. The response time shows that the system is capable of reacting to changes in temperature and material level

efficiently, which is crucial in industrial applications to ensure smooth automation processes. The DHT11 and HC-SR04 sensors performed accurately during the test, providing precise data for system control.

Table 2. Result of Scenario 1 Testing

Time (sec)	Temperature (C)	Level (%)	Motor Active	LED Active	LCD Status
0	85	80	FALSE	FALSE	Temperature: 85.0C Level: 80.0%
30	85.7	80.5	FALSE	FALSE	Temperature: 85.7C Level: 80.5%
60	86.4	81	FALSE	FALSE	Temperature: 86.4C Level: 81.0%
90	87.1	81.5	FALSE	FALSE	Temperature: 87.1C Level: 81.5%
120	87.8	82	FALSE	FALSE	Temperature: 87.8C Level: 82.0%
150	88.5	82.5	FALSE	FALSE	Temperature: 88.5C Level: 82.5%
180	89.2	83	FALSE	FALSE	Temperature: 89.2C Level: 83.0%
210	89.9	83.5	FALSE	FALSE	Temperature: 89.9C Level: 83.5%
240	90.6	84	TRUE	TRUE	Temperature: 90.6C Level: 84.0%
270	91.3	84.5	TRUE	TRUE	Temperature: 91.3C Level: 84.5%
300	92	85	TRUE	TRUE	Temperature: 92.0C Level: 85.0%

B. Scenario 2

The temperature increased linearly from 92°C to 100°C by the 180th second. When the temperature exceeded 95°C, both the motor and LED were turned off, with the motor power reading dropping to 0 W, in accordance with safety protocols. The LCD displayed the message "Temperature: [X]°C - STOP", providing immediate feedback to the operator about the system's status. After the temperature dropped back to 93°C, the motor and LED were reactivated, and the LCD updated the status to "RUNNING". The motor power consumption was 0 W during the shutdown and returned to approximately 150 W when the motor was active again, indicating effective energy savings. Table 3 provides the detailed test data, including temperature, material level, motor status, LED status, and motor power, recorded at 1-second intervals.

Table 3. Result of Scenario 2 Testing

Time (sec)	Temperature (C)	Level (%)	Motor Active	LED Active	LCD Status	Motor power(W)
0	92.0	80	TRUE	TRUE	Temperature: 92.0C Level: 80.0%	150
10	92.4	80	TRUE	TRUE	Temperature: 92.4C Level: 80.0%	150
20	92.9	80	TRUE	TRUE	Temperature: 92.9C Level: 80.0%	150
30	93.3	80	TRUE	TRUE	Temperature: 93.3C Level: 80.0%	150
40	93.8	80	TRUE	TRUE	Temperature: 93.8C Level: 80.0%	150
50	94.2	80	TRUE	TRUE	Temperature: 94.2C Level: 80.0%	150
60	94.7	80	TRUE	TRUE	Temperature: 94.7C Level: 80.0%	150
70	95.1	80	FALSE	FALSE	Temperature: 95.1C - STOP	0
80	95.6	80	FALSE	FALSE	Temperature: 95.6C - STOP	0
90	96.0	80	FALSE	FALSE	Temperature: 96.0C - STOP	0
100	96.4	80	FALSE	FALSE	Temperature: 96.4C - STOP	0
110	96.9	80	FALSE	FALSE	Temperature: 96.9C - STOP	0
120	100.0	80	FALSE	FALSE	Temperature: 97.3C - STOP	0
130	98.8	80	FALSE	FALSE	Temperature: 97.8C - STOP	0
140	97.7	80	FALSE	FALSE	Temperature: 98.2C - STOP	0
150	96.5	80	FALSE	FALSE	Temperature: 98.7C - STOP	0
160	95.3	80	FALSE	FALSE	Temperature: 99.1C - STOP	0
170	94.2	80	FALSE	FALSE	Temperature: 99.6C - STOP	0
180	93.0	80	FALSE	FALSE	Temperature: 100.0C - STOP	0

The response time to detect temperatures above 95°C and stop the motor was recorded as very fast, within less than one second, meeting industrial safety standards aimed at preventing system damage due to overheating. This fast response is attributed to the control logic, which directly reacts to conditions exceeding the temperature threshold.

The recovery process, which took place after the temperature dropped to 93°C, demonstrated that the system could return to normal operation after dealing with overheating conditions. This is essential for maintaining the continuity of automation processes, avoiding long-term damage from overheating, and minimizing downtime.

Furthermore, the recorded 100% power saving during motor shutdown indicates excellent energy control. This is especially important in industrial automation applications where energy management is a top priority, particularly during idle periods or when the system is not operating at full capacity.

C. Scenario 3

The test results, which record the changes in material level, motor status, LED status, and motor, are provided in Table 4. The material level was linearly decreased from 80% to 70% at the 120th second and then increased back to 75% after the 120th second. During the first phase (Level <75%), the motor and LED remained off, and the LCD displayed "Level: [X]% - IDLE," indicating that the system was idle due to the low material level. Once the material level rose above 75%, both the motor and LED were reactivated, and the LCD updated the status to "RUNNING," signaling that the system was now active.

The frequency of false positives recorded during the test showed that level detection accuracy remained within the ±2% range, as specified. Minor fluctuations in the level readings may have been caused by sensor variability or external disturbances, but no significant false positives were observed that impacted system performance.

Tabel 4. Result of Scenario 3 Testing

Time (sec)	Temperature (C)	Level (%)	Motor Active	LED Active	LCD Status
0	92	80.0	TRUE	TRUE	Temperature: 92.0C Level: 80.0%
10	92	79.6	TRUE	TRUE	Temperature: 92.0C Level: 79.6%
20	92	79.2	TRUE	TRUE	Temperature: 92.0C Level: 79.2%
30	92	78.8	TRUE	TRUE	Temperature: 92.0C Level: 78.8%
40	92	78.3	TRUE	TRUE	Temperature: 92.0C Level: 78.3%
50	92	77.9	TRUE	TRUE	Temperature: 92.0C Level: 77.9%
60	92	77.5	TRUE	TRUE	Temperature: 92.0C Level: 77.5%
70	92	77.1	TRUE	TRUE	Temperature: 92.0C Level: 77.1%
80	92	76.7	TRUE	TRUE	Temperature: 92.0C Level: 76.7%
90	92	76.3	TRUE	TRUE	Temperature: 92.0C Level: 76.2%
100	92	75.8	TRUE	TRUE	Temperature: 92.0C Level: 75.8%
120	92	70.0	TRUE	TRUE	Temperature: 92.0C Level: 75.0%
130	92	70.4	FALSE	FALSE	Level: 74.6% - IDLE
140	92	70.8	FALSE	FALSE	Level: 74.2% - IDLE
150	92	71.3	FALSE	FALSE	Level: 73.8% - IDLE
160	92	71.7	FALSE	FALSE	Level: 73.3% - IDLE
170	92	72.1	FALSE	FALSE	Level: 72.9% - IDLE
180	92	72.5	FALSE	FALSE	Level: 72.5% - IDLE
190	92	72.9	FALSE	FALSE	Level: 72.1% - IDLE
200	92	73.3	FALSE	FALSE	Level: 71.7% - IDLE
210	92	73.8	FALSE	FALSE	Level: 71.2% - IDLE
220	92	74.2	FALSE	FALSE	Level: 70.8% - IDLE
230	92	74.6	FALSE	FALSE	Level: 70.4% - IDLE
240	92	75.0	FALSE	FALSE	Level: 70.0% - IDLE

Energy management was a key factor in this scenario, and the system effectively prevented energy wastage by keeping the motor and LED off when the material level was below 75%. This represents an efficient energy management implementation, which is crucial in industrial automation contexts to minimize energy consumption when the system is not operating at full capacity.

The accuracy of level detection within the ±2% range indicates that the ultrasonic sensor performed reliably in detecting level changes, despite minor fluctuations. These fluctuations could be attributed to environmental factors such as dust or interference. However, the system accurately detected level changes without significant impact on performance.

D. Scenario 4

The test data, showing changes in temperature, material level, motor status, LED status, and LCD during the 10 minutes, as well as the error rate during transitions, is presented in Table 5. During the test, the temperature increased rapidly, and the material level fluctuated significantly. When the temperature exceeded 95°C, the motor and LED were immediately turned off, with the LCD displaying the status "STOP" to indicate overheating. When the material level fell below 75%, the motor and LED were also turned off, and the LCD displayed "IDLE."

When either the temperature or material level returned to the operational criteria, the motor and LED were reactivated, and the LCD updated to "ACTIVE." The error rate recorded during extreme transitions was very low, around 5% of the total test time, showing that the system was able to handle rapid temperature and level fluctuations well. The average response time was recorded at around 1 second, meeting the system's criteria for responding in less than 1.5 seconds.

Table 5. Result of Scenario 4 Testing

Time (sec)	Temperature (C)	Level (%)	Motor Active	LED Active	LCD Status	Error Rate
0	85	100	TRUE	TRUE	Temperature: 85.0C Level: 100.0% - ACTIVE	0
60	86.5	95	TRUE	TRUE	Temperature: 86.5C Level: 95.0% - ACTIVE	0
120	88	90	TRUE	TRUE	Temperature: 88.0C Level: 90.0% - ACTIVE	0
180	89.5	85	TRUE	TRUE	Temperature: 89.5C Level: 85.0% - ACTIVE	0
240	91	80	TRUE	TRUE	Temperature: 91.0C Level: 80.0% - ACTIVE	0
300	92.5	75	TRUE	TRUE	Temperature: 92.5C Level: 75.0% - ACTIVE	0
360	94	70	FALSE	FALSE	Temperatur: 94.0C Level: 70.0% - IDLE	1
420	95.5	65	FALSE	FALSE	Temperature: 95.5C Level: 65.0% - STOP	1
480	97	60	FALSE	FALSE	Temperature: 97.0C Level: 60.0% - STOP	1
540	98.5	55	FALSE	FALSE	Temperature: 98.5C Level: 55.0% - STOP	1
600	100	50	FALSE	FALSE	Temperature: 100.0C Level: 50.0% - STOP	1

This test demonstrates that the digester automation system is sufficiently robust to handle extreme stress conditions. The high response speed and low error rate indicate that the system is well-designed and capable of responding quickly and accurately to rapid temperature and level changes. One of the system's strengths is its ability to stop the motor and LED when temperature or material level is outside the desired range, preventing component damage and optimizing energy use by avoiding unnecessary operation.

The system was also able to detect temperature and level changes with high accuracy, despite the sharp fluctuations. However, it should be noted that a slight increase in the error rate was observed during extreme transitions, which could be attributed to sensor limitations or data processing disturbances. Nonetheless, the system managed these conditions effectively and protected its components from damage.

4. Conclusion

The digester automation system performed efficiently across various scenarios, demonstrating robust performance in managing temperature, material level, and rapid fluctuations. It responded quickly to changes, with precise control over the motor and LED, and real-time status updates via the LCD. The system effectively handled overheating conditions by stopping the motor when necessary, optimizing energy usage, and recovering once conditions returned to normal. It also managed low material levels efficiently, activating only when criteria were met. Despite rapid fluctuations, the system showed excellent robustness and low error rates, ensuring reliable operation even in extreme conditions. Overall, the system is efficient, energy-saving, and well-suited for industrial automation applications.

References

[1] B. Trisakti, M. Irvan, I. Zahara, Taslim, and M. Turmuzi, "Effect of Agitation on Acidogenesis Stage of Two-Stage Anaerobic Digestion of Palm Oil Mill Effluent (POME) into Biogas," IOP Conference Series: Materials Science and Engineering, vol. 180, 2017.

[2] B. Santoso, T. Widayati, and B. Hariadi, "Improvement of Fermentation and the In Vitro Digestibility Characteristics of Agricultural Waste-Based Complete Feed Silage with Cellulase Enzyme Treatment," Advances in Animal and Veterinary Sciences, vol. 8, pp. 873-881, 2020.

[3] M. Irvan, T. Husaini, E. Simanungkalit, R. Sidabutar, and B. Trisakti, "Automation of Temperature Sensor in Biogas Production from Palm Oil Mill Effluent (POME)," Journal of Physics: Conference Series, vol. 1116, 2018.

[4] B. Trisakti, M. Irvan, T. Mahdalena, and M. Turmuzi, "Effect of Temperature on Methanogenesis Stage of Two-Stage Anaerobic Digestion of Palm Oil Mill Effluent (POME) into Biogas," IOP Conference Series: Materials Science and Engineering, vol. 206, 2017.

[5] T. D. da Silva, S. Danthine, and S. Martini, "Influence of Sonication, Temperature, and Agitation, on the Physical Properties of a Palm-Based Fat Crystallized in a Continuous System," Ultrasonics Sonochemistry, vol. 74, 2021.

[6] W. Choorit and P. Wisarnwan, "Effect of Temperature on the Anaerobic Digestion of Palm Oil Mill Effluent," Electronic Journal of Biotechnology, vol. 10, pp. 376-385, 2007.

[7] M. A. F. Hamzah, J. Jahim, P. M. Abdul, and A. J. Asis, "Investigation of Temperature Effect on Start-Up Operation from Anaerobic Digestion of Acidified Palm Oil Mill Effluent," Energies, vol. 12, no. 12, 2019.

[8] A. Rajab, A. Sulaeman, S. Sudirham, and S. Suwarno, "A Comparison of Dielectric Properties of Palm Oil with Mineral and Synthetic Types Insulating Liquid under Temperature Variation," Journal of Engineering and Technological Sciences, vol. 43, no. 3, pp. 191-208, 2011.

[9] M. Kellens, V. Gibon, M. Hendrix, and W. Greyt, "Palm Oil Fractionation," European Journal of Lipid Science and Technology, vol. 109, pp. 336-349, 2007.

[10] M. Soleimaninanadegani and S. Manshad, "Enhancement of Biodegradation of Palm Oil Mill Effluents by Local Isolated Microorganisms," International Scholarly Research Notices, vol. 2014, p. 727049, 2014.

[11] S. D. P. Tanjung, “Penerapan Mikrokontroler Arduino dalam Sistem Pengendalian Temperatur Industri,” SABER : Jurnal Teknik Informatika, Sains dan Ilmu Komunikasi, vol. 3, no. 1, pp. 223–234, 2025.

[12] A. A. Rahmansyah, A. R. Taufagus, A. A. Sitinjak, and G. Gultom, “Implementasi Neural Network untuk Monitoring Level CPO dan Pengendalian Pompa Berbasis Arduino dan Aplikasi Android pada Tangki Bulking dalam Rangka Transformasi Industri 4.0,” Joule, pp. 36–42, 2025.

[13] I. As’ad, A. M. Rahmatullah, S. M. Abdullah, F. Fahmi, H. M. Pakka, and A. Andiyan, “Smart clove oil distillation system using IoT and ultrasonic sensors,” J. Sist. Inf., vol. 14, no. 5, p. 2341, 2025.

Vol. 4, No. 2, December 2025, pp. 103-116
p-ISSN: 2963-8577
e-ISSN: 2964-3511
DOI: 10.57102/jescee.v4i2.132

JESCEE
Journal of Emerging Supply Chain, Clean Energy, and Process Engineering

STUDI EKSPERIMENTAL ACTIVE NOISE CONTROL PADA MOTOR PENGGERAK PESAWAT UAV NOISE VIBRATION CENTER BERMESIN DLE GAS ENGINE 30

Alfisyahrin[1*], Ikhwansyah Isranuri[2], Syukriyadin[3], Habiburrahman[4]

[1]Department of Electrical Engineering, Faculty of Engineering, Universitas of Syiah Kuala
[2]Department of Mechanical Engineering, Faculty of Engineering, Universitas of Sumatera Utara
[3]Department of Electrical Engineering, Faculty of Engineering, Universitas of Syiah Kuala
[4]Department of Mechanical Engineering, Faculty of Engineering, Universitas of Sumatera Utara

Abstract
Abstrak—The noise that occurs at the USU UAV Noise and Vibration Center ranges between 90-100 dB. The engine used is a 2-stroke engine which certainly has high noise. The engine drive motor determines the high rotation and contributes to the noise. The method used to reduce noise is ANC. ANC in this study focused only on the drive motor. The results obtained are after comparing the noise before using ANC and after using ANC. The noise reduction obtained is at a rotation of 3000 rpm with a distance of 1.25 m of 1.36 dB.

Keywords:
Drive motor, noise, ANC, UAV, NVC, X,Y,Z axis.

Article History:
Received: November 2nd, 2025
Revised: November 27th, 2025
Accepted: December 21st, 2025
Published: December 31st, 2025

Corresponding Author:
Alfisyahrin
Department of Electrical Engineering, Universitas of Syiah Kuala, Indonesia
Email: alfisyahrin@usk.ac.id

1. Introduction

In today's modern era, unmanned aerial vehicles (UAV) have become a tool that can be used in all aspects of society. They are commonly used for hobbies, commercial purposes, and even in the military. They can also be used for civilian purposes, such as non-military security, firefighting, construction site monitoring, and even for advanced photography and videography. Noise on aircraft is a concentration of research that is continuously carried out to obtain aircraft that have low noise levels and avoid excessive noise pollution that can cause harm to drone users, especially if drones are used in their function as a military tool, of course drones that have vibrations and noise in the engine will not be effective if used as spy planes or as unmanned fighter planes.

However, as with any other machine, noise is unavoidable. Noise issues in unmanned aircraft are a growing focus of research every year. Most aircraft noise originates from the propeller, rotor, and engine systems. Noise from an aircraft engine is a combination of two noise sources: the propeller and the engine itself. The DLE Gas Engine 30 is a key component of the third-generation USU Mechanical Engineering UAV. It functions as a propulsion motor that drives the propeller, generating thrust for the aircraft. It is a 2-stroke engine, making it more noisy than a 4-stroke engine. Therefore, to address this noise, ANC (Active Noise Control) was introduced, which is one possible noise control technique. ANC works by comparing a noise signal from a noise source with a noise signal from a microphone that has the same signal but is in reverse phase with the noise source. By comparing these two signals, the final noise signal is expected to have a reduced noise level.

The measurement method uses a spherical technique by placing the ANC position on the X, Y, Z axes and the measurement point on the X, Y, Z axes with a measuring distance of 1.25 m. Considering the importance of noise reduction, the noise signal approach to unmanned aircraft engines is a technology that is useful for reducing vibrations originating from unwanted engine noise. The principle of its operation is by producing sound waves of sufficient strength to reduce the sound wave signal from the noise source. ANC plays a role in reducing the noise so that the benefits for the work environment do not cause chaos due to noise, both for humans and other objects. In this case, ANC will be applied to unmanned aircraft located in the NVC (Noise and Vibration Research Center) laboratory at the University of North Sumatra. Active Noise Control is a noise control

technique using electronic instruments designed according to the noise parameters of the noise source. The noise countermeasure is carried out by inverting the phase of the source noise using the designed electronic instrument. The experimental study conducted this time was limited only to the UAV propulsion motor with a DLE Gas Engine 30 engine from the USU NVC laboratory.

A. UAV (Unmanned Aerial Vehicle)

Unmanned Aerial Vehicles (UAV) are flying machines that can be controlled remotely, or aircraft that fly without a crew member. There are two main variations of unmanned aircraft: remote control, and autonomous flight based on a program pre-flight. The aircraft's control is entirely handled by an autopilot system, based on parameters set by the user before flight. UAVs can carry cameras, sensors, communications equipment, and various other equipment. These types of aircraft are widely used in the military.

Figure 1.1 Indonesian unmanned aerial vehicle (UAV) (http://tech.dbagus.com/pesawat-tanpa-awak-buatan-indonesia)

B. Unmanned Machine

This drone uses a DLE 30 engine. This type of engine is a gasoline engine similar in size to a glow engine. Electronic ignition provides a quick initial spark. Timing is automatically adjusted for peak power across the rotations per minute (RPM) range and is designed for aviation, ensuring the best power-to-weight ratio and performance.

The DLE 30 gasoline engine can be seen in Figure 2.2 below.

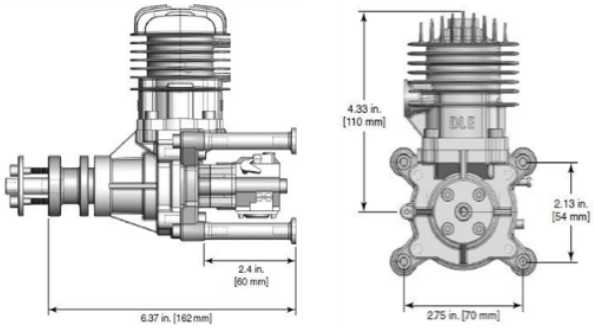

Figure 1.2 DLE Gasoline Engine 30
(https:// =DLE+Gasoline+Engine+30+110cc+engine+pesawat)

C. Aerodynamic Noise.

Sound is defined as a series of waves propagating from a vibrating source as a result of changes in density and air pressure, or changes in pressure that can be detected by the ear. Sound waves in fluids are mostly produced through the vibrating surface of a solid substance within the fluid. The decibel unit indicates the sound pressure level [4]. Its magnitude is above the reference of 20 x 10-6 N/$m2$. The decibel is also a logarithmic unit for describing a ratio.

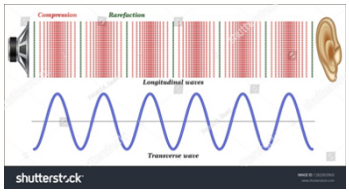

Figure 1.3 Sound waves in media [4]

Humans can only hear sounds within a certain frequency range that elicits a response and does not interfere with the function of the auditory system. The range of frequencies audible to humans is between 20 Hz and 20,000 Hz. Sounds can be grouped into several categories based on their frequency:

1. Infrasonic: frequency < 20 Hz
2. Audiosonic: frequency 20-20,000 Hz
3. Supersonic: frequency > 20,000 Hz

D. Noise

Noise is unwanted sound or noise that can disrupt health and environmental comfort, expressed in decibels (dB). Over time, most production machines, transportation equipment, and anything that improves human quality of life have been associated with noise. Noise can propagate through many pathways, known as noise paths [7].

Noise sources can be grouped into three categories:
1. Intrinsic noise sources arise from random fluctuations within a physical system, such as thermal and shot noise.
2. Man-made noise sources, such as motors, switches, and digital electronics.
3. Noise sources due to natural disturbances, such as lightning and sunspots.

In Table 1.1 you can see examples of the maximum noise levels permitted for several sound sources.

Tabel 1.1 Contoh tingkat kebisingan suara berdasarkan sumbernya [8]

Sound sources (noise) Examples with distance	Sound pressure Level L_p dB SPL
Jet aircraft, 50 m away	140
Threshold of pain	130
Threshold of discomfort	120
Chainsaw, 1 m distance	110
Disco, 1 m from speaker	100
Diesel truck, 10 m away	90
Kerbside of busy road, 5 m	80
Vacuum cleaner, distance 1 m	70
Conversational speech, 1 m	60
Average home	50
Quiet library	40
Quiet bedroom at night	30
Background in TV studio	20
Rustling leaves in the distance	10
Hearing threshold	0

E. How Active Noise Control Works

Active noise control works by providing a noise-controlling sound to the noise source, or in other words, sound counteracts sound. This sound reduction occurs when the "anti-noise" sound wave is 180° out of phase with the noise source.

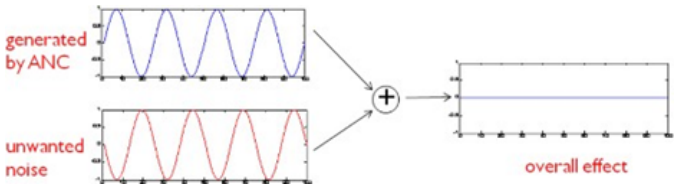

Figure 1.4 Destructive interference process in ANC
(https://Process+interferensi+destruktif+pada+ANC&safe)

Schematically, the noise formation mechanism can be seen in Figure 1.5

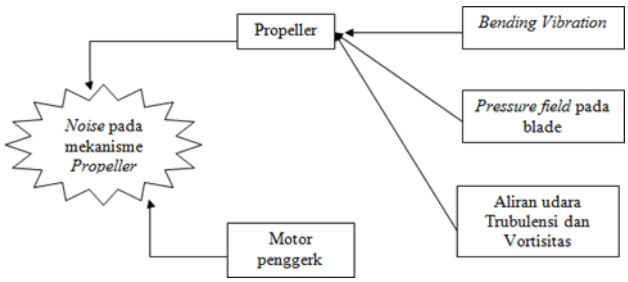

Figure 1.5 Noise Generation Mechanism on the propeller

2. Method

A. Set Up and Data Collection

In this experimental study, reduction was performed by contrasting the primary noise with the secondary noise produced by the loudspeaker. The loudspeaker was placed on a prefabricated stand with a spherical shape on the x+, x-, z+, and z- axes. Testing and data measurements were conducted by placing the sound level meter at varying distances, starting from 0.75 m, 1 m, and 1.25 m. These measurement distances were selected based on the results of experimental studies where the ANC was effective in reducing sound at low frequencies, in this case the low sound frequency range of 20 Hz to 500 Hz.

Measurements were also performed on the x+, x-, y+, y-, z+, and z- axes. In this study, measurements were performed at engine speeds of 3000 rpm, 3500 rpm, 4000 rpm, 4500 rpm, and 5000 rpm. The engine speeds for the measurements were standardized according to ISO 5130.

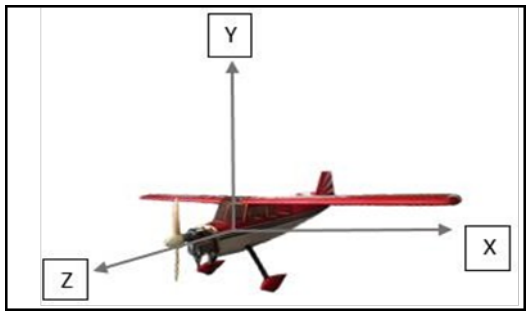

Figure 2.1 Measurement direction

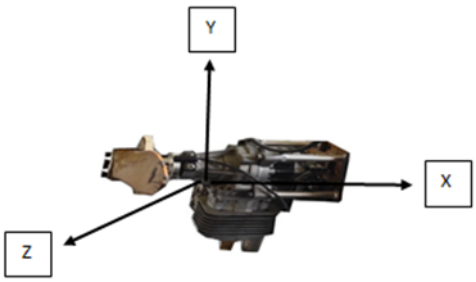

Figure 2.2 Measurement direction on the machine

Figure 2.3 Data collection process

Figure 2.4 ANC Instrument Electronics

In this study, data collection was conducted outdoors at night to achieve the lowest possible environmental noise levels. Testing was conducted by running the engine of the USU NVC drone at varying speeds controlled by a remote control. Engine speed was measured using a tachometer, which directly reads engine speed. Noise levels were then measured using an SPL meter on the USU NVC drone.

B. Parameter Kajian Pada Metode Active Noise Control

To determine the parameters in the kinematic study of the ANC method, the input and output that work on the working principle of the ANC method are identified. Based on the analysis, the parameters that work on the ANC method are input parameters, namely aircraft noise at certain engine speeds, and output parameters, namely the final noise after noise control. And there are also parameters that can affect the output parameters, namely the controlled parameters that surround, environmental noise, measurement distance, and noise counter/ANC. To make it easier, see the illustration in the image below.

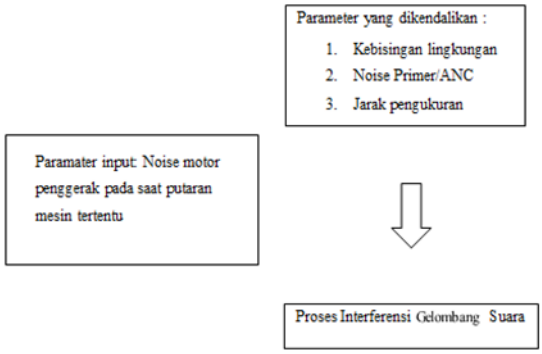

Figure 2.5 Study parameters in the ANC method

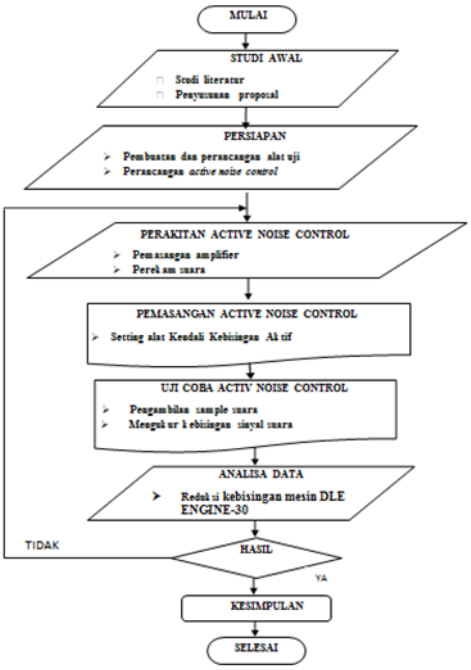

Figure 2.6 Active Noise Control Flowchart

3. Result and Discussion

A. Measurement Result Data After Using Active Noise Control Instrument

After noise measurements were performed using the ANC instrument, the recorded sound was captured using a microphone placed parallel to the speaker at the end of a spherical metal rod. This was done to ensure the sound captured and the sound emitted by the speaker were in phase. The sound was then processed by the ANC instrument to counteract the noise from the source.

1) At a distance of 1.25 meters
From table 4.1, the data on the difference in noise levels are as follows:

Table 3.1 Reduction value at a distance of 1.25 meters

N (rpm)	Sound Pressure Level Reduction (dB) Distance 1.25m					
	x+	x-	y+	y-	z+	z-
2000	-2,5	-1,7	-0,5	-1,6	1,9	3
2500	-1,3	-1,4	-0,8	-1,2	-1,2	-0,6
3000	-0,2	-1,1	-1,8	-2,1	-1,7	-0,6
3500	-0,9	-1	-0,7	-0,9	-0,8	-1,2
4000	-1,2	-0,9	-4,2	-2,2	1	-0,9

• X+ axis

On the x+ axis we can see a comparison of the magnitude of the sound pressure level value at a distance of 1.25 m in the image below:

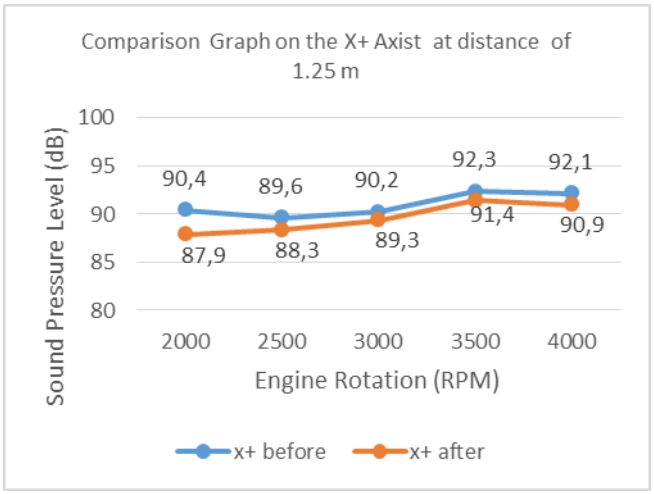

Figure 3.1 Noise comparison graph on the x+ axis at a distance of 1.25 m

From Figure 3.1 above, it can be seen that noise reduction occurs at 3500 rpm with a sound pressure level reduction value of 0.9 dB. Meanwhile, at 2000 rpm, 2500 rpm, and 3000 rpm, there is an increase in noise levels with the largest increase in sound pressure levels at 3000 rpm of 0.2 dB.

• X-axis

On the x-axis we can see a comparison of the magnitude of the sound pressure level values at a distance of 1.25 m in the image below:

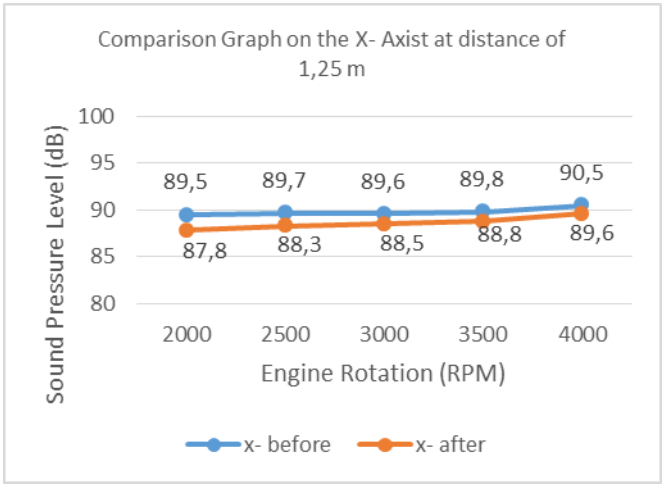

Figure 3.2 Noise comparison graph on the x-axis at a distance of 1.25 m

Figure 3.2 shows that there is no drastic reduction in noise levels at engine speed. The highest increase in sound pressure level occurs at 4000 rpm with an increase of 0.9 dB, and the lowest increase in sound pressure level occurs at 2000 rpm with an increase of 1.7 dB.

• Y+ axis

On the y+ axis we can see a comparison of the magnitude of the sound pressure level value at a distance of 1.25 m in the image below:

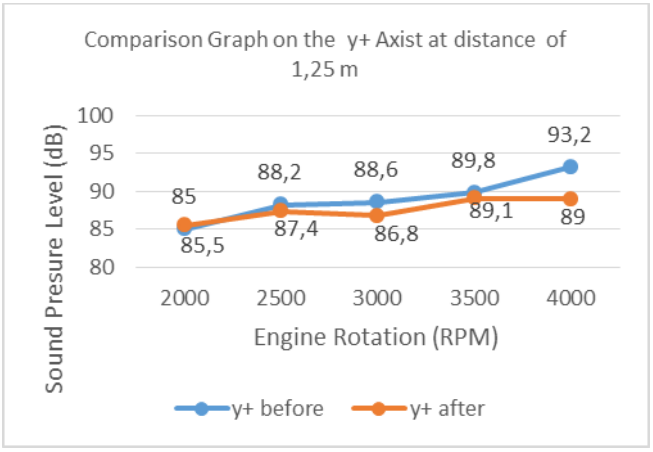

Figure 3.3 Noise comparison graph on the y+ axis at a distance of 1.25 m

Figure 3.3 above shows that there has been an increase in noise reduction. The increase in noise level naturally amplifies the previous noise. The highest increase in noise level occurs at 2000 rpm, with an increase of 0.5 dB, and the lowest increase in sound pressure level occurs at 4000 rpm, with an increase of 4.2 dB.

• Y-axis

On the y-axis we can see a comparison of the magnitude of the sound pressure level values at a distance of 1.25 m in the image below:

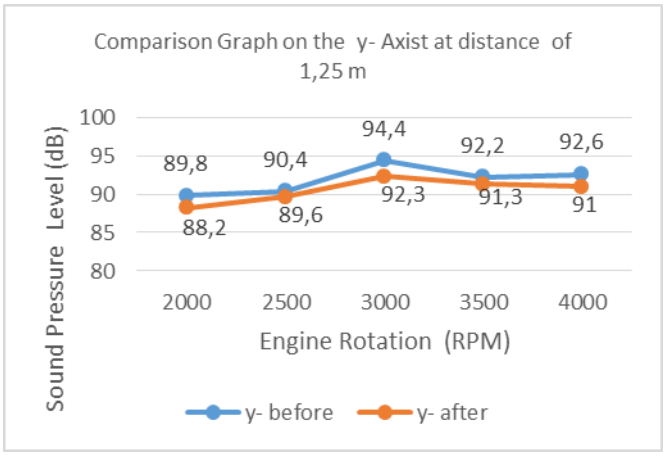

Figure 3.4 Noise comparison graph on the y-axis at a distance of 1.25 m

From Figure 3.4 above, it can be seen that there is no noise reduction, but instead there is an increase in noise at engine speeds of 2000 rpm, 2500 rpm, and 3000 rpm with the largest increase in sound acoustic pressure level occurring at 3000 rpm of 2.1 dB. Meanwhile, at 3500 rpm, there is an increase in reduction of 0.9 dB.

• Z+ axis

On the z+ axis we can see a comparison of the magnitude of the sound pressure level value at a distance of 1.25 m in the image below:

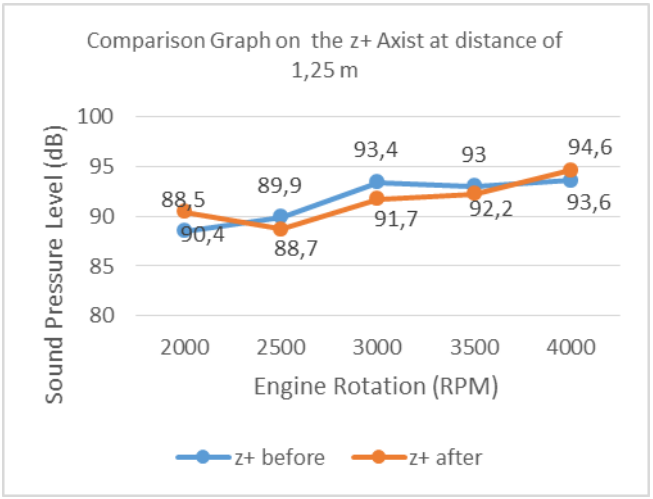

Figure 3.5 Comparison graph on the z+ axis at a distance of 1.25 m

From Figure 3.5 above, it can be seen that there has been an increase in noise reduction at engine speeds of 2000 rpm, 2500 rpm, and 3000 rpm with the largest sound pressure level reduction value occurring at 2000 rpm of 1.9 dB. Meanwhile, at engine speeds of 3500 rpm and 4000 rpm, there was an increase in noise levels with the largest increase in sound pressure levels occurring at 4000 rpm with an increase of 1 dB.

• Z-axis

On the z-axis we can see a comparison of the magnitude of the sound pressure level values at a distance of 1.25 m in the image below:

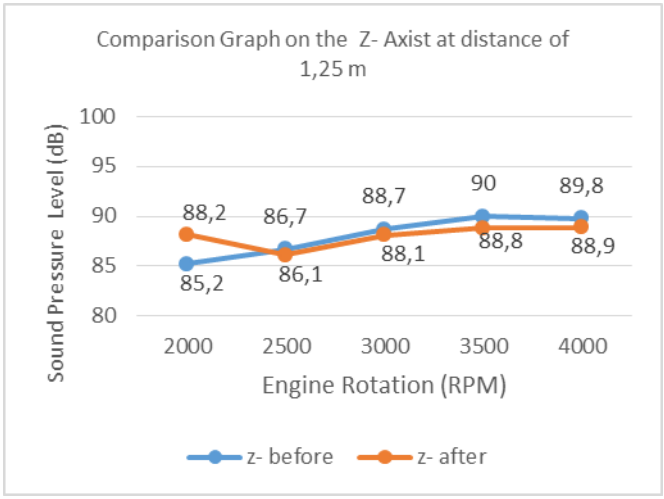

Figure 3.6 Comparison graph of noise in the z-axis at a distance of 1.25 m

From Figure 3.6 above, it can be seen that noise reduction has occurred at 3000 rpm, 3500 rpm, and 4000 rpm, with the largest reduction occurring at 3000 rpm with a sound pressure level of 0.6 dB. The highest increase occurred at 2000 rpm, amounting to 3 dB.

2) Noise contour at a distance of 1.25 meters

Based on the table below, you can see the noise contour for each engine rotation in the graphic image below.

Table 3.1 Measurement results at a distance of 1.25 meters

N (rpm)	Sound Pressure Level (dB) distance 1.25 m					
	x+	x-	y+	y-	z+	z-
2000	90,4	89,5	85	89,8	88,5	85,2
2500	89,6	89,7	88,2	90,4	89,9	86,7
3000	90,2	89,6	88,6	94,4	93,4	88,7
3500	92,3	89,8	89,8	92,2	93	90
4000	92,1	90,5	93,2	92,6	93,6	89,8

Table 3.2 Measurement results at a distance of 1.25 meters

N (rpm)	Sound Pressure Level (dB) Distance 1.25m					
	x+	x-	y+	y-	z+	z-
2000	93	91,7	94,1	95,1	95,4	90,6
2500	93,5	92,5	95,2	95,8	94,6	92,3
3000	94,7	93,9	96,3	96,9	95,5	93,8
3500	95,3	93,3	96,8	96,2	96,8	93,2
4000	95,6	94	98,7	98	98	91,6

Based on table 3.1 and table 3.2above, the noise contour for each engine rotation can be seen in the graphic image below.

• Engine speed 3000 RPM

At an engine speed of 3000 rpm, the shape of the noise contour can be seen as in the image below:

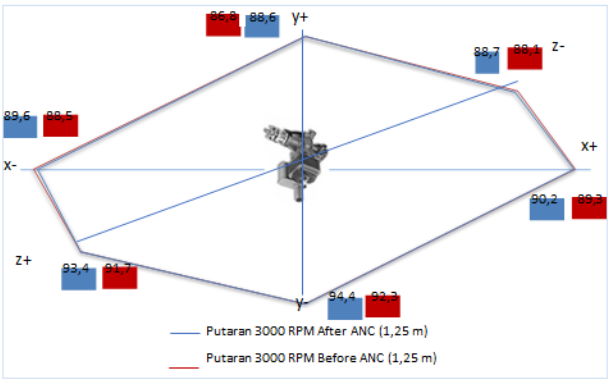

Figure 3.7 Noise contour (dB) at 3000 rpm at a distance of 1.25 m

Figure 3.7 above shows the noise contour at 3000 rpm at a distance of 1.25 meters. It can be seen that noise levels on all measurement axes were reduced after using the active noise control device. The highest noise level was on the y-axis both before and after using the active noise control device.

• Engine speed 3500 RPM

At an engine speed of 3500 rpm, the shape of the noise contour can be seen as in the image below:

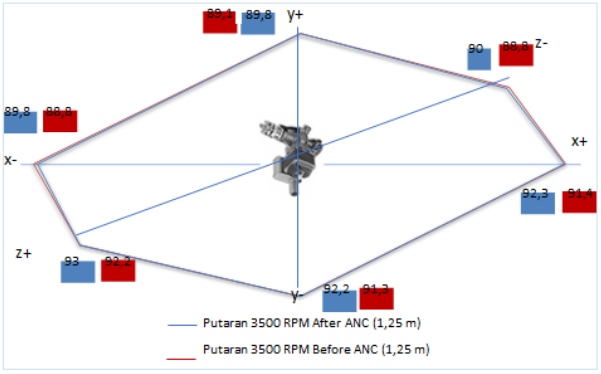

Figure 3.8 Noise contour (dB) at 3500 rpm at a distance of 1.25 m.

From Figure 3.8 above, the noise contour at 3500 rpm at a distance of 1.25 meters can be seen. It can be seen that the noise level on all measurement axes is reduced or reduced after using the active noise control device, while the highest noise level is on the z+ axis both before and after using the active noise control device.

• Engine speed 4000 RPM

At an engine speed of 4000 rpm, the shape of the noise contour can be seen as in the image below:

p-ISSN: 2963-8577
e-ISSN: 2964-3511

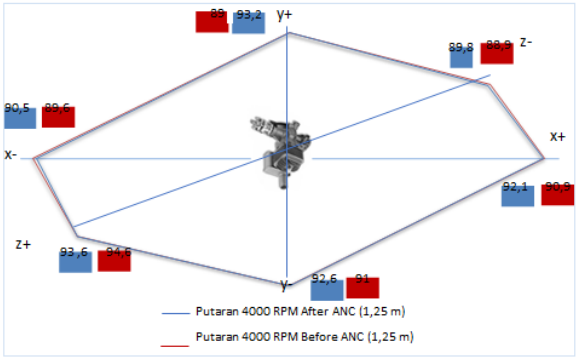

Figure 3.9 Noise contour (dB) at 4000 rpm at a distance of 1.25 m

From Figure 3.9 above, we can see the noise contour at 4000 rpm at a distance of 1.25 meters. It can be seen that the noise level on the x+, x-, y+, and y- axes experienced noise reduction after using the active noise control device. Meanwhile, on the z+ and z- axes, noise amplification occurred after using the active noise control device.

• Average Noise Value After Using Active Noise Control Devices.

Using the same formula to calculate the average noise value above, the average noise value after using active noise control equipment is obtained as shown in the table below:

Table 3.3 Average noise values after using active noise control devices

N (rpm)	Average Sound Pressure Level (dB)		
	Distance 0,75 m	Distance 1 m	Distance 1,25m
2000	89,4	88,1	88
2500	91	90	88
3000	93,6	91,2	89,4
3500	93,9	92,7	90,2
4000	93,9	92	90,6

The table above shows the average noise levels after using the active noise control device at all engine speeds at each measurement distance. The highest noise levels were at 4,000 rpm and 3,500 rpm at a distance of 0.75 meters, and the lowest noise levels were at 2,000 rpm and 2,500 rpm at a distance of 1.25 meters. The noise levels at each distance did not increase consistently. This may be due to uneven noise reduction.

3) Noise Reduction Rate (NRR)

Noise Reduction Rate or NRR is the reduction rate obtained from the average reduction value that occurs, namely the total noise value before using the active noise control device minus the total noise value after using the active noise control device and divided by the number of measurement axes, which can be formulated as follows:

$$NRR = \frac{\Sigma \text{ Noise Level before ANC} - \Sigma \text{ Noise Level After ANC}}{Number\ of\ Data\ Capture\ Axes}$$

With the formula above, the noise reduction rate value is obtained for each distance rotation in the table below:

Table 3.4 NRR Values

N (rpm)	Average Sound Pressure Level (dB)		
	Distance Jarak 0,75 m	Distancen 1 m	Distance 1,25 m
2000	-10,3	0,93	-4,53
2500	-1,76	0,85	0,98
3000	0,1	0,86	1,36
3500	0,88	0,9	0,91
4000	1	0,96	1,3

The table above shows that at engine speeds of 3000 rpm, 3500 rpm, and 4000 rpm, the NRR value at all measurement distances is positive, indicating that no noise reduction occurs. The highest NRR value that does not reduce noise is at 3000 rpm at a distance of 1.25 meters, where the NRR value obtained is 1.36 dB.

4. Conclusion

The reduction occurred after averaging several variations of rotation at 3000 rpm, at a measuring distance of 1.25 m, with a value of 1.36 Db.

Acknowledgment

Thank you to the USU Noise and Vibration Center Laboratory team, as well as to the resource persons and discussion partners for carrying out this research.

References

[1] Alfisyahrin, “Simulasi Pemrosesan Sinyal Suara Untuk Sistem Aktif Kendali Kebisingan Pada Knalpot (Noise Silencer),” Thesis, Medan; Indonesia, 2008.
[2] Alfisyahrin and I. Isranuri, “Cancelation and its simulation using Matlab according to active noise control case study of automotive noise silencer,” IOP Conf. Ser. Mater. Sci. Eng., vol. 308, no. 1, 2018, doi: 10.1088/1757-899X/308/1/012039.
[3] S. Fields, Basic Concepts of Sound Contents : Definitions.
[4] https://www.shutterstock.com/image-vector/sound-reflection-reverberation-1282003960
[5] Microcontroler, “What is a Microcontroller?,” The Bare Necessities. .
[6] T. Technopreneur, “Introduction ATMega16,” Technopreneur.
[7] N. Nishant, “Introduction to Atmega Microcontrollers,” My experiences with Tech"crazy"onology. .
[8] https://fiveable.me/noise-control-engineering/unit-3/point-line-plane-sources/study-guide/WudQtcwpEoEOi8gs
[9] Beginer, “Proses Perubahan Sinyal Analog Ke Digital,” Beginer welcom.
[10] E. Galery, “ADC0808,” Engineer Galery.
[11] E. Dasar, “Frekuensi, Periode Dan Fasa Gelombang Listrik,” Teori Dasar Elektronika, Karakteristik Komponen Elektronika, Rangkaian Elektronika Dasar, Artikel Dan Aplikasinya.
[12] S. Stock, “Sound Propagation Images,” Stock, Shutter. .
[13] MPS, “Analog Signals vs. Digital Signals,” MPS.
[14] H. Zhu, R. Rajamani, J. Dudney, and K. A. Stelson, “Active noise control using a distributed mode flat panel loudspeaker,” ISA Trans., vol. 42, no. 3, pp. 475–484, 2003, doi: 10.1016/S0019-0578(07)60148-7..
[15] P. Micheau and S. Renault, “Active control of the complex envelope associated with a low damped mode,” Mech. Syst. Signal Process., vol. 20, no. 3, pp. 646–661, 2006, doi: 10.1016/j.ymssp.2005.05.004
[16] M. Guldenschuh and R. Höldrich, “Prediction filter design for active noise cancellation headphones,” IET Signal Process., vol. 7, no. 6, pp. 497–504, 2013, doi: 10.1049/iet-spr.2012.0161.
[17] T. Watanabe, H. H. Nigim, and H. S. Koyama, “The effects of propeller tip vane on flow-field behavior,” Exp. Fluids, vol. 23, no. 5, pp. 410–417, 1997, doi: 10.1007/s003480050129.
[18] C. Kestell and C. H. Hansen, “The Active Noise Control of a Light Aircraft Cabin Interior ; A work in progress .,” pp. 1–5.

[19] S. M. Hashemi-Dehkordi, M. Mailah, and A. R. Abu-Bakar, "A robust active control method to reduce brake noise," 2008 IEEE Int. Conf. Robot. Biomimetics, ROBIO 2008, pp. 739–744, 2009, doi: 10.1109/ROBIO.2009.4913092.
[20] C. H. Hansen, "Fundamentals of Acoustics," Phys. Today, vol. 16, no. 8, pp. 56–57, 1963, doi: 10.1063/1.3051072.
[21] T. Robert, "Active Noise Cancelling (ANC) Technology Types Explaned," Soundguys.
[22] A. and Vibration, "Acoustics and Vibration: FEA and CFD for VibroAcoustics and NVH Analysis," Enteknograte.
[23] M. O'Brien and P. Pratt, "Active noise control using robust feedback techniques," ICASSP, IEEE Int. Conf. Acoust. Speech Signal Process. - Proc., vol. 5, pp. 3209–3212, 2001, doi: 10.1109/icassp.2001.940341.
[24] F. T. Calkins and J. H. Mabe, "Variable Geometry Jet Nozzle Using Shape Memory Alloy Actuators," no. 425, 2007
[25] T. Nestorovic, "Active control of mechanical structures in research and education," Theor. Appl. Mech. i Primenj. Meh., vol. 40, no. 2, pp. 203–221, 2013, doi: 10.2298/tam1302203n.
[26] C. Doolan, "Wind turbine noise mechanisms and some concepts for its control," Aust. Acoust. Soc. 2011, Acoust. 2011 Break. New Gr., vol. 40, no. 1, pp. 494–500, 2011.
[27] T. H. Jung, J. H. Kim, K. J. Kim, and S. W. Nam, "Active noise reduction system using multi-channel ANC," Int. Conf. Control. Autom. Syst., no. 2, pp. 36–39, 2011

ISSN 2963-8577
ISSN 2964-3511

Faculty of
Industrial Technology
Universitas Pertamina
Jl. Teuku Nyak Arief, RT.7/RW.8, Simprug, Kec. Kby. Lama, Kota Jakarta Selatan, Daerah Khusus Ibukota Jakarta 12220